

الجمهورية الجزائرية الديمقراطية
الشعبية
وزارة التعليم العالي والبحث العلمي
جامعة غرداية



حاضنة الأعمال لجامعة غرداية

كلية العلوم والتكنولوجيا

قسم الآلية والكهروميكانيك.

مذكرة تخرج لنيل شهادة الماستر في تخصص آلية وأنظمة في إطار القرار الوزاري
1275

شهادة تخرج – مؤسسة ناشئة / براءة اختراع

بعنوان:

**DairAI (درعي): AI-based firefighting
system using drones for fire prediction,**

تحت إشراف:

حسن ناصر

من إعداد الطلبة:

عمير منال
فارح أسامة
أولاد العيد فاطمة الزهرة

الموسم الجامعي: 2022/ 2023 م

People's Democratic Republic of Algeria
Ministry of Higher Education and Scientific Research



N° d'ordre :

N° de série :

University of Ghardaia
Faculty of Science and Technology
Department of Automation and Electromechanics

Thesis presented for the graduation of

MASTER'S DEGREE

Field: Science and Technology

Die: Automatic

Specialty: Automatic and Systems

By: *AMIEUR Manal*

FAREH Oussama

Theme

**Intelligent control for stabilization and
trajectory tracking of unmanned aerial
vehicles UAVs (drones)**

Publicly supported on: 06/25/2023 In front of the jury :

	Univ. Ghardaïa	President
	Univ. Ghardaïa	Examiner
	Univ. Ghardaïa	Examiner
HACENE Nacer	MCA Univ. Ghardaïa	Supervisor

Academic year 2020/2023

People's Democratic Republic of Algeria
Ministry of Higher Education and Scientific Research



N° d'ordre :

N° de série :

University of Ghardaia
Faculty of Science and Technology
Department of Automation and Electromechanics

Thesis presented for the graduation of

MASTER'S DEGREE

Field: Science and Technology

Die: Automatic

Specialty: Automatic and Systems

By: OULAD LAID Fatima Zohra

Theme

**Autonomous Drone-Based System for Fire
Detection and Firefighting**

HACENE Nacer

MCA

Univ. Ghardaïa

President

Univ. Ghardaïa

Examiner

Univ. Ghardaïa

Examiner

Univ. Ghardaïa

Supervisor

Academic year 2022/2023

Thanks

First of all, we thank God for giving us strength, will and the courage to accomplish this humble work.

These thanks are addressed to our families who have always helped us and to encourage during long years of study.

We thank our supervisor **Dr. Nacer HACENE** for all that he gave, for his valuable advice and patience with us, to all those who helped and supported us in our work.

Our deep thanks to the jury members who approved the evaluation this work.

Finally, we would like to express our deep gratitude to everyone who has supported us in our journey from colleagues and friends.....

Dedication



**First, we thank God, our Lord , who gave us strength and
Patience to get this job done.**

I dedicate this diary to my dear mom

**Whatever you do or say, I can't thank you enough. Your passion
Overwhelms me, your mercy guides me, and your presence beside
me has**

**I have always been the source of my strength in the face of various
obstacles.**

**To my dear Dad, you have always been by my side to support and
encourage me. I hope that this work reflects my gratitude and affection.**

To my dear grandmother, God healed her

To my sisters, Warda, Asma, Bouchra, Hadjar, Roukia and Aicha

To my niece Anfal

To my friend Abd Rahman



FARAH Oussama



Dedication

**First, we thank God, our Lord, who gave us strength and
Patience to get this job done.**

I dedicate this diary to my dear mom

**Whatever you do or say, I can't thank you enough. Your passion
Overwhelms me, your mercy guides me, and your presence beside me has
I have always been the source of my strength in the face of various
obstacles.**

**To my dear father You have always been by my side to support and
encourage me. I hope this is**

The work reflects my gratitude and affection.

**To my dear sister Kaouthar and to my brothers Mohammed Habib
Noureddine and Abdeldjebbar**

**To my future partner ABDEIDJEBBAR Mohammed, who
provided me with psychological and moral support, I sincerely thank him
for everything**

To my friends.

**To the enemies of success, I have reached and overcome challenges
thanks to my strong will and diligence.**



OULAD LAID Fatima Zohra



Dedication



First, we thank God, our Lord , who gave us strength and

Patience to get this job done.

I dedicate this diary to my dear mom

**Whatever you do or say, I can't thank you enough. Your passion
Overwhelms me , your mercy guides me, and your presence beside
me has**

**I have always been the source of my strength in the face of various
obstacles.**

**To my dear Dad, you have always been by my side to support and
encourage me. I hope that this work reflects my gratitude and affection.**

To my dear grandmother, God healed her

**To my dear sister Hadil and to my brothers mouhoub and
Rodouan**

**To my sister Lamia and her husband GHRBOUZ Saiid and her
daughter Yaqine**

To my uncles, each in his own name, and their daughters and sons

To my friends.

**To the enemies of success, I have reached and overcome challenges
thanks to my strong will and diligence.**

AMIEUR Manel



ملخص:

في أعقاب الحرائق الأخيرة في تيزي وزو وما خلفته من مآسي وخسائر في الأرواح والممتلكات والزرور والغابات، خاصة في ظل التغيرات المناخية المفاجئة وسنوات الجفاف الأخيرة، فإن حرائق الغابات تشكل مشكلا أمنيا واقتصاديا واجتماعيا كبيرا، ليس على المستوى الوطني فحسب، بل على المستوى العالمي. وحتى الإمكانيات الضخمة للدول المتطورة تعجز عن محاربة هذه الظاهرة الخطيرة.

وكحل واعد لمكافحة هذه الظاهرة يقترح عملنا حلا من مجموعة متكاملة من الإستراتيجيات التي تعتمد على استخدام الطائرات بدون طيار والذكاء الاصطناعي: الأولى هي إستراتيجية التنبؤ بالحرائق باستخدام الذكاء الاصطناعي Fire prediction. الثانية هي استراتيجية للإنذار المبكر وكشف الحرائق باستخدام الدرونز والذكاء الاصطناعي Fire detection. والثالثة هي استراتيجية مكافحة الحرائق Firefighting. والرابعة والأخيرة أطلقنا عليها استراتيجية مطر الدرون DronesRain، وتستخدم عندما يكون الحريق كبيرا وتعجز درون واحدة على إخماده.

من أجل ثبات الدرون في القيام بمهمته، تم استخدام التحكم من نوع PID وكذلك من نوع المنطق الغامض في تتبع مسار معين.

الكلمات المفتاحية: طائرات بدون طيار، الذكاء الاصطناعي، التنبؤ بالحريق، الكشف عن الحرائق، مكافحة الحريق، مطر الدرون

Abstract

In the aftermath of the recent fires in Tizi Ouzou and the tragedies and losses they caused in terms of lives, properties, crops, and forests, especially in light of sudden climate changes and recent years of drought, forest fires have become a significant security, economic, and social problem, not only at the national level but also globally. Even the vast resources of advanced countries are unable to combat this dangerous phenomenon.

As a promising solution to tackle this issue, our work proposes a solution from an integrated set of strategies that rely on the use of unmanned aerial vehicles (UAVs) and artificial intelligence. The first strategy is fire area prediction, utilizing artificial intelligence for fire prediction. The second strategy is early warning and fire detection using drones and artificial intelligence. The third strategy is firefighting. The fourth and final strategy, which we call DronesRain, is deployed when the fire is large and a single drone is unable to extinguish it.

To ensure the stability of the drone in carrying out its mission, a PID control system and fuzzy logic are used to track a specific path.

key words: Drones; Artificial intelligence; Fire prediction; Fire detection; Firefighting; DroneRain

Résumé

À la suite des récents incendies à Tizi Ouzou et des tragédies et pertes qu'ils ont entraînées en termes de vies humaines, de biens, de cultures et de forêts, notamment dans un contexte de changements climatiques soudains et d'années de sécheresse récentes, les incendies de forêt posent un problème majeur sur les plans de la sécurité, de l'économie et de la société, non seulement au niveau national mais aussi à l'échelle mondiale. Même les ressources

considérables des pays développés ne parviennent pas à lutter contre ce phénomène dangereux.

En tant que solution prometteuse pour faire face à ce problème, notre travail propose une solution basée sur un ensemble intégré de stratégies qui reposent sur l'utilisation de drones et d'intelligence artificielle. La première stratégie est la prédiction des zones de feu en utilisant l'intelligence artificielle. La deuxième stratégie est la détection précoce des incendies à l'aide de drones et d'intelligence artificielle. La troisième stratégie est la lutte contre les incendies. La quatrième et dernière stratégie, que nous appelons DronesRain, est mise en œuvre lorsque l'incendie est d'une grande ampleur et qu'un seul drone ne peut l'éteindre.

Pour assurer la stabilité du drone dans l'exécution de sa mission, deux contrôleurs PID et flou sont utilisés pour suivre un chemin spécifique.

Mots clés: Drones ; Intelligence artificielle; prévision d'incendie ; Détection d'incendie; Lutte contre l'incendie ; DronePluie

Table of contents

Abstract I	
List of figure.....	XVI
List of tables.....	XVII
List of symbols.....	XVIII
General introduction.....	1

Chapter I

I.1. Introduction.....	4
I.2. Quadcopter	5
I.3. Components of U.A.V (Quadcopter)	5
I.3.1. Quadcopter frame.....	5
I.3.2. Motors.....	6
I.3.3. Electronic Speed controller (ESC).....	6
I.3.4. Flight/Board control	6
I.3.5. Propellers	7
I.3.6. Transmitter	7
I.3.7. Batteries, Electronic & Power Distribution	7
I.3.8. Camera	7
I.4. Forces Acting on U.A.V. (Quadcopter)	8
I.4.1. Setup for a Drone Flight	9
I.4.2. Taking off	9
I.4.3. Moving on.....	9
I.4.4. Roll	9
I.4.5. Voice	10
I.4.6. Yaw	10
I.5. Applications of UAVs	10
I.5.1. Agriculture	10
I.5.2. Conservation	11
I.5.3. Delivery/fulfillment	12
I.5.4. Disaster mitigation and relief	12
I.5.5. Filmmaking and photography	12
I.5.6. Law enforcement	13
I.5.7. Real Estate	13

Table of contents

I.6.Conclusion.....	14
---------------------	----

Chapter II

II.1 Introduction.....	20
II.2 .The principle of quadrotor flight.....	20
II.3 Kinematics.....	21
II.3.1 Translation Kinematics.....	24
II.3.2.Rotation Kinematics	26
II.4. Dynamics.....	26
II.4.1 Newton-Euler.....	26
II.5. DC-Motor.....	33
II.6 Simulation Values.....	38
II.7. Simulink Modeling.....	39
II.8. Conclusion.....	41

Chapter III

III.1. Introduction.....	44
III.2. Trajectory.....	44
III.3. Control modeling.....	46
III.4. PID controller.....	47
III.4.1 Role of Proportional Action (P).....	48
III.4.2. Role of Integral Action (I).....	48
III.4.3 Role of Derivative Action (D).....	48
III.5. Controller Synthesis	49
III.5.1 The design of a PID controller.....	49
III.5.2 Height control.....	49
III.5.3 Roll control	51
III.5.4 Pitch control	52
III.5.5 Yaw control	53
III.6 MATLAB Simulink model	54
III.7. Simulation result.....	55
III.8. Conclusion.....	56

Chapter IV

IV.1. Introduction.....	59
-------------------------	----

Table of contents

IV.2. Fuzzy Logic	59
IV.3. Principe de la commande floue.....	59
IV.4. Structure of a fuzzy controller	60
IV.4. 1. Fuzzification Block.....	60
IV.4. 2.Rule Base and Inference Mechanism.....	60
IV.4. 2.1.Max-Min Inference Method (Mamdani Method).....	61
IV.4. 2.2.Max-Product Inference Method (Larsen Method).....	62
IV.4. 2.3.Sugeno Method	62
IV.4.3. Defuzzification Block.....	62
IV.4.3.1. Center of Gravity Method.....	63
IV.4.3.2. Maximum Value Method	64
IV.4.3.3. Mean of Maximums Method.....	65
IV.5 Membership functions: Parameterization and Formulatio.....	64
IV.6 Application of Fuzzy Control to UAV	64
IV.7. MATLAB Simulink model	66
IV.8. Simulation result.....	66
IV.9 Comparison of PID and Fuzzy.....	67
IV.10.Conclusion.....	68

Chapter V

V.1Introduction.....	70
V.2The processing of images.....	70
V.2.1 Definition.....	70
V.2.2 Definition of Image.....	71
V.2.2.1 Digital image.....	71
V.3 Artificial Neural Networks.....	71
V.3.1 Definition.....	71
V.3.2 Different models of neural networks.....	73
V.3.2.1Single-layer neural networks.....	73
V.3.2.2Multilayer neural networks.....	73
V.3.3 Applications.....	74
V.4Learning a neural network.....	74
V.4.1 Machine learning according to the nature of the input data.....	74
V.4.1.1 Supervised learning.....	74

Table of contents

V.4.1.2 Unsupervised learning.....	75
V.4.1.3 Reinforcement learning.....	75
V.4.2 Machine learning by type of result classification.....	75
V.5 Convolutional neural networks.....	76
V.5.1 CNN architecture principle.....	76
V.5.2 The different layers of the CNN.....	77
V.5.2.1 The convolution layer (CONV).....	77
V.5.2.2 Pooling layer (POOL).....	78
V.5.2.3 ReLU.....	79
V.5.2.4 Fully connected layer.....	79
V.5.2.5 Loss Layer (LOSS).....	79
V.5.3 Advantages of CNN.....	80
V.6 Model development and implementation of CNN.....	80
V.6.1 Introduction to Teachable Machine.....	80
V.6.2 Target Audience of Teachable Machine.....	80
V.6.3 Working Principle of Teachable Machine.....	81
V.6.4 Initial Steps for Using Teachable Machine.....	81
V.6.5 Saving Projects in Teachable Machine.....	82
V.7 Wildfire detection and prediction using CNN.....	82
V.7.A Fire prediction.....	82
V.7.A.1 Prediction based on historical fire records.....	82
V.7.A.1.1 Data Mining Algorithms.....	83
V.7.A.1.2 Simulated actions.....	84
V.7.A.2 Prediction base of Thermal Data Analysis.....	84
V.7.A.2.1 Monitoring of temperature and humidity.....	86
V.7.A.2.2 Check for fire.....	87
V.7.A.3 Prediction by aerial imaging using drones.....	89
V.7.B Fire detection using machine learning.....	90
V.7.B.1 Preparing the dataset (data segmentation).....	93
V.7.B.2 Experimentation.....	94
V.7.B.3 Results and Discussion.....	95
V.7.C Firefighting using UAV.....	99
V.8 Conculsion.....	101
General conclusion.....	103

Table of contents

References.....106

List of Figures

Chapter I: Unmanned Aerial Vehicles: An Overview

Figure I.1: schema working Principle of Drone.....	08
Figure I.2: Agriculture drone.....	11
Figure I.3: Conservation drone.....	11
Figure I.4: Delivery drone.....	12
Figure I.5: Disaster mitigation drone.....	12
Figure I.6: photography drone.....	13
Figure I.7: Law enforcement drone.....	13
Figure I.8: Real Estate drone.....	14

Chapter II: Modeling of a quadcopter

Figure II.1: Movement around Angles on the Coordinates System because of Force.....	21
Figure II.2: The two frames and their relation.....	22
Figure II.3: The structure of a quadrotor and the relative coordinate systems.....	26
Figure II.4: DC Motor Diagram.....	34
Figure II.5: Motor model.....	34
Figure II.6: Drone model.....	39
Figure II.7: Result simulation in open loop.....	40
Figure II.8: Trajectories 3D in open loop.....	41

Chapter III: Stabilization and control of a quadcopter

Figure III.1: Description of rotational angles.....	45
Figure III.2: Enhanced PID structure.....	49
Figure III.3: Block diagram of the height control.....	50
Figure III.4: Block diagram of the roll control.....	51

Liste of figures

Figure III.5: Block diagram of the pitch control.....	52
Figure III.6: Block diagram of the Yaw control.....	53
Figure III.7: PID control Model	54
Figure III.4: Z (height) &Phi(roll)&Theta (pitch) & Psi (yaw) pid controls Results.....	55
Figure III.5: The final simulation PID result of global in Trajectories 3D.....	56

Chapter IV: Fuzzy control of quadcopter

Figure IV.1: The general structure of a fuzzy controller.....	76
Figure IV.2: Fuzzification into 5 fuzzy subsets.....	77
Figure IV.3: The MAX/MIN Inference Method.....	79
Figure IV.4: Defuzzification by Center of Gravity.....	79
Figure IV.5: Maximum Value Defuzzification Method.....	80
Figure IV.6: Various type of Fuzzy membership functions.....	81
Figure IV.7: controller Z, ϕ , θ , ω , diagram.....	82
Figure IV.8. The numbership functions of the thrust controller: a) error, b) U1.....	85
Figure IV.9. The numbership functions of the Roll controller: a) error, b) U2.....	86
Figure IV.10. The numbership functions of the pitch controller: a) error, b) U3.....	86
Figure IV.11. The numbership functions of the Yaw controller: a) error, b) U4.....	87
Figure IV.12: Fuzzy Controle model.	88
Figure IV.13. Z (height) & Phi (roll)&Theta (pitch) & Psi (yaw) Fuzzy controls Results.....	88
Figure IV.14: Z (height)& Phi(roll)&Theta(pitch)&Psi(yaw)Fuzzy and pid controls Results	89
Figure IV.15: The final simulation Fuzzy result of global in Trajectories 3D.....	90

Chapter V: Firefighting Strategy

Figure V.1: artificiel Neurone	90
Figure V.2: the activation Fonction.....	90

Liste of figures

Figure V.3: Model of a simple (single layer) perceptron.....	93
Figure V.4: Model of a Multilayer perceptron.....	93
Figure V.5: Supervised learning.....	95
Figure V.6: Unsupervised learning.....	95
Figure V.7: The convolutional neural networks.....	95
Figure V.8: Set of neurons (circles) creating the depth of a convolution layer (blue) They are linked to the same receiver field (red).	96
Figure V.9: Pooling with a 2x2 filter and a step of 2.....	96
Figure V.10: The ReLu function.....	79
Figure V.11: Operation of a convolutional neural network.	98
Figure V.12: The main interface of Teachable Machine.....	99
FigureV.13: Start of work	100
Figure V.14: Steps in simulating the dataset	102
Figure V.15: System overview for monitoring forests.....	104
Figure V.15: Temperature and humidity fire modle.....	105
Figure V.16: Heat index.....	105
Figure V.17: Forest affected with fire & forest without fire.....	106
Figure V.18: an overview of convolutional neural network architecture for image classification.....	107
Figure V.19: Ditection fire modle.....	110
Figure V.20: Segmentation of the model data.....	111
Figure V.21: Fire images (Training)	112
Figure V.22: No Fire images (Training)	112
Figure V.23: Examples of Fire and No Fire images (Tasting)	112
Figure V.24: Preparation the dateset.....	113

Liste of figures

Figure V.25: preparation of training data.....	113
Figure V.26: Training dataset.....	114
Figure V.27: Tasting the dataset	114
Figure V.28: Result Tasting 'fire'	115
Figure V.29: Result Tasting 'No fire'.....	115
Figure V.30: Result Tasting 'fire'.....	116
Figure V.31: Export the model.....	116

List of Tables

Chapter II: Modeling of a quadcopter

Table II.1: Physical parameters of the quadrotor.....	38
--	-----------

Chapter III: Stabilization and control of a quadcopter

Table III.1: Parameters of different PID controllers.....	54
--	-----------

Chapter IV: Fuzzy control of quadcopter

Table.IV.1: Inference table with five fuzzy subsets.....	78
---	-----------

Liste of Symbols

AUAV	Autonomous Unmanned Aerial Vehicle
GPS	Global Positioning Systems
PID	Proportionnelle Intégrale Dérivée
AC-DC	Direct Current-Alternating-Curren
UAS	Unmanned Aerial Systems
ESC	Electronic Speed Controller
TBS	Team Black Sheep
MPC	Model predictive control
RL	Reinforcement learning



**General
Introduction**

General introduction

Unmanned aerial vehicles (UAVs) have proliferated widely across various fields and have become highly popular due to their ability to efficiently and accurately execute tasks. One of the most commonly used and relied-upon types of UAVs is the quadcopter, which plays a significant role in diverse areas such as aerial surveillance, reconnaissance, aerial photography, firefighting, and other applications.

Modeling a quadcopter requires a precise understanding of the technical factors and variables that impact its performance. This includes analyzing the quadcopter's characteristics, such as its design, propulsion system, sensors used, motion control and axis, and response to external commands. By accurately representing these factors in mathematical and computational models, the performance of the quadcopter can be evaluated, analyzed, and continuously improved.

After achieving an accurate model of the quadcopter, the next challenge is to achieve stability and effective control. Stability is crucial for a quadcopter as it greatly influences its ability to maintain a stable position in the air and execute specific tasks. Achieving stability requires the use of appropriate and advanced control techniques to guide the quadcopter's movements properly and accurately.

Although the most commonly used control unit is the PID controller, it can sometimes lead to uncertainty and disturbances during flight. One innovative approach to achieve control in a quadcopter is the use of fuzzy control. Fuzzy control technology relies on fuzzy logic and predefined rules to control the system, enabling the quadcopter to effectively and flexibly deal with unexpected changes and challenges in the environment.

Additionally, quadcopters are employed in various practical applications, such as firefighting strategies. Quadcopter aircraft are used for early fire detection and monitoring fire spread, contributing to faster and more effective responses by firefighting crews. Firefighting strategies rely on utilizing quadcopters to quickly and accurately transmit information related to fires and fire-prone areas.

In the aftermath of the recent fires in Tizi Ouzou and the resulting tragedies, loss of life, property, crops, and forests, particularly in light of sudden climate changes and recent years of drought, forest fires pose a significant security, economic, and social problem, not only at the

national level but also globally. Even the extensive capabilities of developed countries are insufficient to combat this perilous phenomenon.

As a promising solution to tackle this issue, our work proposes an integrated set of strategies that utilize drones and artificial intelligence. The first strategy is fire prediction using artificial intelligence (fire area prediction). Artificial intelligence is trained on historical fire data in the region, utilizing maps of previous fires. This enables early prediction of potential fire outbreaks and directs drones to focus on those areas, facilitating more effective intervention. This approach reduces the number of drones required and lowers costs.

The second strategy is early warning and fire detection using drones and artificial intelligence (fire detection). Drones and artificial intelligence are employed for the early detection of fires and precise location identification. This aids in limiting fire spread and enhances the chances of swift extinguishment. Drones operate autonomously within predetermined areas.

The third strategy is firefighting. Upon fire detection, drones are directed to intervene and extinguish the fire in its initial stage before it expands and spreads.

The fourth and final strategy is named DronesRain. In instances where a fire is large and a single drone is unable to extinguish it, this drone invokes the strategy by calling nearby drones, particularly those stationed at the base level, forming a swarm of drones. These drones release dampening material simultaneously, akin to rain, to suppress the fire.

Following the introduction, the first chapter will present some key concepts on UAV systems.

Then, in the second chapter, we will conduct the quadrotor's modeling, including the kinematic and dynamic models.

The third chapter will address the stabilization and trajectory tracking problem using a PID controller.

The fourth chapter will explore fuzzy control as an alternative solution to the same problem.

The final chapter will focus on the firefighting problem based on the proposed strategies.

Lastly, a comprehensive conclusion will present the findings of this work.

Chaptre I:

Unmanned Aerial Vehicles:

An Overview

Unmanned Aerial Vehicles: An Overview

I. Introduction

An unmanned aerial vehicle (UAV), also known as an unmanned aircraft system (UAS) or drone, is an aircraft that operates without a human pilot or crew on board. UAVs can be controlled remotely by a ground-based operator or operate autonomously using pre-programmed flight plans and onboard sensors.

Initially developed for military purposes, UAVs have become an essential tool for military operations, particularly in situations that are considered too dull, unclean, or dangerous for human pilots. However, advancements in control technology and cost reduction have led to the widespread adoption of UAVs in various non-military applications as well.

Drones have found applications in fields such as aerial photography and videography, product delivery, law enforcement, infrastructure inspection, scientific research, and even racing. The versatility and accessibility of UAVs have made them popular tools across different industries.

Among the various types of drones available, quadcopters are indeed one of the most widely used and relevant models today. Quadcopters are multi-rotor drones with four propellers, providing stability, maneuverability, and the ability to hover in place. They are commonly used for aerial photography, videography, recreational flying, and even racing due to their agility and ease of control. [A.Rahuldeo and all.2022].

Since the quadcopter's introduction a few decades ago, more research has been done on the device due to the demand for more maneuverable and hovering aircraft.

The most popular and current drones available today, quadcopters are made simple to build while maintaining their high levels of reliability and maneuverability because to their four-rotor architecture. Since the quadcopter's introduction a few decades ago, more research has been done on the device due to the demand for more maneuverable and hovering aircraft.

The four-rotor architecture of quadcopters ensures their high levels of durability and maneuverability while making them easy to build.

II. Quadcopter

A quadcopter, also referred to as a multirotor, drone, or quadrotor, is a mechanical vehicle with four arms, each equipped with a motor and propeller. While it's possible to have multi copters with different numbers of arms, the quadcopter configuration is the most commonly used. Two rotors spin in an anticlockwise direction, while the other two spin in a clockwise direction. This configuration enables the quadcopter to achieve stability and controlled flight.

Unlike helicopters or fixed-wing aircraft that rely on wings for lift, quadcopters generate lift by using the thrust produced by their propellers. In a helicopter, the main rotor generates lift and also controls pitch and yaw. In contrast, quadcopters depend solely on the propellers for lift generation and maneuverability.

Although the concept of quadcopters dates back to the 1920s and 1930s, early designs faced challenges such as poor performance and high instability, requiring significant pilot input. However, with advancements in electronic technology, including flight control computers, miniaturized processors, brushless motors, batteries, cameras, accelerometers, and GPS systems, flying quadcopters has become more feasible and accessible [CC,Chang, and all. 2016].

The simplicity of the quadcopter design has contributed to its popularity in various fields, particularly in photography and videography. The ability to hover, maneuver in tight spaces, and capture aerial footage from unique perspectives has made quadcopters an invaluable tool for aerial photography and videography enthusiasts and professionals alike.

III. Components of U.A.V. (Quadcopter)

III.1 Quadcopter Frame

The TBS Oblivion is a specific frame used in quadcopters and is known for its strength and durability. The frame's design allows for additional weight and surface area, which can enhance drag and stability during flight.

The framework of a quadcopter serves as a skeleton or structure where all the components are mounted. It helps distribute the drone's center of gravity and provides support

for various components such as motors, flight controller, battery, and other electronics. Quadcopter frames typically have multiple fitting gaps for propellers, with a minimum of three gaps commonly used in drone designs. [J.Bright, and all 2019].

III.2 Motors

Only the use of motors allows the propeller to rotate. As a result, the drone's propulsion thrust is increased. However, the ratio of motors to propellers should be the same.[A. Sanchez ·L. R. García Carrillo. E. Rondon · R. Lozano · O. Garcia.2010] .The motors are positioned in a way that allows the controller to easily rotate them. Because of their rotation, drones may move in a more controlled manner. The motor a drone employs has a direct impact on its effectiveness.

III.3 Electronic Speed Controller (ESC)

The Electronic Speed Controller (ESC) plays a crucial role in controlling the speed of the motors. It is an electronic control board that allows the ground pilot to vary the motor speed, and it also incorporates a dynamic brake function. This device enables the pilot to monitor the drone's altitude by measuring the power consumption of all the motors.

As the drone flies higher, the power stores, such as the battery, may experience depletion due to increased power requirements. Monitoring power consumption can provide valuable information about the drone's performance, battery life, and the potential impact of altitude on power usage. It is important for pilots to carefully consider these factors to ensure safe and efficient drone operation. [H.L. Chan, K. T. Woo, 2015].

III.4 Flight/Board Control

Drones often have a "Return to Home" feature, which allows them to autonomously return to their takeoff position. This feature is typically facilitated by the flight controller board, which keeps a record of the drone's initial location. In addition to the location record,

The flight controller board can also estimate the drone's height by considering factors such as the amount of power consumed by the motors or the barometric pressure sensor readings. These measurements help the flight controller calculate the drone's altitude during flight. [A. Kendall, K.A STOL .2014] by utilizing this information, the drone's autonomous system can guide it back to the takeoff position accurately and safely. The "Return to Home" feature is particularly useful when the drone is operating beyond the line of sight or in case of an emergency.

III.5 Propellers

When propellers rotate at high speeds, they create a pressure differential between the top and bottom surfaces of the blades. This pressure differential is a result of the aerodynamic forces acting on the blades as they move through the air. The difference in air pressure between the top and bottom surfaces of the propellers contributes to the generation of lift. [T.A. Brungarta and all. 2019].

In the case of quadcopters, the propellers create lift by generating a lower air pressure on the top surface compared to the bottom surface. This difference in air pressure helps the drone achieve upward thrust and maintain flight. The design and configuration of the propellers, including factors such as their size, shape, and pitch, affect the efficiency and performance of the drone. By optimizing these factors, drone manufacturers can enhance the lift generated by the propellers and improve the overall flight capabilities of the drone.

III.6 Transmitter

For stable and precise control of a drone, it is common for the transmitter to have multiple channels. A minimum of four channels is typically required, as this allows control over essential drone movements such as throttle (for altitude control), yaw (rotation), pitch (forward and backward movement), and roll (sideways movement).

Additional channels can be utilized for controlling other features or functionalities of the drone, such as camera tilt, auxiliary modes, or advanced flight maneuvers. [K, SA Khuwaja, and all. 2018].

III.7 Batteries, Electronic & Power Distribution

The battery is indeed a crucial component in generating electrical power for the drone. It provides the necessary energy to power the motors, flight controller, camera, and other electronic systems onboard the drone. The cables, or wires, serve as the connections that transfer power from the battery to these components [D, Baek, and all. 2014].

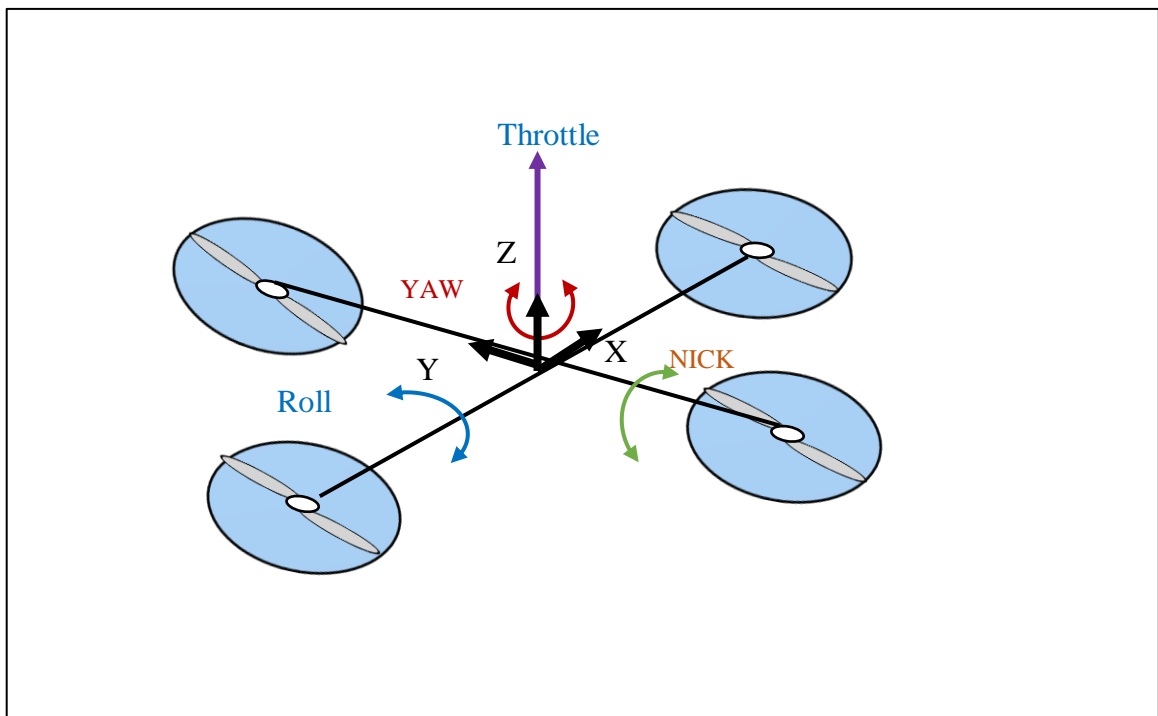
III.8 Camera

Drones equipped with cameras have a wide range of applications, including wedding photography, aerial surveys, cinematography, thermal imaging, surveillance, and many others. Each of these applications may have specific camera requirements, such as image resolution,

sensor type, lens options, stabilization features, and compatibility with the drone's payload capacity.

IV. Forces Acting on U.A.V (Quadcopter)

The principles of flight and how they relate to quadcopter drones In air travel, lift is the upward force that acts perpendicular to the direction of motion. It is generated when there are differences in air pressure, resulting in an upward lift force. [DR, Borah, L., Debnath and M., Gogoi. 2016] Thrust, on the other hand, is the forward force that propels flight machines, including quadcopter drones. Engines generate this thrust force.



FigureI.1: schema working Principle of Drone

Drag is the force that acts in the opposite direction of motion and is caused by factors such as friction and differences in air pressure. It opposes the motion of the quadcopter drone.

Quadcopter drones use rotors that function similarly to wings in generating lift. By rapidly spinning the rotors and pulling air downward, the drone generates the necessary lift to ascend into the air. If the lift force is equal to the force of gravity, the net force is balanced, and the quadcopter remains airborne.

IV.1. Setup for a Drone Flight

Stating that the polarity of rotation is reversed between two adjacent motors in a quadcopter drone, while the same direction of rotation is shared by two opposing motors. This configuration helps to maintain stability and control during flight. In a quadcopter drone, the motors are arranged in a cross-like configuration, with two motors spinning clockwise (e.g., motors 1 and 3) and the other two spinning counterclockwise (e.g., motors 2 and 4). This arrangement creates a balanced distribution of torque. When all the rotors of a quadcopter drone rotate in the same direction, it can generate a net torque that causes the entire drone to rotate as a whole. This would result in instability and hinder the drone's control. To counteract this, the motor rotation directions are configured such that the opposing torques generated by the motors cancel each other out, providing stability and allowing for precise control of the drone's orientation.

IV.2. Taking Off

In stating that to get off the ground, a drone needs a net upward force that exceeds the force of gravity, In order for a drone to achieve lift and take off, the propellers or rotors create a force called thrust. This thrust force is generated by the engines or motors, which create higher air pressures below the drone compared to the force of gravity acting upon it. The resulting pressure difference between the top and bottom surfaces of the rotors generates an upward force known as lift.

IV.3. Moving on

Drones achieve movement and control through various means, including the use of propellers or rotors, which generate lift and thrust. The engines or motors in a drone create the thrust necessary to propel the drone forward, backward, or in other directions.

IV.4. Roll

In a drone or quadcopter, the elevator control surface is not used to turn left or right. The elevator control surface primarily controls the pitch of the drone, which is the up-and-down movement. To turn left or right, a drone typically utilizes a control surface called the aileron. By adjusting the ailerons, the drone can generate differential lift on the wings or rotors, causing it to roll and turn in the desired direction.

IV.5. Voice

To make a drone move straight towards you, the power applied to all the motors should be increased or decreased equally. By increasing the power to all motors, the drone will generate a net-forward force that propels it in the desired direction. Similarly, reducing the power to all motors will slow down or stop the forward movement.

In general, adjusting the power distribution between the motors is not a typical method for controlling the angular pressure or attitude of a drone. The angular pressure or attitude control of a drone is typically achieved through the use of other control surfaces, such as the pitch, roll, and yaw controls. These control surfaces, along with flight control algorithms, are responsible for maintaining the drone's stability and controlling its orientation.

IV.6. Yaw

To make a drone rotate clockwise (yaw), the rotational speed of the motors rotating clockwise should be increased, while the rotational speed of the motors rotating counterclockwise should be decreased. This speed differential creates a torque that causes the drone to rotate in the desired direction.

The elevator control surface is primarily responsible for controlling the pitch of the drone, not yaw. Pitch control is achieved by adjusting the elevator control surface to control the drone's forward or backward tilt.

V. Applications of UAVs

V.1. Agriculture

Drones equipped with various sensors, such as multispectral or thermal cameras, can provide valuable data on crop health, identify areas of concern, and optimize irrigation and fertilizer application. This data can help farmers make informed decisions to improve crop yield and reduce resource waste. [S. Ahirwar and all. 2019]



FigureI.2: Agriculture drone [<https://fr.freepik.com/>]

V.2. Conservation

In addition to monitoring wildlife, drones can be utilized to assess and monitor changes in various ecosystems, such as forests, wetlands, and marine environments. They enable researchers to survey large areas quickly, map habitats, detect deforestation or illegal activities, and monitor changes over time. This data can contribute to a better understanding and management of ecosystems, leading to more targeted conservation efforts .



Figure I.3: Conservation drone [<https://phys.org/news/2020-11-drones.html>]

V.3. Delivery/fulfillment

One of the key advantages of using drones for delivery is their ability to navigate quickly through urban environments and bypass traffic congestion. This can significantly reduce delivery times, especially for time-sensitive items such as food or perishable goods. Drones can take a direct route from the fulfillment center to the destination, avoiding the need to navigate complex road networks. [M.O.Baloola, Ibrahim, and Mas S. Mohktar, 2022]



Figure I.4: Delivery drone [<https://www.rolandberger.com>]

V.4. Disaster mitigation and relief

Drones are also valuable in delivering emergency supplies to remote and inaccessible areas. Traditional means of transportation may be limited or disrupted during emergencies, making it challenging to deliver essential items like medical supplies, food, water, or communication equipment. Drones can overcome these challenges by quickly transporting lightweight payloads over difficult terrain or areas with damaged infrastructure [B. Rabta, C. Wankmüller, and G. Reiner, 2018]. They can navigate obstacles and deliver supplies directly to affected communities, providing life-saving resources in a timely manner.



Figure I.5: Disaster mitigation drone [<https://aerizone.com>]

V.5. Filmmaking and photography

In the world of news reporting, drones have become valuable tools for capturing top news stories from above. News agencies can use drones to quickly deploy aerial cameras to cover events such as natural disasters, protests, or traffic incidents. Drones provide a bird's-eye view of the scene, offering unique perspectives and real-time coverage. This enhances the quality

and depth of news reporting, providing viewers with a more comprehensive understanding of the situation. [S. Maharana. 2017].



Figure I.6: photography drone [<https://www.bhphotovideo.com>]

V.6. Law enforcement

During major public events, such as festivals, parades, or protests, drones can enhance the police presence by providing an aerial perspective and real-time situational awareness. They can be used to monitor crowd movements, identify potential security risks, and assist in maintaining public safety. [E,Brumfield,2014]. Drones equipped with cameras and sensors can quickly survey large areas, monitor traffic flow, and detect any suspicious activities or threats.



Figure I.7: Law enforcement drone [<https://www.istockphoto.com>]

V.7. Real Estate

Real estate agents and property sellers are utilizing drone technology to create captivating virtual tours and promotional materials. Drones can capture aerial views of the property, showcasing its size, layout, and exterior features from different angles. Additionally, drones

can navigate through interior spaces, offering immersive experiences for potential buyers by providing a comprehensive view of each room. [Y,Mohd Yamani, and all.2021].



Figure I.8: Real Estate drone [https://www.boxbrownie.com]

VI.Conclusion

Unmanned aerial vehicles (UAVs) have seen increasing utilization across both military and civilian sectors. These UAVs can be classified into different types based on their size, which can range from ultra-small to medium-sized and large UAVs. Classification criteria such as range, endurance, maximum altitude, and weight are used to differentiate and discuss these UAVs.

The applications of UAVs are diverse and extend to various fields. In the realm of planetary exploration, UAVs have proven to be valuable tools for gathering data and conducting research in remote and challenging environments. They can be used to explore and study areas that are difficult to access by traditional means, aiding in the understanding of celestial bodies and their environments.

Chapter II:

Modeling of a quadcopter

Modeling of a quadcopter

II.1. Introduction

Modeling and simulation are important in research. They code real systems, either by physical reproduction on a smaller scale, Either by mathematical models that explain the dynamics of a system through simulation, you agree to explore the behavior of the system, which may be the case risky in the real world. Modeling is the first job to do develop censorship laws. For the quadricopter, it will represent the kinematic model and the dynamic model the relationship between the aerodynamic forces and the torque generated by the rotation the rotors and a machine, on the other hand, are accelerations (translation and rotation) of a quadricopter block center. We can distinguish two modeling categories,

Euler-Lagrange's method and Newton-Eulaler method

II.2.The principle of quadrotor flight:

The operation of a quadrotor is quite special. By cleverly varying the power of the engines, it is possible to raise it/descend, to tilt it on the left/right (roll) or in front/rear (pitch) or even to rotate it on itself (lacet). The quadrotor has six degrees of freedoms (three rotation movements and three translational movements). [C.Agho.2017] These six degrees should be ordered using only four actuators; So it is a system under activated (the number of inputs is lower than the number of outputs)

The possible movements of the quadrotor are:

- **The vertical movement** (Lift) is obtained from the contribution of the four propellers at the same time.
- **The displacement along the X axis** occurs following a rotation around the Y axis, the latter being created because of the difference in lift of the rotors 1-3 (Pitch θ).

- **The displacement along the Y axis** occurs as a result of a rotation around the X axis, the latter is created because of the difference in lift of the rotors 2-4 (Roll ϕ).
- The yaw movement requires that two rotors of the same axis rotate in one direction while the other two in the other direction (yaw ψ)

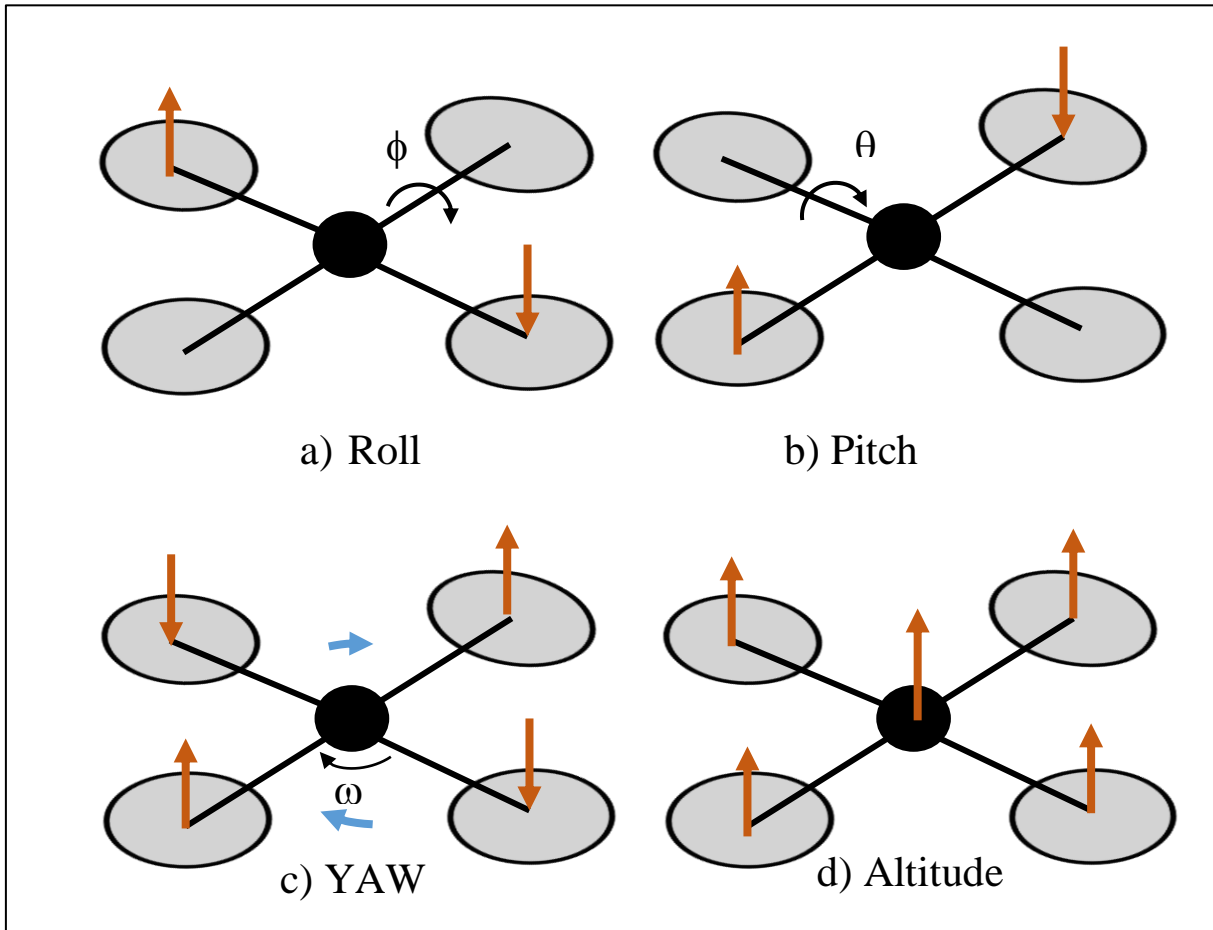


Figure II.1: Movement around Angles on the Coordinates System because of Force

II.2 Kinematics

Kinematics is a branch of mechanics that focuses on the study of motion without considering the forces and torques that cause that motion. It deals with the description and analysis of the position, velocity, and acceleration of objects or systems.

In the context of describing the motion of a body or a system of bodies, there are two commonly used reference frames:

The Earth inertial reference frame (E-frame)

The body-fixed reference frame (B-frame).

The E-frame ($O_E \ X_E \ Y_E \ Z_E$) is chosen as the inertial right-hand reference. X_E points toward the North, Y_E points toward the West, Z_E points upwards respect to the earth and O_E is

the axis origin.[M,Mokhtari.2015] This frame is used to define the linear position (ξ^E [m]) and the angular position (Π^E [rad]) of the quadrotor

The B-frame (O_B X_B Y_B Z_B) is attached to the body. X_B points toward the quadrotor front, Y_B points toward the quadrotor left, Z_B points upwards and O_B is the axis origin. O_B is chosen to coincide with the center of the quadrotor cross structure. This reference is right-hand too. The linear velocity (V^B [$m \ s^{-1}$])the angular velocity(w^E [$rad \ s^{-1}$]), the forces (F^B [N])and the torques (τ^E [$n \ m$])are defined in this frame.

The linear position ξ^E of the helicopter is determined by the coordinates of the vector between the origin of the B-frame and the origin of the E-frame respect to the E-frame according to equation (2.1).

$$\xi^E = (X \ Y \ Z)^T \tag{2.1}$$

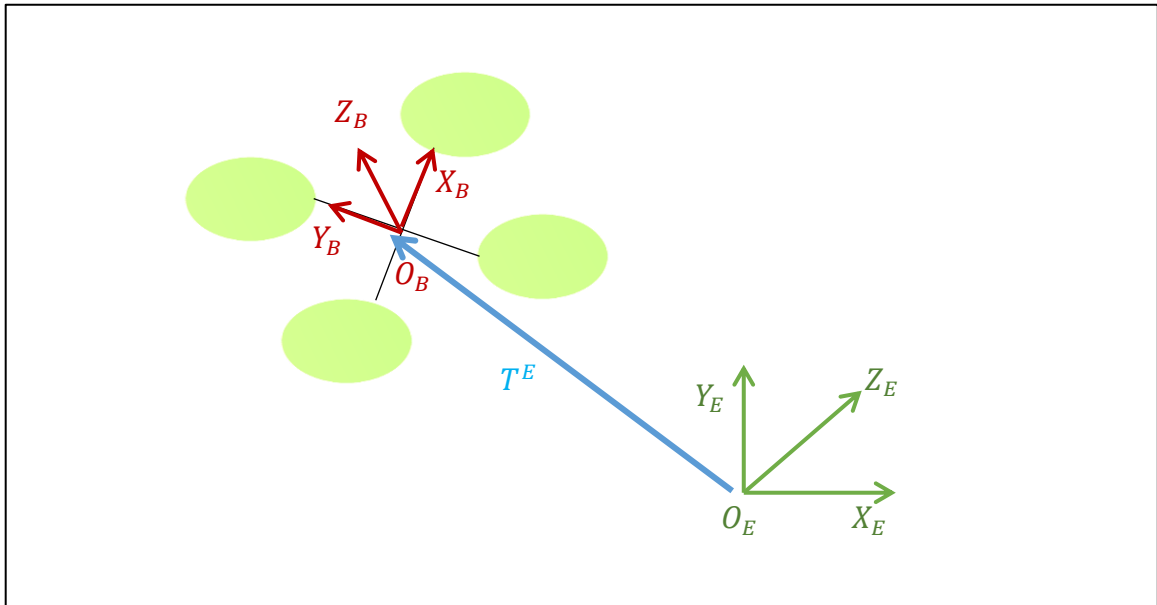


Figure II .2: The two frames and their relation

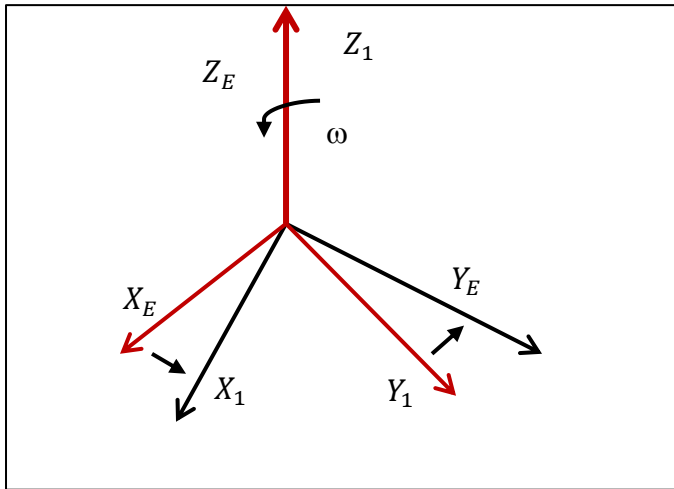
Π^E is the angular position the helicopter is defined by the orientation of the B-frame respect to the E-frame. This is given by three consecutive rotations about the main axes which take the E-frame into the B-frame.

In this work the”roll-pitch-yaw” set of Euler angles were used. Equation (2.2) shows the attitude vector.

$$\Pi^E = (\phi \ \theta \ \omega)^T \tag{2.2}$$

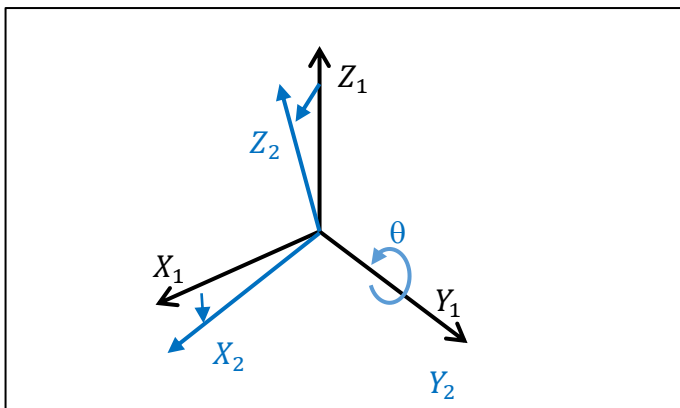
R_{II} [-] The rotation matrix is obtained by post-multiplying the three basic rotation matrices in the following order:

- Rotation about the Z_E axis of the angle ω (yaw) through $R(\omega, z)$ [-].



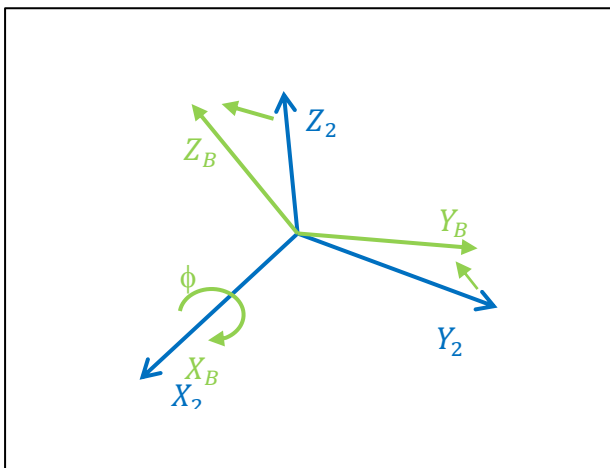
$$R(\omega, z) = \begin{bmatrix} C_\omega & -S_\omega & 0 \\ S_\omega & C_\omega & 0 \\ 0 & 0 & 1 \end{bmatrix} \quad (2.3)$$

- Rotation about the y_1 axis of the angle θ (pitch) through $R(\theta, y)$ [-].



$$R(\theta, y) = \begin{bmatrix} C_\theta & 0 & S_\theta \\ 0 & 1 & 0 \\ -S_\theta & 0 & C_\theta \end{bmatrix} \quad (2.4)$$

- Rotation about the x_2 axis of the angle ϕ (roll) through $R(\phi, x)$ [-].



$$R(\phi, x) = \begin{bmatrix} 1 & 0 & 0 \\ 0 & C_\phi & -S_\phi \\ 0 & S_\phi & C_\phi \end{bmatrix} \quad (2.5)$$

The linear V^B and angular w^B velocities are given in the body-fixed frame, as was previously mentioned. The definitions of their compositions are given by equations (2.7) and (2.8).

$$V^B = [u \quad v \quad w]^T \quad (2.7)$$

$$w^B = [p \quad q \quad r]^T \quad (2.8)$$

It is possible to combine linear and angular quantities to give a complete representation of the body in the space. Two vectors can be thus defined: the generalized velocity v [+] and the generalized position ξ [+]. As reported in equations (2.9) and (2.10).

$$\xi = [I^E \quad \Pi^E] = [x \quad y \quad z \quad \phi \quad \theta \quad \omega]^T \quad (2.9)$$

$$v = [V^B \quad w^B] = [u \quad v \quad w \quad p \quad q \quad r]^T \quad (2.10)$$

The relationship between the linear velocities in the body-fixed frame V^B and the earth frame V^E [$m \quad S^{-1}$] according to equation (2.11), involves the rotation matrix R_{Π} .

$$V^B = \dot{I}^B = R_{\Pi} V^E \quad (2.11)$$

II.2.1. Translation Kinematics

$$\begin{bmatrix} \dot{x} \\ \dot{y} \\ \dot{z} \end{bmatrix} = \begin{bmatrix} C_{\omega}C_{\theta} & -S_{\omega}C_{\phi} + C_{\omega}S_{\theta}S_{\phi} & S_{\omega}S_{\phi} + C_{\omega}S_{\theta}C_{\phi} \\ S_{\omega}C_{\theta} & C_{\omega}C_{\phi} + S_{\omega}S_{\theta}S_{\phi} & -C_{\omega}S_{\phi} + S_{\omega}S_{\theta}C_{\phi} \\ -S_{\theta} & C_{\theta}S_{\phi} & C_{\theta}C_{\phi} \end{bmatrix} \begin{bmatrix} p \\ q \\ r \end{bmatrix} \quad (2.12)$$

Regarding the linear velocity, it is also possible to establish a relationship between the angular velocity in the earth frame (or Euler rates) \dot{I}^E [$rad \quad S^{-1}$] and the angular velocity in the body-fixed frame w^B , thanks to the transfer matrix B_{Π} [-]. Equations (2.13) and (3.14) depict the specified relationship.

$$w^B = T_{II}^{-1} \dot{\Pi}^B \quad (2.13)$$

$$\dot{\Pi}^B = T_{II} w^B \quad (2.14)$$

The transfer matrix T_{II} is determined by resolving the Euler rates $\dot{\Pi}^B$ into the body-fixed frame. Equations (2.15), (2.16), and (2.17) likely represent the specific equations or relationships used to calculate the components of the transfer matrix.

$$\begin{bmatrix} p \\ q \\ r \end{bmatrix} = \begin{bmatrix} \dot{\phi} \\ 0 \\ 0 \end{bmatrix} + \mathbf{R}(\phi, x)^{-1} \begin{bmatrix} 0 \\ \dot{\theta} \\ 0 \end{bmatrix} + \mathbf{R}(\phi, x)^{-1} \mathbf{R}(\theta, y)^{-1} \begin{bmatrix} 0 \\ 0 \\ \dot{\omega} \end{bmatrix} = T_{II}^{-1} \begin{bmatrix} \dot{\phi} \\ \dot{\theta} \\ \dot{\omega} \end{bmatrix} \quad (2.15)$$

$$T_{II}^{-1} = \begin{bmatrix} 1 & 0 & -S_{\theta} \\ 0 & C_{\phi} & C_{\theta} S_{\phi} \\ 0 & -S_{\phi} & C_{\theta} C_{\phi} \end{bmatrix} \quad (2.16)$$

$$T_{II} = \begin{bmatrix} 1 & S_{\phi} t_{\theta} & C_{\phi} t_{\theta} \\ 0 & C_{\phi} & -S_{\phi} \\ 0 & -S_{\phi}/C_{\theta} & C_{\phi}/C_{\theta} \end{bmatrix} \quad (2.17)$$

It is possible to describe equations (2.11) and (2.14) in just one equivalence which relate the derivate of the generalized position in the earth frame $\dot{\xi}^+$ to the generalized velocity in the body frame v . The transformation is possible thanks to the generalized matrix J_{II}^- . In this matrix, the notation $0_{3 \times 3}$ means a sub-matrix with dimension 3 times 3 filled with all zeros. Equations (2.18) and (2.19) show the relation described above.

$$\dot{\xi} = J_{II} v \quad (2.18)$$

$$J_{II} = \begin{bmatrix} R_{II} & 0_{3 \times 3} \\ 0_{3 \times 3} & T_{II} \end{bmatrix} \quad (2.19)$$

II.2.2 Rotation Kinematics

$$\begin{bmatrix} \dot{\phi} \\ \dot{\theta} \\ \dot{\omega} \end{bmatrix} = \begin{bmatrix} 1 & t_{\theta}S_{\phi} & t_{\theta}C_{\phi} \\ 0 & C_{\phi} & -S_{\phi} \\ 0 & S_{\phi}/C_{\theta} & C_{\phi}/C_{\theta} \end{bmatrix} \begin{bmatrix} p \\ q \\ r \end{bmatrix} \quad (2.20)$$

II.3 Dynamics:

Dynamics is indeed a branch of mechanics that focuses on studying the effects of forces and torques on the motion of a body or a system of bodies. It seeks to understand how these forces and torques influence the acceleration, velocity, and position of objects.

In the context of analyzing the motion of a rigid body with six degrees of freedom (6 DOF), various techniques can be employed to derive the equations that describe its dynamics. One commonly used formulation is the Newton-Euler formulation.

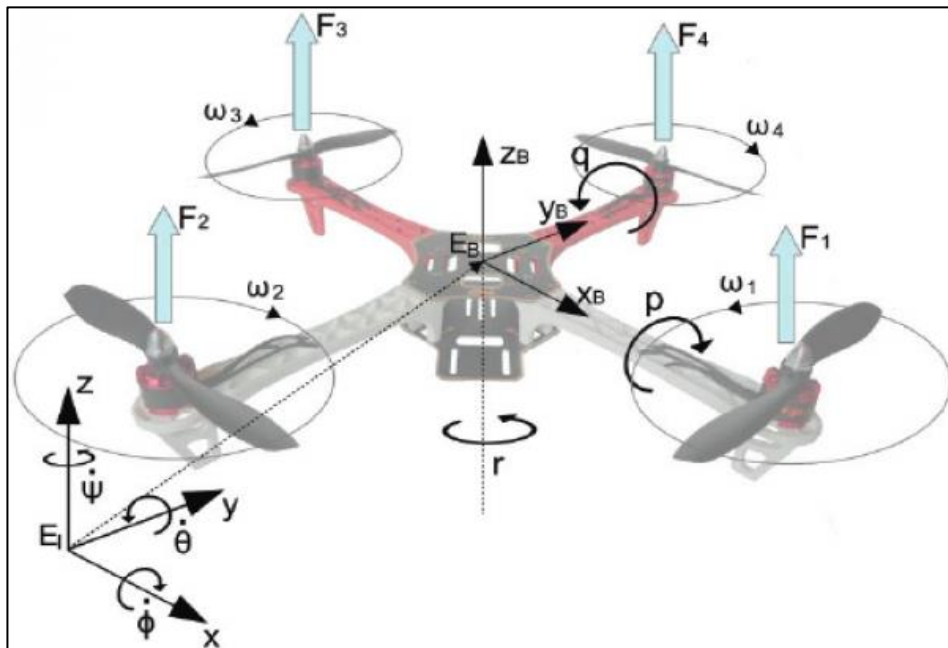


Figure.II.3: The structure of a quadrotor and the relative coordinate systems

III.3.1. Newton-Euler:

In the context of the dynamics of a generic 6 DOF rigid body, the dynamics equations typically take into account the mass of the body m [kg] and its inertia matrix I [$N \ m \ S^2$].

The inertia matrix represents the distribution of mass and moments of inertia of the body around its principal axes.

The dynamics of the rigid body is described by the following equation :

$$\begin{bmatrix} m \mathbf{I}_{3 \times 3} & \mathbf{0}_{3 \times 3} \\ \mathbf{0}_{3 \times 3} & \mathbf{I}_{3 \times 3} \end{bmatrix} \begin{bmatrix} \dot{V}^B \\ \dot{W}^B \end{bmatrix} + \begin{bmatrix} W^B \times (m V^B) \\ W^B \times (I W^B) \end{bmatrix} = \begin{bmatrix} F^B \\ \tau^B \end{bmatrix} \quad (2.21)$$

Equation (2.21) can be used to define a generalized force vector Λ .

$$\Lambda = [F^B \quad \tau^B]^T = [F_x \quad F_y \quad F_z \quad \tau_x \quad \tau_y \quad \tau_z]^T \quad (2.22)$$

Therefore it is possible to rewrite equation (2.22) in a matrix form

$$M_B \dot{v} + C_B(v)v = \Lambda \quad (2.23)$$

Where \dot{v} is the generalized acceleration vector WRT B-frame. M_B is the system inertia matrix and $C_B(v)$ is the Coriolis-centripetal matrix, both WRT B-frame. [T.B.2016] Equation (2.24) shows the system inertia matrix.

$$M_B = \begin{bmatrix} m \mathbf{I}_{3 \times 3} & \mathbf{0}_{3 \times 3} \\ \mathbf{0}_{3 \times 3} & \mathbf{I}_{3 \times 3} \end{bmatrix} = \begin{bmatrix} m & 0 & 0 & 0 & 0 & 0 \\ 0 & m & 0 & 0 & 0 & 0 \\ 0 & 0 & m & 0 & 0 & 0 \\ 0 & 0 & 0 & I_{XX} & 0 & 0 \\ 0 & 0 & 0 & 0 & I_{YY} & 0 \\ 0 & 0 & 0 & 0 & 0 & I_{ZZ} \end{bmatrix} \quad (2.24)$$

Given the aforementioned presumptions, it is clear that M_B is diagonal and constant. The Coriolis-centripetal matrix is shown in equation (2.25).

$$C_B(v) = \begin{bmatrix} \mathbf{0}_{3 \times 3} & -m\mathcal{S}(V^B) \\ \mathbf{0}_{3 \times 3} & -\mathcal{S}(I W^B) \end{bmatrix} = \begin{bmatrix} 0 & 0 & 0 & 0 & m w & -m v \\ 0 & 0 & 0 & -m w & 0 & m u \\ 0 & 0 & 0 & m v & -m u & 0 \\ 0 & 0 & 0 & 0 & I_{ZZ} r & -I_{YY} q \\ 0 & 0 & 0 & -I_{ZZ} r & 0 & I_{XX} p \\ 0 & 0 & 0 & I_{YY} q & -I_{XX} p & 0 \end{bmatrix} \quad (2.25)$$

The skew-symmetric operator $\mathcal{S}(\cdot)$ has been used in the previous equation. Equation (2.26) defines the skew-symmetric matrix of the k ($\mathcal{S}(k)$) for a generic three-dimensional vector k .

$$\mathcal{S}(k) = -\mathcal{S}^T(k) = \begin{bmatrix} 0 & -k_3 & k_1 \\ k_3 & 0 & -k_1 \\ -k_2 & k_1 & 0 \end{bmatrix} \quad k = \begin{bmatrix} k_1 \\ k_2 \\ k_3 \end{bmatrix} \quad (2.26)$$

Equation (2.23) is completely universal and applicable to any stiff body that follows the previously stated assumptions (or simplifications). The last vector, however, offers special information on the dynamics of the quadrotor helicopter because it was employed in this work to simulate the device. can be broken down into three parts based on the type of the quadrotor contributions.

The gravitational vector $G_B(\xi)$ [+] derived from the acceleration owing to gravity g [$m \ S^{-2}$] is the initial contribution. Since it is a force rather than a torque, it is simple to realize that it only influences the linear equations and not the angular equations. The adjustments to obtain $G_B(\xi)$ are shown in Equation (2.27).

$$G_B(\xi) = \begin{bmatrix} F_G^B \\ 0_{3 \times 1} \end{bmatrix} = \begin{bmatrix} R_{II}^{-1} F_G^E \\ 0_{3 \times 1} \end{bmatrix} = \begin{bmatrix} R_{II}^{-1} \begin{bmatrix} 0 \\ 0 \\ -mg \end{bmatrix} \\ 0_{3 \times 1} \end{bmatrix} = \begin{bmatrix} m g S_\theta \\ -m g C_\theta S_\phi \\ -m g C_\theta S_\phi \\ 0 \\ 0 \\ 0 \end{bmatrix} \quad (2.27)$$

Where the gravitational force vector F_G^B [N] is the one in the WRT B-frame and the one in the WRT E-frame is F_G^E [N] . Three zeros make up the vertical vector $0_{3 \times 1}$ [-] . The fact that R_{II} is an orthogonal normalized matrix means that its inverted R_{II}^{-1} is equivalent to the transposed R_{II}^T .

The second component accounts for the gyroscopic effects caused by the rotation of the propeller. When the algebraic sum of the rotor speeds is not zero, there is an overall imbalance since two of them rotate clockwise and the other two counterclockwise. According to equation (2.28), the quadrotor feels a gyroscopic torque if the roll or pitch rates are also vary from zero.

$$O_B(\nu) \Omega = \begin{bmatrix} 0_{3 \times 1} \\ -\sum_{k=1}^4 J_{TP} \begin{pmatrix} 0_{3 \times 1} \\ w^{B \times} \begin{bmatrix} 0 \\ 0 \\ 1 \end{bmatrix} \end{pmatrix} (-1)^k \Omega^k \end{bmatrix} = \begin{bmatrix} 0_{3 \times 1} \\ J_{TP} \begin{bmatrix} -q \\ p \\ 0 \end{bmatrix} \Omega \end{bmatrix} = J_{TP} \begin{bmatrix} 0 & 0 & 0 & 0 \\ 0 & 0 & 0 & 0 \\ 0 & 0 & 0 & 0 \\ q & -q & q & -q \\ -p & p & -p & p \\ 0 & 0 & 0 & 0 \end{bmatrix} \Omega \quad (2.28)$$

The gyroscopic propeller matrix is $O_B(\nu)$ [+], and J_{TP} [$N \ m \ S^{-2}$] is calculated in the following section as the entire rotating moment of inertia around the propeller axis. It is clear that the gyroscopic effects caused by propeller rotation only pertain to angular not linear equations.

The overall propeller speed Ω [$rad\ S^{-1}$] and the propeller speed vector Ω [$rad\ S^{-1}$] used in equation (2.28) are defined in equation (2.29).

$$\Omega = -\Omega_1 + \Omega_2 - \Omega_3 + \Omega_4 \quad \Omega = \begin{bmatrix} \Omega_1 \\ \Omega_2 \\ \Omega_3 \\ \Omega_4 \end{bmatrix} \quad (2.29)$$

Where Ω_1 [$rad\ S^{-1}$] represents the speed of the front propeller, Ω_2 [$rad\ S^{-1}$] represents the speed of the right propeller, and Ω_3 [$rad\ S^{-1}$] represents the speed of the back propeller. The speed of the left propeller is Ω_4 [$rad\ S^{-1}$]

The third contribution accounts for the pressures and torques that the primary movement inputs directly produce. It derives from an aerodynamics analysis that forces and torques are related to the squared propellers' speed. In order to obtain the movement vector $U_B(\Omega)$ [+], the movement matrix E_B [+] is multiplied by Ω^2 . The calculation of the aerodynamic contributions, including the thrust and drag factors (thrust b [$N\ S^2$] and drag d [$N\ m\ S^2$] factors).

Equation (2.30), demonstrates how the quadrotor helicopter dynamics are affected by the movement vector.

$$U_B(\Omega) = E_B \Omega^2 = \begin{bmatrix} 0 \\ 0 \\ U_1 \\ U_2 \\ U_3 \\ U_4 \end{bmatrix} = \begin{bmatrix} 0 \\ 0 \\ b(\Omega_1^2 + \Omega_2^2 + \Omega_3^2 + \Omega_4^2) \\ b l(\Omega_4^2 - \Omega_2^2) \\ b l(\Omega_3^2 - \Omega_1^2) \\ d(\Omega_2^2 + \Omega_4^2 - \Omega_3^2 + \Omega_1^2) \end{bmatrix} \quad (2.30)$$

Where l [m] is the distance between the center of the quadrotor and the center of a propeller. U_1, U_2, U_3 and U_4 , are the movement vector components introduced in the previous section. Their relation with the propellers' speeds comes from aerodynamic calculus. The expression of the torque produced by U_4 has been simplified by neglecting its $\dot{\Omega}$ component. Therefore all the movements have a similar expression and are easier to control.

As stated before (and shown in the previous equation), it is possible to identify a constant matrix E_B which multiplied by the squared propellers' speed Ω_2 produces the movement vector $U_B(\Omega)$. Equation (2.31) shows the movement matrix.

$$E_B = \begin{bmatrix} 0 & 0 & 0 & 0 \\ 0 & 0 & 0 & 0 \\ b & b & b & b \\ 0 & -b l & 0 & b l \\ -b l & 0 & b l & 0 \\ -d & d & -d & d \end{bmatrix} \quad (2.31)$$

From equation (2.23), it is possible to describe the quadrotor dynamics considering these last three contributions according to equation (2.32)

$$M_B \dot{v} + C_B(v) v = G_B(\xi) + O_B(v) \Omega + E_B \Omega^2 \quad (2.32)$$

The derivate of the generalized velocity vector WRT B-frame \dot{v} can be isolated by rearranging equation (2.32).

$$\dot{v} = M_B^{-1}(-C_B(v) v + G_B(\xi) + O_B(v) \Omega + E_B \Omega^2) \quad (2.33)$$

Equation (2.34) demonstrates the preceding expression as a system of equations rather than a matrix form.

$$\left\{ \begin{array}{l} \dot{u} = (v r - w q) + g S_\theta \\ \dot{v} = (w p - u r) - g C_\theta S_\phi \\ \dot{w} = (u q - v p) - g C_\theta S_\phi + \frac{U_1}{m} \\ \dot{p} = \frac{I_{YY} - I_{ZZ}}{I_{XX}} q r - \frac{J_{TP}}{I_{XX}} q \Omega + \frac{U_2}{m} \\ \dot{q} = \frac{I_{ZZ} - I_{XX}}{I_{YY}} p r - \frac{J_{TP}}{I_{YY}} p \Omega + \frac{U_3}{m} \\ \dot{r} = \frac{I_{XX} - I_{YY}}{I_{ZZ}} p q + \frac{U_4}{m} \end{array} \right. \quad (2.34)$$

Where equation (2.35) is used to provide the propellers' speed inputs.

$$\begin{cases} U_1 = b (\Omega_1^2 + \Omega_2^2 + \Omega_3^2 + \Omega_4^2) \\ U_2 = b l (-\Omega_2^2 + \Omega_4^2) \\ U_3 = b l (-\Omega_1^2 + \Omega_3^2) \\ U_4 = d (-\Omega_1^2 + \Omega_2^2 - \Omega_3^2 + \Omega_4^2) \\ \Omega = -\Omega_1 + \Omega_2 - \Omega_3 + \Omega_4 \end{cases} \quad (2.35)$$

The quadrotor dynamic system in equation (2.34) is written in the bodyfixed frame. As stated before, this reference is widely used in 6 DOF rigidbody equations. However in this case it can be useful to express the dynamics with respect to a hybrid system composed of linear equations WRT E-frame and angular equations WTR B-frame. Therefore the following equations will be expressed in the new "hybrid" frame called H-frame. This new reference is adopted because it's easy to express the dynamics combined with the control (in particular for the vertical position in the earth inertial frame). Equation (2.36)

Shows the quadrotor generalized velocity vector WRT H-frame (ζ [+]).

$$\xi = [j^E \quad w^B]^T = [\dot{X} \quad \dot{Y} \quad \dot{Z} \quad p \quad q \quad r]^T \quad (2.36)$$

The dynamics of the system in the H-frame can be rewritten in a matrix form according to equation (2.37).

$$M_H \dot{\xi} + C_H(\zeta) \xi = G_B(\zeta) + O_H(\zeta) \Omega + E_H(\xi) \Omega^2 \quad (2.37)$$

Where $\dot{\xi}$ [+] the quadrotor is generalized acceleration vector WRT H-frame. It now follows the definitions of all the matrices and vectors used in equation (2.37). The system inertia matrix WRT H-frame M_H [+] is equal to that one WRT B-frame and defined according to equations (2.24) and (2.38)

$$M_H = M_B = \begin{bmatrix} m \mathbf{I}_{3 \times 3} & \mathbf{0}_{3 \times 3} \\ \mathbf{0}_{3 \times 3} & \mathbf{I}_{3 \times 3} \end{bmatrix} = \begin{bmatrix} m & 0 & 0 & 0 & 0 & 0 \\ 0 & m & 0 & 0 & 0 & 0 \\ 0 & 0 & m & 0 & 0 & 0 \\ 0 & 0 & 0 & I_{XX} & 0 & 0 \\ 0 & 0 & 0 & 0 & I_{YY} & 0 \\ 0 & 0 & 0 & 0 & 0 & I_{ZZ} \end{bmatrix} \quad (2.38)$$

The Coriolis-centripetal matrix WRT H-frame $C_H(\zeta)$ [+] on the other hand is not equivalent to that particular WRT B-frame and determined by equation (2.39).

$$C_H(\zeta) = \begin{bmatrix} 0_{3 \times 3} & 0_{3 \times 3} \\ 0_{3 \times 3} & -S(I \mathbf{w}^B) \end{bmatrix} = \begin{bmatrix} 0 & 0 & 0 & 0 & 0 & 0 \\ 0 & 0 & 0 & 0 & 0 & 0 \\ 0 & 0 & 0 & 0 & 0 & 0 \\ 0 & 0 & 0 & 0 & I_{ZZ} r & -I_{YY} q \\ 0 & 0 & 0 & -I_{ZZ} r & 0 & I_{XX} p \\ 0 & 0 & 0 & -I_{YY} q & -I_{XX} p & 0 \end{bmatrix} \quad (2.39)$$

Equation (2.40) gives the definition of the gravitational vector WRT the H-frame G_H [+]. As can be observed, it affects all three linear equations as opposed to just the third in the prior scenario.

$$G_H = \begin{bmatrix} F_G^E \\ 0_{3 \times 1} \end{bmatrix} = \begin{bmatrix} 0 \\ 0 \\ -m g \\ 0 \\ 0 \\ 0 \end{bmatrix} \quad (2.40)$$

Equation (2.38) defines the gravitational vector WRT H-frame G_H [+]. It is clear that this time, rather than only the third linear equation as in the prior instance, it impacts all three of them.

$$O_H(\zeta) \Omega = O_B(\nu) \Omega = \begin{bmatrix} 0_{3 \times 1} \\ J_{TP} \begin{bmatrix} -q \\ p \\ 0 \end{bmatrix} \Omega \end{bmatrix} = J_{TP} \begin{bmatrix} 0 & 0 & 0 & 0 \\ 0 & 0 & 0 & 0 \\ 0 & 0 & 0 & 0 \\ q & -q & q & -q \\ -p & p & -p & p \\ 0 & 0 & 0 & 0 \end{bmatrix} \Omega \quad (2.41)$$

The input U_1 impacts all three linear equations via the rotation matrix R_{II} , hence the movement matrix WRT H-frame $E_H(\zeta)$ [+] differs from that in the B-frame. Equation (2.42) displays the product of the movement matrix and the squared propellers' speed vector.

$$E_H(\zeta) \Omega^2 = \begin{bmatrix} R_{II} & 0_{3 \times 3} \\ 0_{3 \times 3} & I_{3 \times 3} \end{bmatrix} E_B \Omega^2 = \begin{bmatrix} (S_\omega S_\phi + C_\omega S_\theta C_\phi) U_1 \\ (-C_\omega S_\phi + S_\omega S_\theta C_\phi) U_1 \\ (C_\theta C_\phi) U_1 \\ U_2 \\ U_3 \\ U_4 \end{bmatrix} \quad (2.42)$$

The derivate of the generalized velocity vector WRT H-frame $\dot{\zeta}[+]$. can be isolated by rearranging equation (2.37).

$$\dot{\zeta} = M_H^{-1} \left(-C_H(\zeta)\zeta + G_H + O_H(\zeta) \Omega + E_H(\zeta) \Omega^2 \right) \quad (2.43)$$

Equation (2.44) demonstrates the preceding expression as a system of equations rather than a matrix form.

$$\left\{ \begin{array}{l} \ddot{X} = (\sin \omega \sin \phi + \cos \omega \sin \theta \cos \phi) \frac{U_1}{m} \\ \ddot{Y} = (-\cos \omega \sin \phi + \sin \omega \sin \theta \cos \phi) \frac{U_1}{m} \\ \ddot{Z} = -g + (\cos \theta \cos \phi) \frac{U_1}{m} \\ \dot{p} = \frac{I_{YY} - I_{ZZ}}{I_{XX}} q r - \frac{J_{TP}}{I_{XX}} q \Omega + \frac{U_2}{m} \\ \dot{q} = \frac{I_{ZZ} - I_{XX}}{I_{YY}} p r - \frac{J_{TP}}{I_{YY}} p \Omega + \frac{U_3}{m} \\ \dot{r} = \frac{I_{XX} - I_{YY}}{I_{ZZ}} p q + \frac{U_4}{m} \end{array} \right. \quad (2.44)$$

The system in equation (2.44) will be simplified and utilized extensively in the Control algorithms chapter, where the propellers' speed inputs are the same as in the system WRT B frame and given by equation (2.35). Additionally, using the kinematics, the angular equations will be connected to angular fixed references.

II.4 DC-motor

A DC motor is an electromechanical device that converts electrical energy into mechanical energy through the interaction of magnetic fields. It consists of two essential components: the rotor and the stator.

The rotor is the rotating part of the motor, while the stator is the stationary part [T, Bresciani.2008]. The rotor contains copper windings that are arranged in groups and connected in series. These windings are externally accessible through a component called a commutator.

The stator, on the other hand, houses two or more permanent magnets that create a magnetic field. This magnetic field interacts with the rotor and generates a force that causes the rotor to rotate.

To operate the DC motor, a direct current (DC) is supplied to the windings. The flow of current through the windings creates an electromagnetic field. The interaction between this electromagnetic field and the magnetic field of the stator produces a torque, which causes the rotor to rotate.

The design of the rotor and the commutator ensures continuous rotation of the motor when a DC voltage is applied to its terminals. The commutator allows the direction of the current in the windings to be reversed at the appropriate time, ensuring smooth and continuous rotation

Overall, a DC motor is an efficient and widely used actuator that converts electrical energy into mechanical motion, making it suitable for various applications in industries such as robotics, automation, and transportation.

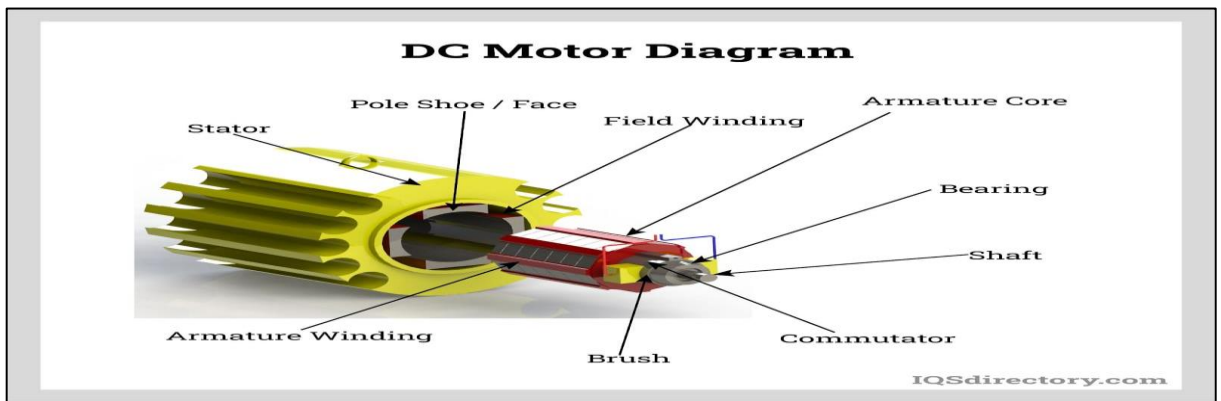


Figure II.4: DC Motor Diagram [<https://www.iqsdirectory.com>]

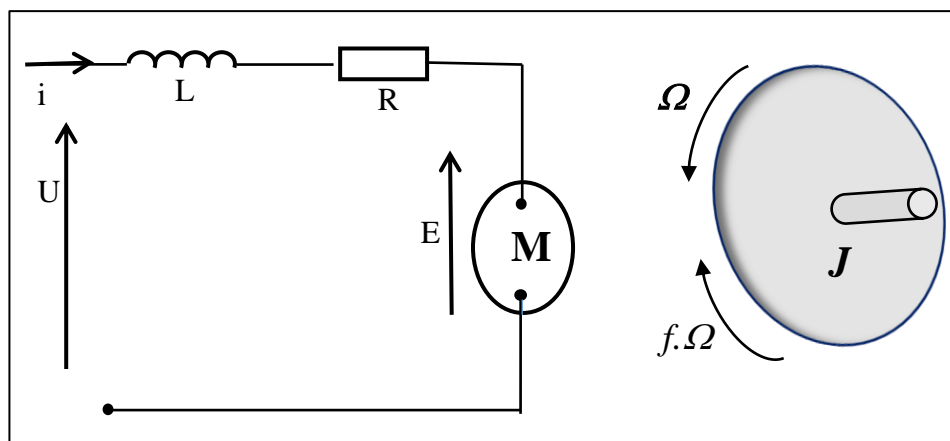


Figure II.5: Motor model

Equation (2.45). Is obtained by employing the Kirchhoff's voltage law.

$$u = u_R + u_L + e \tag{2.45}$$

Where the voltage across the resistor R is $u_R [v]$ and the voltage across the inductor L is $u_L [v]$. It is possible to rewrite equation (2.46) as the following one.

$$u = R i + L \frac{\partial i}{\partial t} + K_E w_M \quad (2.46)$$

The motor constant $K_E [v \ s \ rad^{-1}]$ is also known as the motor constant, and the angular speed of the motor is represented as $w_M [rad \ s^{-1}]$. Ohm's law has been used to modify the initial addend.

The first uses the inductor differential equation, $u_R = R i$ and the second, $u_L = L \frac{\partial i}{\partial t}$. The final component of equation (2.46) demonstrates the relationship between mechanics and electricity.

The dynamics of the motor is described by the following equation.

$$J_{TM} \dot{w}_M = T_M - T_L \quad (2.47)$$

Electrical current i through is inversely correlated with motor torque T_M

$$K_M [N \ m \ A^{-1}]: T_M = K_M i .$$

As a result, equation (2.47) can be revised using equation (2.49).

$$J_{TM} \dot{w}_M = k_M i - T_L \quad (2.48)$$

By connecting equations (2.46) and (2.48) a differential equation in w_M can be derived.

$$J_{TM} \dot{w}_M = -\frac{K_E K_M}{R} w_M - T_L + \frac{K_M}{R} u \quad (2.49)$$

The two constants K_E and K_M share the same value despite the fact that the units of measurement are different. The mechanic $P_M [N \ m \ S^{-1}]$ and electric $P_E [W]$ are the sources of this discrepancy. Balance of power

$$P_E = P_M = \left\{ \begin{array}{l} P_E = e i = K_E i w_M \\ P_M = T_M w_M = K_M i w_M \end{array} \right\} \Rightarrow K_E = K_M \quad (2.50)$$

The reduction ratio of the gearbox, $N [-]$, is equal to the product of the motor speed w_M and the propeller speed w_P : $N = \frac{w_M}{w_P}$ can also be calculated as the difference between the number of teeth on the motor gear and the number of teeth on the propeller gear. The

conversion efficiency η [-] of the gear box, which connects the mechanical force of the motor axis P_M to the propeller axis one P_P [$N \cdot m \cdot s^{-1}$], is another parameter.

$$\begin{aligned} P_M \eta &= P_P \\ \omega_M T_{P_M} \eta &= \omega_P T_{M_P} \end{aligned} \quad (2.51)$$

Consequently, the following steps can be used to determine the dynamics of the gear box system:

$$J_M \dot{\omega}_M = T_M - T_{P_M} \quad (2.52)$$

$$J_P \dot{\omega}_P = T_{M_P} - T_P \quad (2.53)$$

In any case $\dot{\omega}_P$ [$rad \cdot s^{-1}$] is the angular acceleration of the propeller. With equations (2.52) and (2.53) in mind, equation (2.51) can be rewritten as follows.

$$\begin{aligned} \omega_M (T_M - J_M \dot{\omega}_M) \eta &= \omega_P (T_M - J_P \dot{\omega}_P) \\ &\vdots \\ \left(J_M + \frac{J_P}{\eta N^2} \right) \omega_M &= T_M - \frac{T_P}{\eta N^2} \end{aligned} \quad (2.54)$$

In equation (2.54) the following two substitutions were done.

$$\dot{\omega}_P = \frac{\omega_P}{\omega_M} \dot{\omega}_M \quad \text{AND} \quad \frac{\omega_P}{\omega_M} = N$$

Equation (2.54) is crucial since it shares the same structure as equation (2.49). The real values of the load torque T_L and the total motor moment of inertia J_{TM} can be determined in accordance with equations (2.55) and (2.56) by comparing the two equations.

$$T_L = \frac{T_P}{\eta N^2} \quad (2.55)$$

$$J_{TM} = J_M + \frac{J_P}{\eta N^2} \quad (2.56)$$

Geometric, dynamic, and aerodynamic analyses of the mechanism can be used to calculate the parameters in equations (2.55) and (2.56).

$$T_P = d w_p^2 = \frac{d w_M^2}{N^2} \quad (2.57)$$

Where the aerodynamic drag factor, $d [N \ m \ s^2]$, is present. It is possible to get the final load torque expression from equations (2.55) and (2.57)

$$T_L = \frac{d w_M^2}{\eta N^3} \quad (2.58)$$

Equations (2.49) can be rewritten according to equations (2.56) and (2.58).

$$\left(J_M + \frac{J_P}{\eta N^2} \right) \dot{w}_M = - \frac{K_E K_M}{R} w_M - \frac{d}{\eta N^3} w_M^2 + \frac{K_M}{R} u \quad (2.59)$$

The propeller axis (rather than the motor axis) can be used to rewrite all of the previous equations. Therefore, the following differential equation can also be used to simulate the motor system.

$$\left(J_P + \eta N^2 J_M \right) \dot{w}_P = - \frac{K_E K_M}{R} \eta N^2 w_P - d w_P^2 + \frac{K_M}{R} \eta N u \quad (2.60)$$

According to equation (2.61), the \dot{w}_P coefficient is equal to the total rotational moment of inertia about the propeller axis ($J_{TP} [N \ m \ s^2]$).

$$J_{TP} = J_P + \eta N^2 J_M \quad (2.61)$$

A suitable strategy is to linearize the differential equation (2.60) around its working point because it is nonlinear. It has been decided to derive equation (2.62) using the first order Taylor series approach.

$$\dot{w}_P = A_P w_P + B_P u + C_P \quad (2.62)$$

The linearized propeller speed coefficient is represented in the preceding equation by $A_P [rad \ s^{-1}]$, the linearized input voltage coefficient is represented by $B_P [rad^2 \ s^{-2} \ V^{-1}]$ and the linearized constant coefficient is represented by $C_P [rad^2 \ s^{-2}]$. Equations (2.63), (2.64), and (2.65) define their values. [T.Bresciani,2008]

$$A_P = \left. \frac{\partial \dot{w}_P}{\partial w_P} \right|_{w_P = w_H} = -\frac{K_E K_M \eta N^2}{J_{TPR}} - \frac{2d}{J_{TP}} w_H = -22. [rad \ s^{-1}] \quad (2.63)$$

$$B_P = \left. \frac{\partial \dot{w}_P}{\partial u} \right|_{w_P = w_H} = \frac{K_M \eta N}{J_{TPR}} = 514 [rad^2 \ s^{-2} \ V^{-1}] \quad (2.64)$$

$$C_P = (\dot{w}_P - (A_P w_P + B_P u)) \left. \frac{d}{J_{TP}} w_H^2 \right|_{w_P = w_H} = 494 [rad^2 \ s^{-2}] \quad (2.65)$$

As a result, the dynamics of all four motor systems may be described using just these three parameters. The differential equation can be seen in matrix form in equation (2.66).

$$\dot{\Omega} = A_P \Omega + B_P u + C_P \quad (2.66)$$

Where u [V] is the input voltage vector, $\Omega [rad \ s^{-1}]$ is the propellers' speed vector, and $\dot{\Omega} [rad \ s^{-2}]$ is their acceleration vector.

II.6 Simulation Values

The following table represents the values used during the simulation of the system dynamics in Matlab-Simulink:

Parameters	Description	Value	Unit
d	drag factor	1.1×10^{-6}	$(N \ m \ s^2)$
l	center of quadrotor	0.24	(m)
m	mass of the quadrotor	1	(kg)
b	thrust factor	54.2×10^{-6}	$(N \ s^2)$
g	acceleration due to gravity	9.8	$(m \ s^{-2})$
I_{XX}	body moment of inertia around the x-axis	8.1×10^{-3}	$(N \ m \ s^2)$
I_{YY}	body moment of inertia around	8.1×10^{-3}	$(N \ m \ s^2)$

	the y-axis		
I_{ZZ}	body moment of inertia around the Z-axis	14.2×10^{-3}	$(N m s^2)$
J_{TP}	total rotational moment of inertia	104×10^{-6}	$(N m s^2)$
L	Motor inductance	15×10^{-6}	(H)
R	Motor resistance	0.6	(Ω)
K_E	Electric motor constant	6.3×10^{-3}	$(V s rad^{-1})$
J_R	rotor rotational moment of inertia	1.08×10^{-6}	$(N m s^2)$
C_P	linearized constant coefficient	494	$(rad^2 s^{-2})$
B_P	linearized input voltage coefficient	514	$(rad^2 s^{-2} V^{-1})$
A_P	linearized propeller's speed coefficient	-22.7	$(rad s^{-1})$

Table II.1:Physical parameters of the quadrotor

II.7. Matlab-Simulink

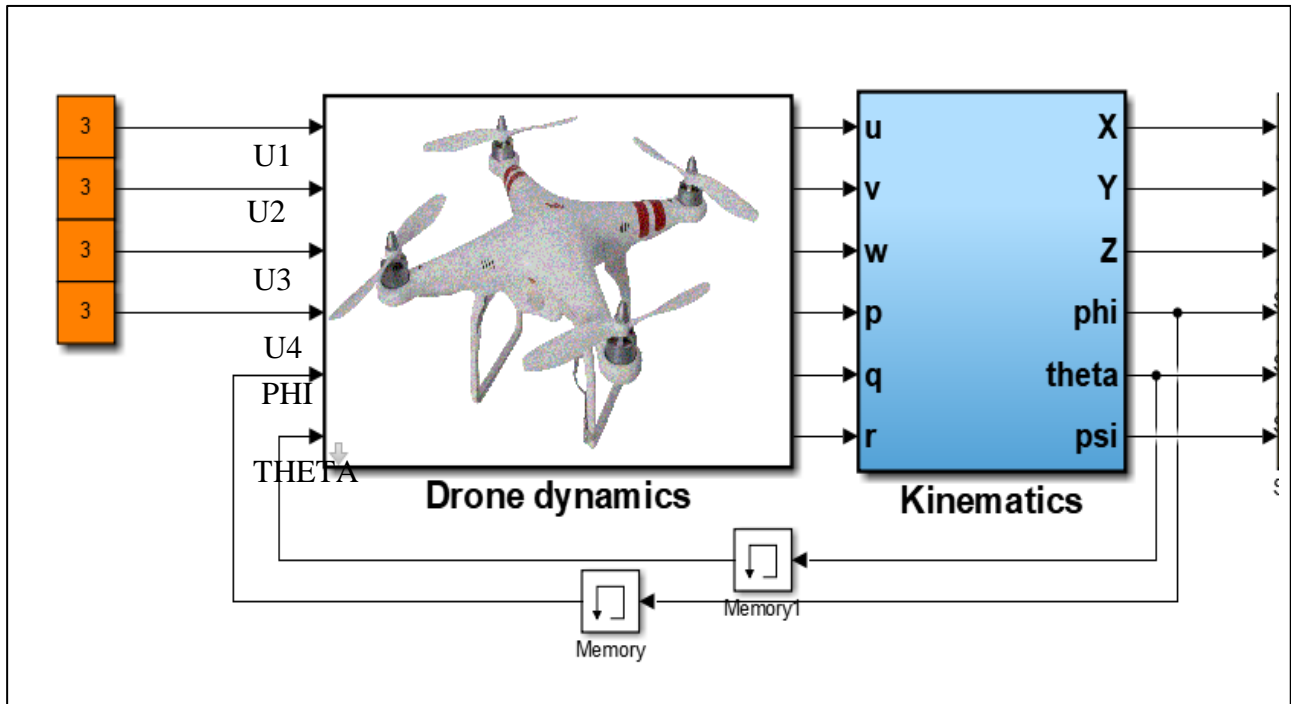


Figure II.6: Drone Model

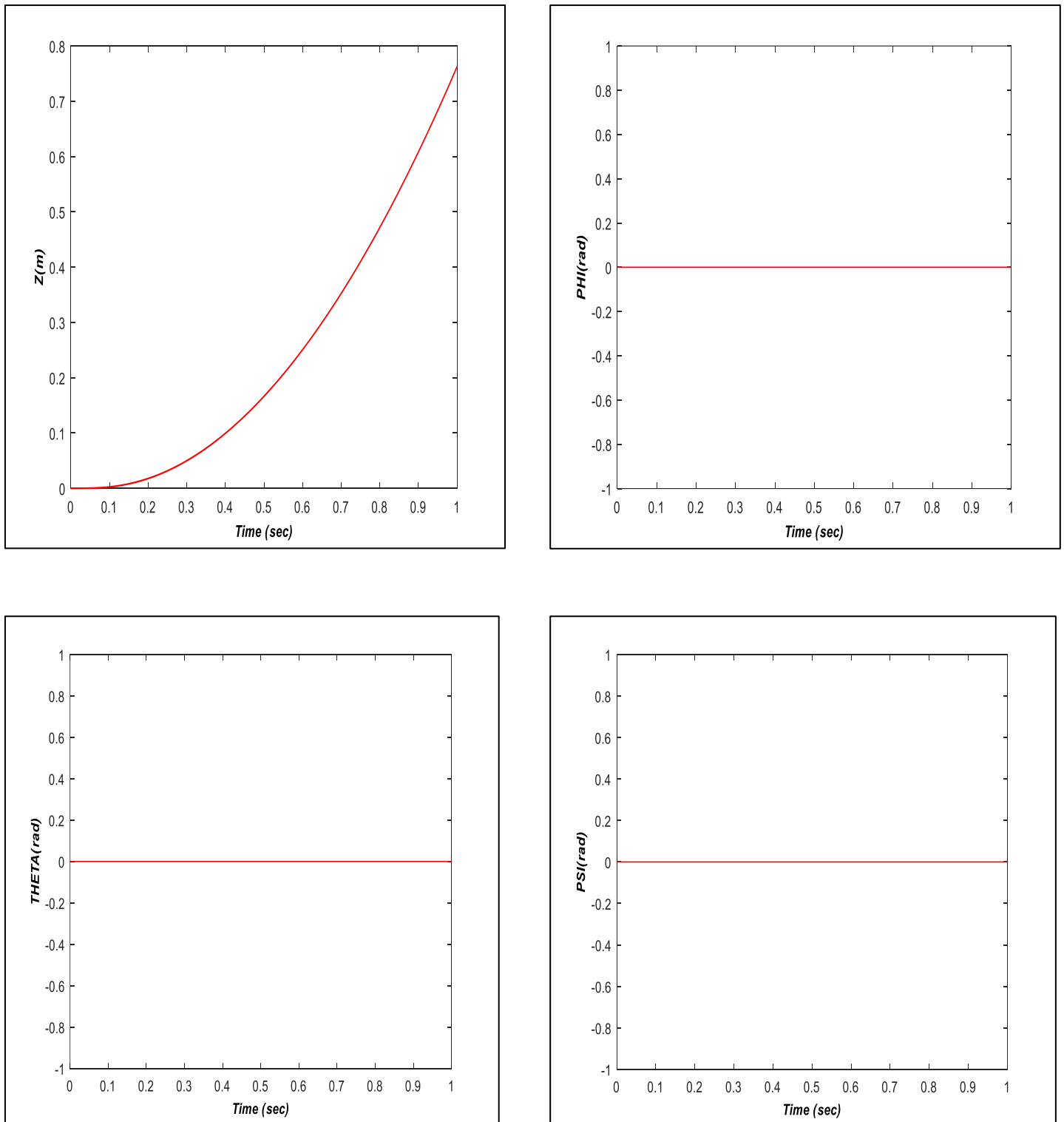


Figure II.7: Result simulation in open loop

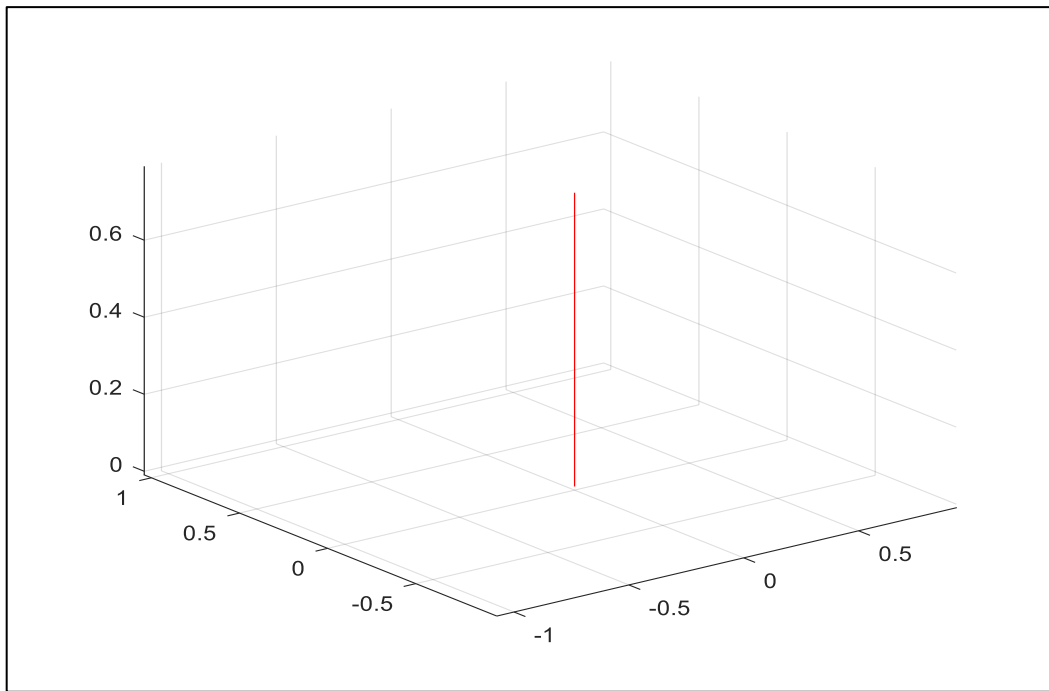


Figure II.9: Trajectories 3D in open loop

II.8. Conclusion

In this chapter, our objective was to present a comprehensive modeling approach for a quadrotor. We began by providing a general overview of how a quadrotor functions and the various maneuvers it can perform during flight. Subsequently, we defined the physical factors that influence quadrotor flight. Finally, we introduced a mathematical model that describes the quadrotor's dynamics based on the Newton-Euler formalism, represented in a state model.

Through this modeling process, we concluded that the quadrotor is a nonlinear and underactuated system with significant interdependencies among its states. In the upcoming chapter, we will proceed with the implementation of a Proportional-Integral-Derivative (PID) control for the quadrotor.

The upcoming chapter will focus on designing the PID controller, which will be responsible for monitoring the quadrotor's states and generating suitable control signals to stabilize the flight and track the desired trajectories.

Chapter III:

**Stabilization and control
of a quadcopter**

Stabilization and control of a quadcopter

III.1 Introduction

It is crucial to construct a control system to regulate how the quadcopter operates.

Since closed loop control records the output rather than the input, it is preferred for all designs and the dynamic model of the quadcopter uses an open loop.

Adapts its output to a desired situation. We require four controllers that are made to act as input to the quadcopter's model in order to successfully navigate the machine. If this were a real quadcopter, the four controllers reflect the transmitter's four inputs. They are inputs for the throttle, roll, pitch, and yaw. The altitude controller or translational controller in the z axis can be used to express and refer to the throttle coming from the transmitter. Roll, pitch, and yaw input from the transmitter is what is referred to as a rotational controller because it depends on the angle,. Because the rotational subsystem is under-actuated, the translational subsystem of the model is partially dependent on it.

The X and Y axes are the dependent axes on the translational controller. Therefore, a controller that accepts desired X and Y values and generates an angular desired output that would be supplied to a rotating controller must be created. Small angle approximation would be used to linearize the dynamic model of the system for the quadrotor's PID controller.

III.2 Trajectory

A good controller should be able to find a location where the yaw, pitch, and roll angles are stable and constant [Satla _Z, Elajrami_M , Bendine_K.2018].

By applying the Pythagoras Theorem and the aforementioned presumptions and cancellations:

1. The quadrotor is regarded as having a symmetrical structure and a constant mass.
2. The vehicle's inertia matrix (I) is quite modest and should be disregarded.
3. The center of gravity and the center of mass are identical.
4. The square of the propeller's speed determines how much thrust there is.

The entire process is shown in **(Figure III.2)** and is based on the presumption that the drone serves as a material point whose rotational angles can be determined using a desired position. Angles (Roll, Pitch, and Yaw) that are desired

$$\phi_d = \tan^{-1}(Z_d/Y_d) \quad (3.1)$$

$$\theta_d = \sin^{-1}\left(X_d/\sqrt{Z_d^2 + X_d^2}\right). \quad (3.2)$$

$$\omega_d = \cos^{-1}\left(Y_d/\sqrt{X_d^2 + Y_d^2 + Z_d^2}\right) \quad (3.3)$$

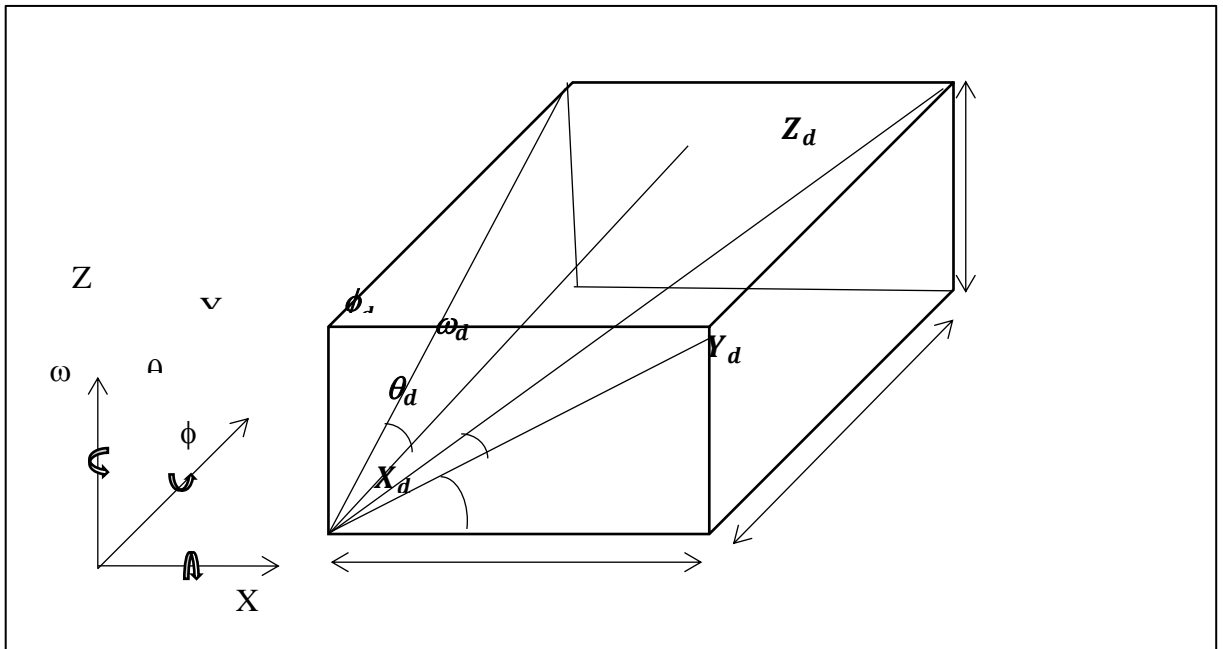


Figure III.1: Description of rotational angles.

Figure III.1 depicts the roll, pitch, and yaw angles as the quadrotor moves. This graphic demonstrates how to develop a very good tracking of the desired angles to improve position. In order to calculate rotational angles in this stage, we created a cube with an inertial frame that took into account each instantaneous position. The dimensions of this cube fluctuate at each instant, thus in order to account for blockage cases, we used the critical value of the pitch angle, which is $\theta < \pi/2$.

III.3 Control modeling:

The previous chapter provides a thorough description of the quadrotor's dynamics.

However, equations (3.4), (3.5), and (3.6) provide concise summaries of the most crucial ideas. [T_Bresciani.2008], The first one displays the quadrotor's acceleration as described in

The instructions given for basic movement.

$$\left\{ \begin{array}{l} \ddot{X} = (\sin \omega \sin \phi + \cos \omega \sin \theta \cos \phi) \frac{U_1}{m} \\ \ddot{Y} = (-\cos \omega \sin \phi + \sin \omega \sin \theta \cos \phi) \frac{U_1}{m} \\ \ddot{Z} = -g + (\cos \theta \cos \phi) \frac{U_1}{m} \\ \dot{p} = \frac{I_{YY} - I_{ZZ}}{I_{XX}} q r - \frac{J_{TP}}{I_{XX}} q \Omega + \frac{U_2}{m} \\ \dot{q} = \frac{I_{ZZ} - I_{XX}}{I_{YY}} p r - \frac{J_{TP}}{I_{YY}} p \Omega + \frac{U_3}{m} \\ \dot{r} = \frac{I_{XX} - I_{YY}}{I_{ZZ}} p q + \frac{U_4}{m} \end{array} \right. \quad (3.4)$$

The second set of equations illustrates how the fundamental motions relate to the squared speed of the propellers.

$$\left\{ \begin{array}{l} U_1 = b (\Omega_1^2 + \Omega_2^2 + \Omega_3^2 + \Omega_4^2) \\ U_2 = b l (-\Omega_2^2 + \Omega_4^2) \\ U_3 = b l (-\Omega_1^2 + \Omega_3^2) \\ U_4 = d (-\Omega_1^2 + \Omega_2^2 - \Omega_3^2 + \Omega_4^2) \\ \Omega = -\Omega_1 + \Omega_2 - \Omega_3 + \Omega_4 \end{array} \right. \quad (3.5)$$

The third equation demonstrates the relationship between propeller speed and motor voltage while accounting for the dynamics of the motors.

$$\left(J_p + \eta N^2 J_M \right) \dot{\Omega} = - \frac{K_E K_M}{R} \eta N^2 \Omega - d \Omega^2 + \frac{K_M}{R} \eta N u \quad (3.6)$$

This method makes it (theoretically) possible to calculate the quadrotor position by twice integrating its linear and angular accelerations. Only the internal state and the four motor voltages must be controlled in order to complete this procedure Direct dynamics and direct kinematics are other names for this method. The correct signals are sent to the propellers using the entire control system.

There can only be four variables controlled in the loop because there are only four of them. The decision to stabilize the project has been made from the beginning.

Height and attitude (Euler angles). The equations that explain the X and Y positions have been removed in accordance with this decision.

The quadrotor dynamics employed in the control are shown in equation (3.7).

$$\left\{ \begin{array}{l} \ddot{Z} = -g + (\cos \theta \cos \phi) \frac{U_1}{m} \\ \ddot{\phi} = \frac{U_2}{I_{XX}} \\ \ddot{\theta} = \frac{U_3}{I_{YY}} \\ \ddot{\omega} = \frac{U_4}{I_{ZZ}} \end{array} \right. \quad (3.7)$$

III.4 PID controller

A proportional-integral-derivative (PID) controller is a feedback control loop mechanism. As the name suggests, the PID algorithm consists of three basic coefficients: proportional, integral, and derivative, which are varied to achieve an optimal response using the values of the constants KP, KD, and KI. KP depends on the current errors, KI depends on the accumulation of past errors, and KD is a prediction of future errors [R,BAHAZ.2020]. They provide control signals that are proportional to the error between the reference signal and the actual output (proportional action), the integral of the error (integral action), and the derivative of the error. The control input used to control the position and angle of the drone with respect to the reference input was designed as follows:

$$\mathbf{u}(t) = \mathbf{k}_p \mathbf{e}(t) + \mathbf{k}_i \int \mathbf{e}(t) dt + \mathbf{k}_d \dot{\mathbf{e}}(t). \quad (3.8)$$

\mathbf{k}_p : is the proportional gain.

\mathbf{k}_i : is the integral gain.

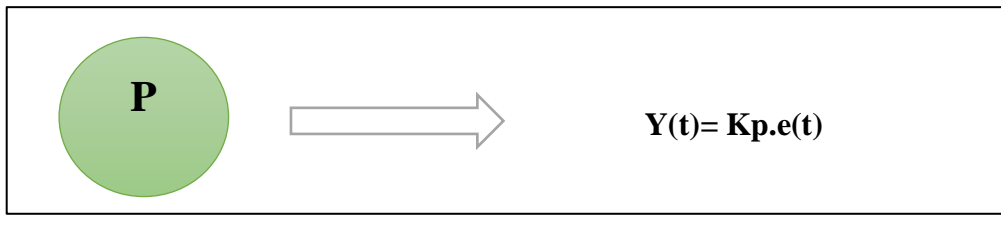
\mathbf{k}_d : is the derivation gain.

The PID controller is based on three main blocks, and we need to know the role of each block.

III.3.1 Role of Proportional Action (P)

The purpose of proportional action is to quicken the measurement's reaction, which lowers the measurement's deviation from the setpoint. According to research on proportional action in a naturally stable closed-loop system, the steady-state approaches a residual deviation during a setpoint change. [D. Dubois].

Forme:

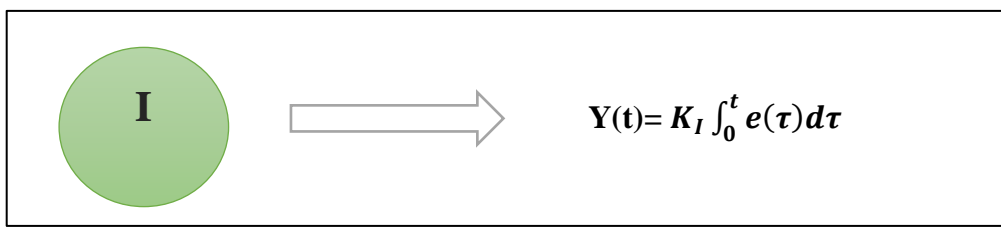


$$Y(t) = K_p \cdot e(t) \quad (3.9)$$

III.3.2 Role of Integral Action (I)

Integral action has the responsibility of removing the difference between the measurement and the set point. In integral-only mode, the controller's output signal is proportional to the measurement-setpoint error's integral. With the help of this controller's integrator, the open-loop transfer function gains a zero pole. [D. Dubois].

Forme:

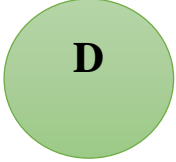


$$Y(t) = K_I \int_0^t e(\tau) d\tau \quad (3.10)$$

III.3.3 Role of Derivative Action (D)

By figuring out the error's slope and dividing it by the derivative gain K_d , the process error's derivative may be derived. The derivative term reduces the controller output's rate of change. A derivative control, K_d , will improve transient response, decrease overshoot, and increase system stability.

Forme:



→

$$Y(t) = K_d \frac{de(t)}{dt}$$

(3.11)

III.5. Controller Synthesis

The objective of a control system is to endow the system with certain properties.

- The stability of the controlled system
- The quality of the transient response (speed, overshoot)
- The precision in steady-state
- The robustness (stability margins, disturbance rejection)
- The response time

III.5.1 The design of a PID controller

Shows the enhanced PID structure:

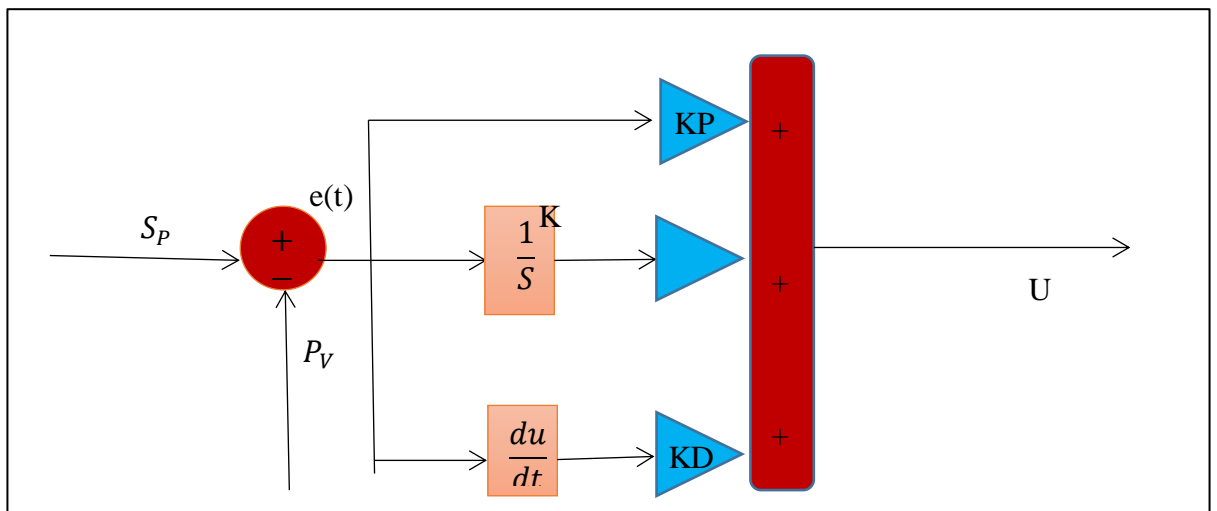


Figure III .2: Enhanced PID structure

With error can be formulated as:

$$e(t) = S_p - P_V(t) \quad (3.12)$$

S_p : is the setpoint or desired position

$P_V(t)$: is the process variable at instantaneous time according to S_p

III.5.2. Height control:

$$u_z = k_p(Z_d - Z) + k_i \int_0^t (Z_d - Z) + k_d \frac{d(Z_d - Z)}{dt} \quad (3.13)$$

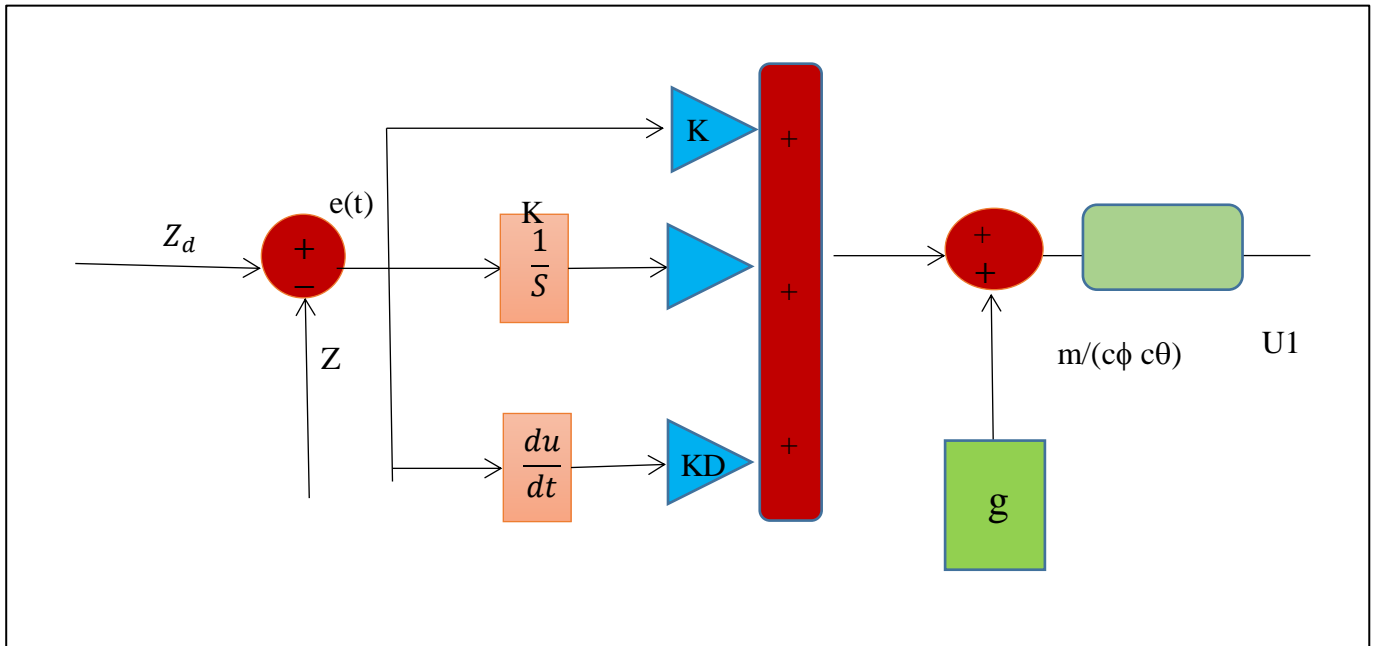


Figure III.3: Block diagram of the height control

Z_d represents the desired height, Z is the height measured e (m) is the height error and U_1 is the required thrust. Along with k_p , k_i and k_d are gains for coordinate position from PID controllers.

The following equations describe how the orientation angles are controlled.

III.5.3. Roll control

$$u_\phi = k_p(\phi_d - \phi) + k_i \int_0^t (\phi_d - \phi) + k_d \frac{d(\phi_d - \phi)}{dt} \quad (3.14)$$

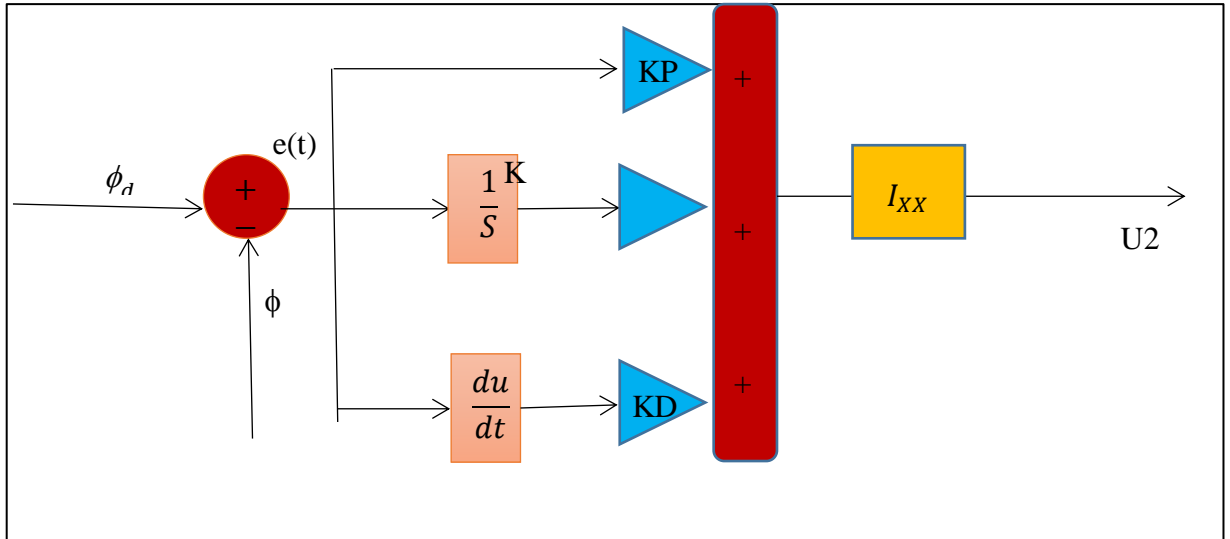


Figure III.4: Block diagram of the roll control

ϕ_d [rad] Represents the desired roll angle, ϕ [rad] is the measured roll angle e_ϕ [rad] is the roll error and $U2$ [N m] is the required roll torque

III.5.4. Pitch control

$$u_{\theta} = k_p(\theta_d - \theta) + k_i \int_0^t (\theta_d - \theta) + k_d \frac{d(\theta_d - \theta)}{dt} \quad (3.15)$$

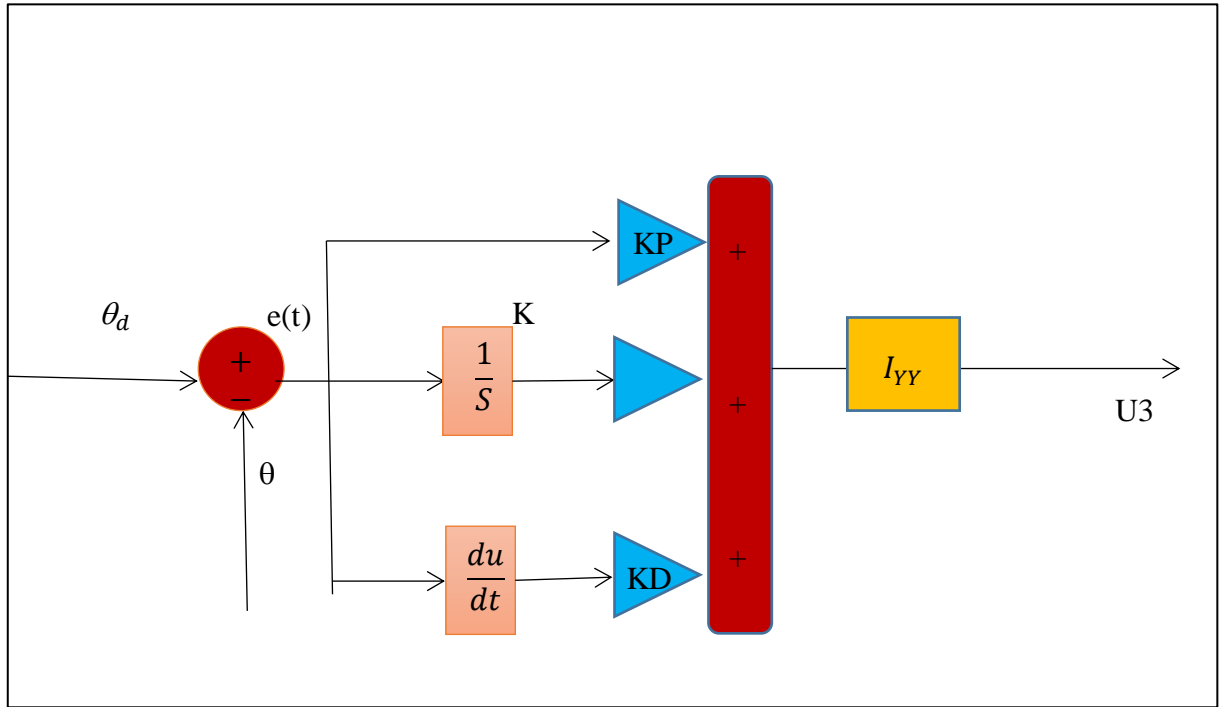


Figure III.5: Block diagram of the pitch control

$\theta_d [rad]$ Represents the desired pitch angle, $\theta [rad]$ is the measured pitch angle, $e_{\theta} [rad]$ is the pitch error and $U3 [N \cdot m]$ is the required pitch torque.

III.5.5. Yaw control

$$u_\omega = k_p(\omega_d - \omega) + k_i \int_0^t (\omega_d - \omega) + k_d \frac{d(\omega_d - \omega)}{dt} \quad (3.16)$$

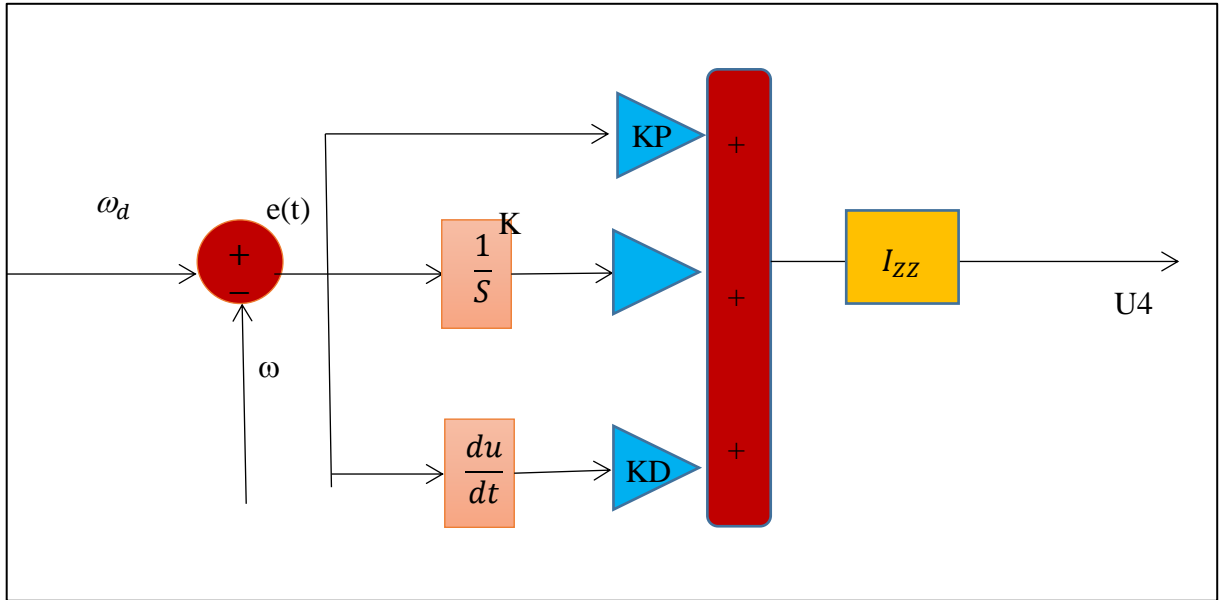


Figure III.6: Block diagram of the Yaw control

ω [rad] Represents the desired yaw angle, ω_d [rad] represents the desired yaw angle, e_ω [rad] is the yaw error and $U4$ [N m] is the required yaw torque.

k_p , k_i and k_d are the PID controller's parameters for controlling Roll, Pitch, and Yaw, angles.

III.6 MATLAB Simulink model

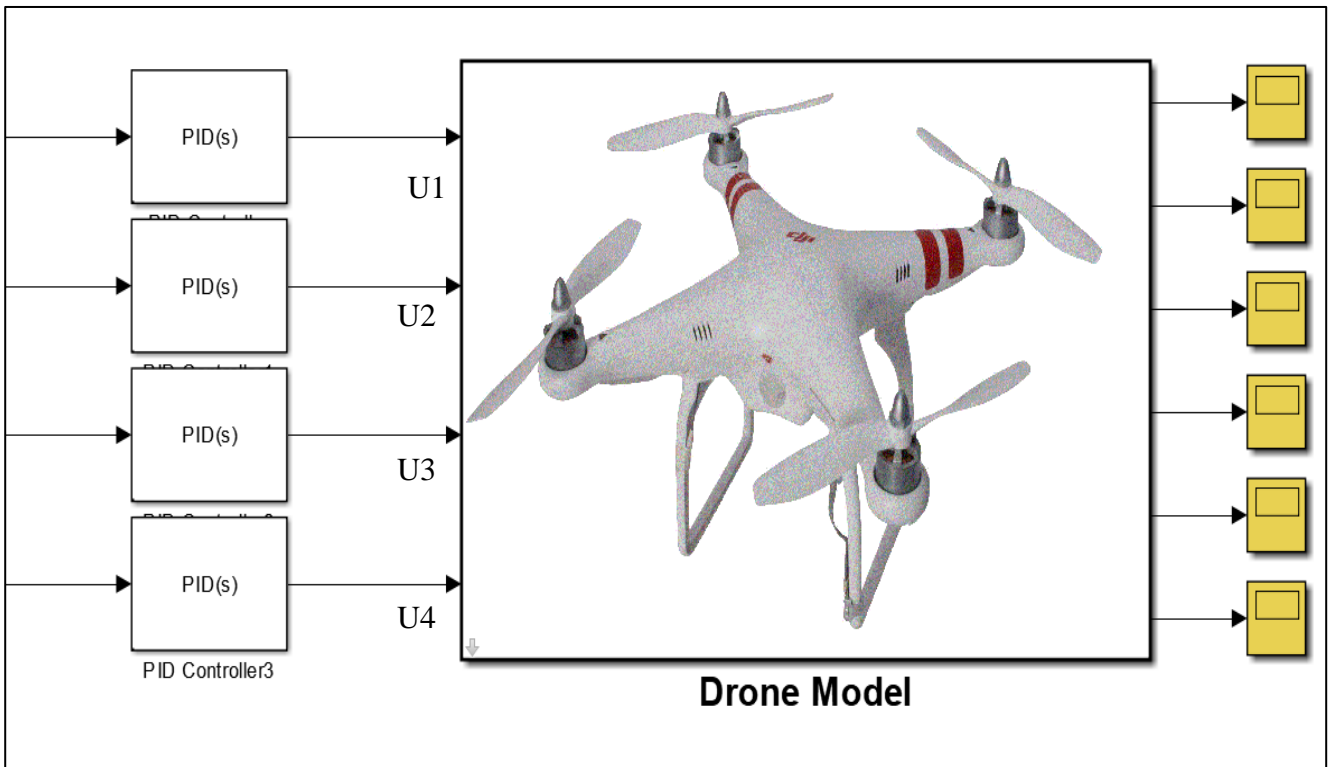


Figure III.6: PID Control Model

Initial Parameter Selection:

We have determined initial parameters that ensure a certain level of stability. These parameters are summarized in the following table:

	Z	PHI	Theta	Psi
P	40	0.05	0.05	0.05
D	10	0.1	0.1	0.1

Table III.1: Parameters of different PD controllers

III.7 Simulation result:

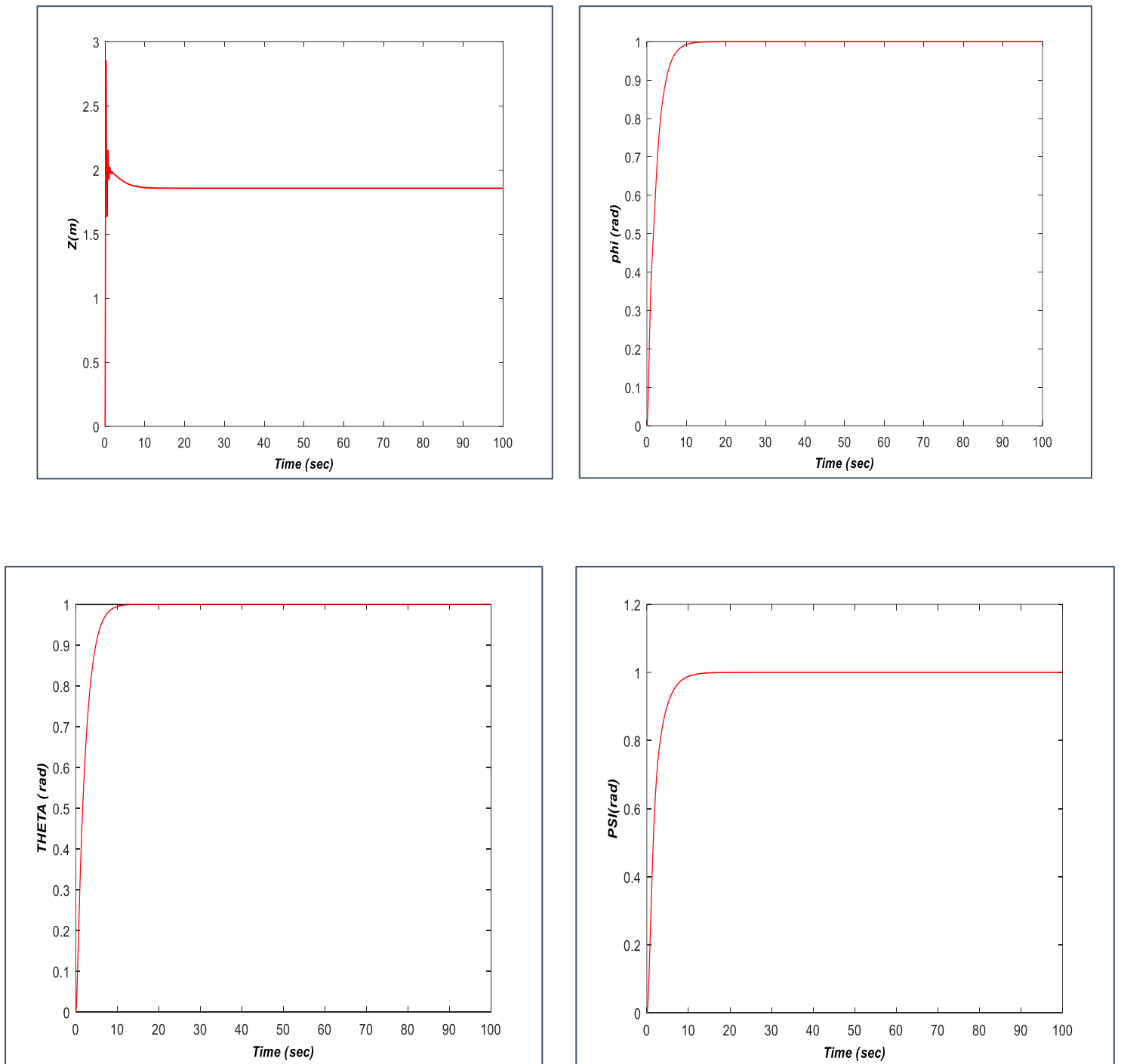


Figure III.4: Z (height) & Phi (roll) & Theta (pitch) & Psi (yaw) pid controls Results

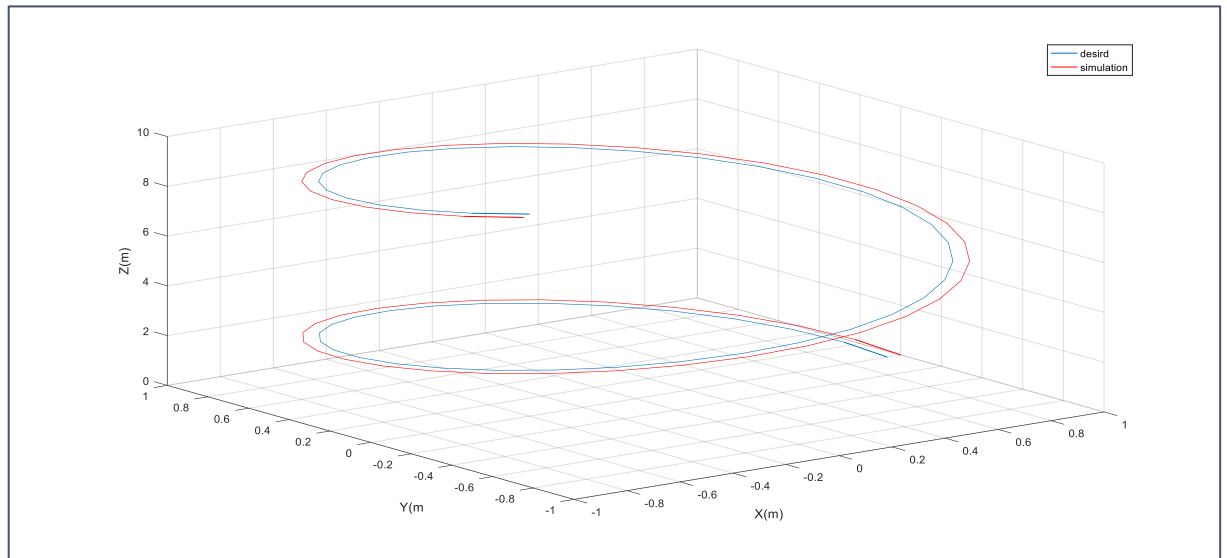


Figure III.5: The final simulation PID result of global in Trajectories 3D

Note:

After applying the classical controller...

The error is significant in terms of altitude, but in terms of response speed and stability, it is acceptable.

III.8 Conclusion:

In this chapter, our primary focus was on the trajectory tracking problem. By using PID control, we effectively adjusted the proportional, integral, and derivative gains to manage the error between the desired and actual states. This allowed us to improve the quadrotor's response and reduce deviations from the intended trajectory.

Although we observed an improvement in the quadrotor's performance with PID control, it was not sufficient to achieve its stability and reach the desired altitude. Therefore, in the next chapter, we will turn to intelligent control for precise trajectory tracking.

Chapter IV:
Fuzzy control of quadcopter

Fuzzy control of quadcopter

IV.1. Introduction

Fuzzy logic, which deals with uncertainty and imprecision, is used in fuzzy control to improve the stability, maneuverability, and flight performance of drones. It can maintain aircraft stability, allow for autonomous navigation, guarantee precise trajectory monitoring, and maximize battery life. Based on drone states, sensor inputs, and external factors, fuzzy control modifies control inputs. Depending on the needs and resources of the application, additional control techniques like PID control, MPC, or RL are also accessible.

By using fuzzy control, engineers can design control systems that can adapt and respond to changing and uncertain environments, leading to improved system performance, stability, and robustness. [Ch, CHUEN.1990].

IV.2. Fuzzy Logic

Control systems may handle complex and uncertain settings by using fuzzy control. Fuzzy logic, on which it is built, enables the representation and manipulation of ambiguous and imperfect information.

Fuzzy control describes the behavior of the system and the control operations using linguistic variables and rules rather than accurate mathematical models.

Vague notions and ill-defined interactions between inputs and outputs can be modelled using fuzzy logic [R. R. Yager.1992].

IV.3. Principe de la commande floue:

Lorsqu'un opérateur humain commande manuellement un système, les actions qu'il réalise sont dictées par une connaissance subjective du fonctionnement de ce système. Par exemple, si l'eau est chaude dans une piscine, on la refroidit, si elle est très chaude on la refroidit plus. Cette commande du système peut être envisagée de façon différente selon la personne qui la

réalise. Ce principe est la base de la commande floue. La mesure «température» réalisée sur le système est prise en compte par l'intermédiaire d'une variable linguistique («froid», «tiède», «chaud»), qui est issue de l'analyse d'un expert humain. Ensuite, l'action à réaliser est déduite à la fois d'un ensemble de règle de commande («s'il fait froid, on chauffe plus...») et de l'état du système, qualifiée par la variable linguistique.

IV.4. Structure of a fuzzy controller:

Fuzzy control is the most widely used application of fuzzy logic. The general structure of a fuzzy controller is shown in the following figure

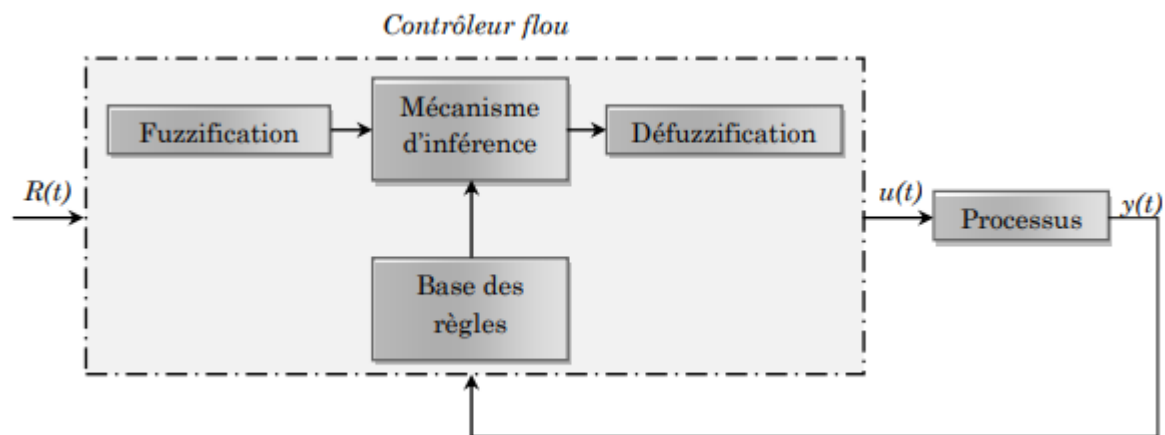


Figure IV.1: The general structure of a fuzzy controller

$R(t)$: is the reference signal.

$u(t)$: is the control signal.

$y(t)$: is the output of the system to be controlled.

The fuzzy controller essentially consists of four parts: a fuzzification block, a rule base, an inference mechanism, and a defuzzification block.

IV.4. 1.Fuzzification Block: It is used to transform crisp numerical variables from the inputs into fuzzy linguistic variables. Fuzzification involves defining membership functions for the different input and output variables. In the case of fuzzy logic control, trapezoidal and triangular shapes are commonly used for the membership functions.

To fuzzify a numerical variable, you need to provide the following:

1. Universe of Discourse: This refers to the range of possible values for the inputs and outputs. It defines the overall scope within which the variable operates.
2. Fuzzy Partition: This involves dividing the universe of discourse into fuzzy classes or sets. These classes represent different linguistic terms or categories that describe the variable's

behavior. For example, for a temperature variable, fuzzy classes like "cold," "warm," and "hot" can be defined.

3. Membership Functions: For each fuzzy class, you need to define a membership function. A membership function assigns a degree of membership to each value within the universe of discourse, indicating the extent to which a value belongs to a particular fuzzy class. Commonly used membership function shapes include triangular, trapezoidal, or Gaussian.

Example:

Figure (Figure.IV.2) illustrates an example of fuzzifying a variable x into five (5) fuzzy subsets.

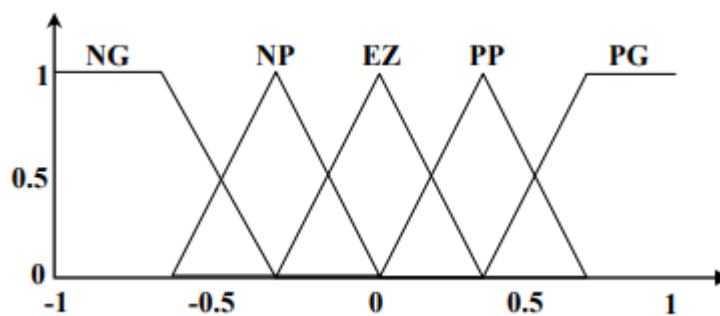


Figure.IV.2: Fuzzification into 5 fuzzy subsets

The different fuzzy sets are characterized by standard designations, where the symbols have the following meanings:

NG: Negative Grande.

NP: Negative Petite.

EZ: Approximately Zero.

PP: Positive Petite.

PG: Positive Grande.

IV.4. 2.Rule Base and Inference Mechanism:

Using the rule base provided by the expert and the fuzzy subsets of the corresponding inputs and outputs obtained through fuzzification, the inference mechanism establishes a relationship between the membership functions of the inputs and the membership functions of the outputs. By applying rules of the form "if condition then conclusion," the inference block serves as the core of a fuzzy controller, simulating human decision-making and deducing (inferring) fuzzy control actions. A graphical representation of the rule set, called an inference matrix or rule table, helps summarize the core of the fuzzy controller. The table (Table.IV.1) represents an

inference table with five fuzzy subsets for two input variables, namely, error 'e' and its derivative 'de,' and one output variable, the control 'du.'

Inference or decision-making is the heart of the fuzzy controller. It has the ability to simulate human decision-making based on fuzzy concepts and expertise. For fuzzy logic control, generally one of the following three methods is used:

<i>du</i>		<i>E</i>				
		<i>NG</i>	<i>NP</i>	<i>EZ</i>	<i>PP</i>	<i>PG</i>
<i>de</i>	<i>NG</i>	<i>NG</i>	<i>NG</i>	<i>NP</i>	<i>NP</i>	<i>EZ</i>
	<i>NP</i>	<i>NG</i>	<i>NP</i>	<i>NP</i>	<i>EZ</i>	<i>PP</i>
	<i>EZ</i>	<i>NP</i>	<i>NP</i>	<i>EZ</i>	<i>PP</i>	<i>PP</i>
	<i>PP</i>	<i>NP</i>	<i>EZ</i>	<i>PP</i>	<i>PP</i>	<i>PG</i>
	<i>PG</i>	<i>EZ</i>	<i>PP</i>	<i>PP</i>	<i>PG</i>	<i>PG</i>

Table.IV.1: Inference table with five fuzzy subsets

IV.4. 2.1.Max-Min Inference Method (Mamdani Method): The max-min inference method uses the "AND" operator through the minimum formulation. The conclusion in each rule, introduced by "THEN," is achieved by taking the minimum value. Finally, the "OR" operator combines the different rules by taking the maximum value.

IV.4. 2.2.Max-Product Inference Method (Larsen Method): The max-product inference method achieves the "AND" operator through the product formulation. The conclusion in each rule, introduced by "THEN," is achieved by taking the product. The "OR" operator that combines the different rules is achieved by taking the maximum value.

IV.4. 2.3.Sugeno Method: The "AND" operator is achieved by taking the minimum value, and the conclusion of each fuzzy rule takes a polynomial form.

Example of Fuzzy Inference:

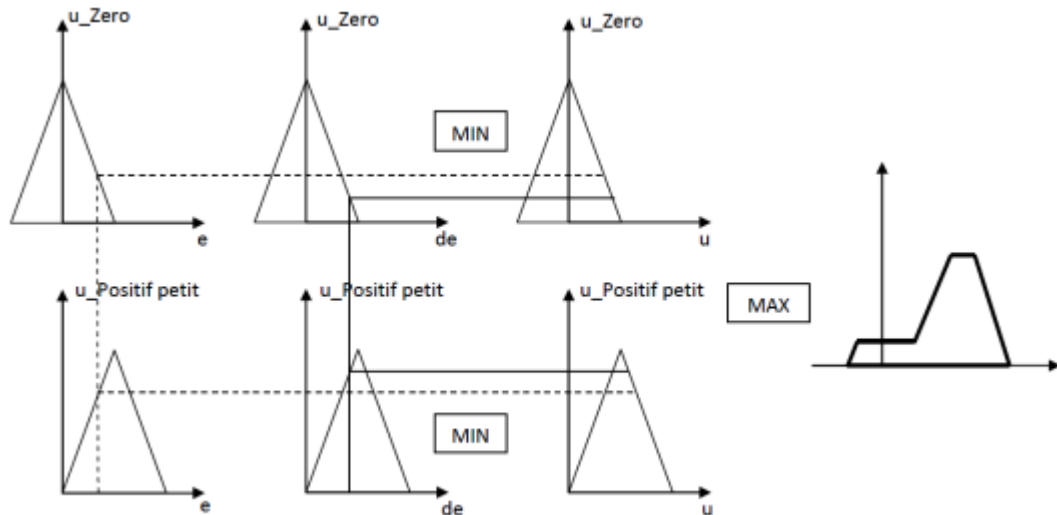


Figure.IV.3: The MAX/MIN Inference Method

IV.4.3. Defuzzification Block:

This block is the inverse of the fuzzification block. It is used to transform the fuzzy decision into a numerical value to be sent to the system. There are several defuzzification methods, with the main ones being:

IV.4.3.1. Center of Gravity Method:

This is the most common defuzzification method. The abscissa of the center of gravity of the membership function resulting from the inference corresponds to the output value of the controller.

$$x_G = u = \frac{\int_{x_0}^{x_1} x u(x) dx}{\int_{x_0}^{x_1} u(x) dx} \quad (\text{IV.1})$$

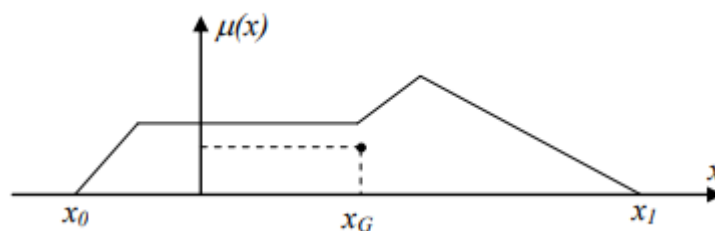


Figure.IV.4: Defuzzification by Center of Gravity

IV.4.3.2. Maximum Value Method:

This method is much simpler and is used only in discrete cases. The output value is chosen as the abscissa of the maximum value of the membership function. The figure below illustrates the principle of this method.

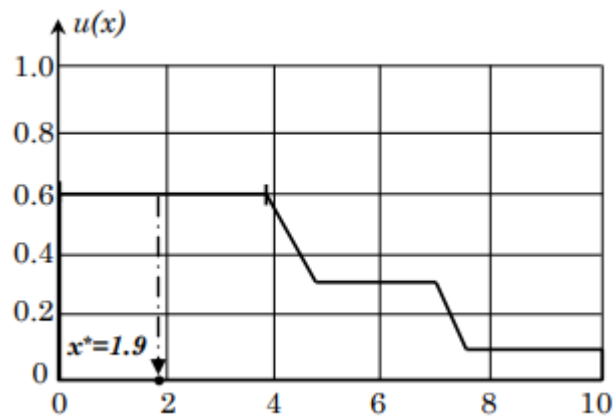


Figure.IV.5: Maximum Value Defuzzification Method

IV.4.3.3. Mean of Maximums Method:

In this method, the output value is estimated by the abscissa of the point corresponding to the center of the interval for which the membership function is maximum. This value is obtained using the following expression:

$$y_{cm} = \frac{\inf M + \sup M}{2} \quad (\text{IV.2})$$

Where M is the set of points for which the membership function is maximum.

IV.5. Advantages of fuzzy logic

- **Handling uncertainty:** Fuzzy logic can handle ambiguous and inaccurate input, making it appropriate for use in systems where it may not be possible or feasible to derive precise numerical values.
- **Intuitive reasoning:** Fuzzy logic offers intuitive modeling based on human-like reasoning by allowing the use of language variables and rules.
- **Robustness:** Systems based on fuzzy logic are typically more resistant to system fluctuations and disruptions.
- **Nonlinear system control:** Traditional control methods may have trouble with nonlinear systems; however, fuzzy logic excels in this area.

IV.6. Membership functions: Parameterization and Formulation

- 1) Triangular Membership function
- 2) Trapezoidal MF
- 3) Gaussian MF
- 4) Generalized bell MF

5) Sigmoid membership function

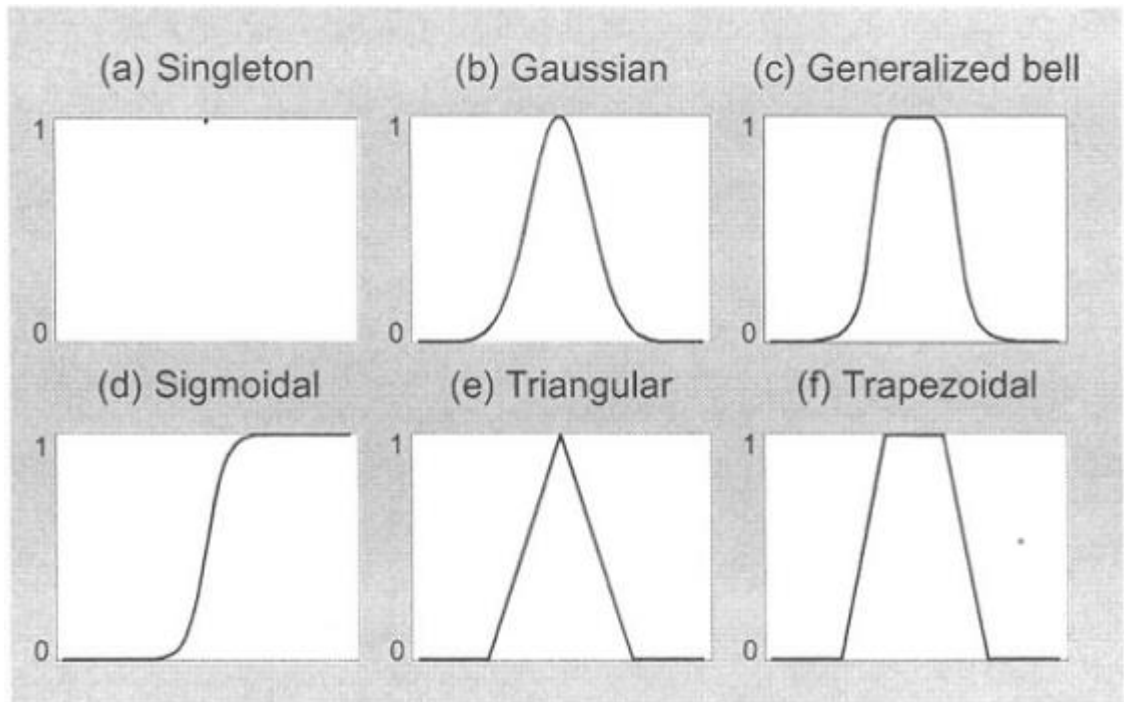


Figure IV.6: Various type of Fuzzy membership functions

IV.7. Quadcopter fuzzy controller design

The concept of fuzzy logic systems draws its inspiration from the impressive ability of humans to make sense of information based on perception. Rule-based fuzzy logic offers a structured approach for dealing with linguistic rules that emerge from reasoning and decision-making processes involving uncertain and imprecise data. Unlike a dynamic system, a fuzzy controller represents a static, nonlinear relationship between its inputs and outputs. The inputs and outputs of the fuzzy controller are precise and expressed as real numbers, rather than fuzzy sets.

The overall fuzzy control architecture is given in Figure IV.7, it comprises four controllers each for one input of the quadcopter.

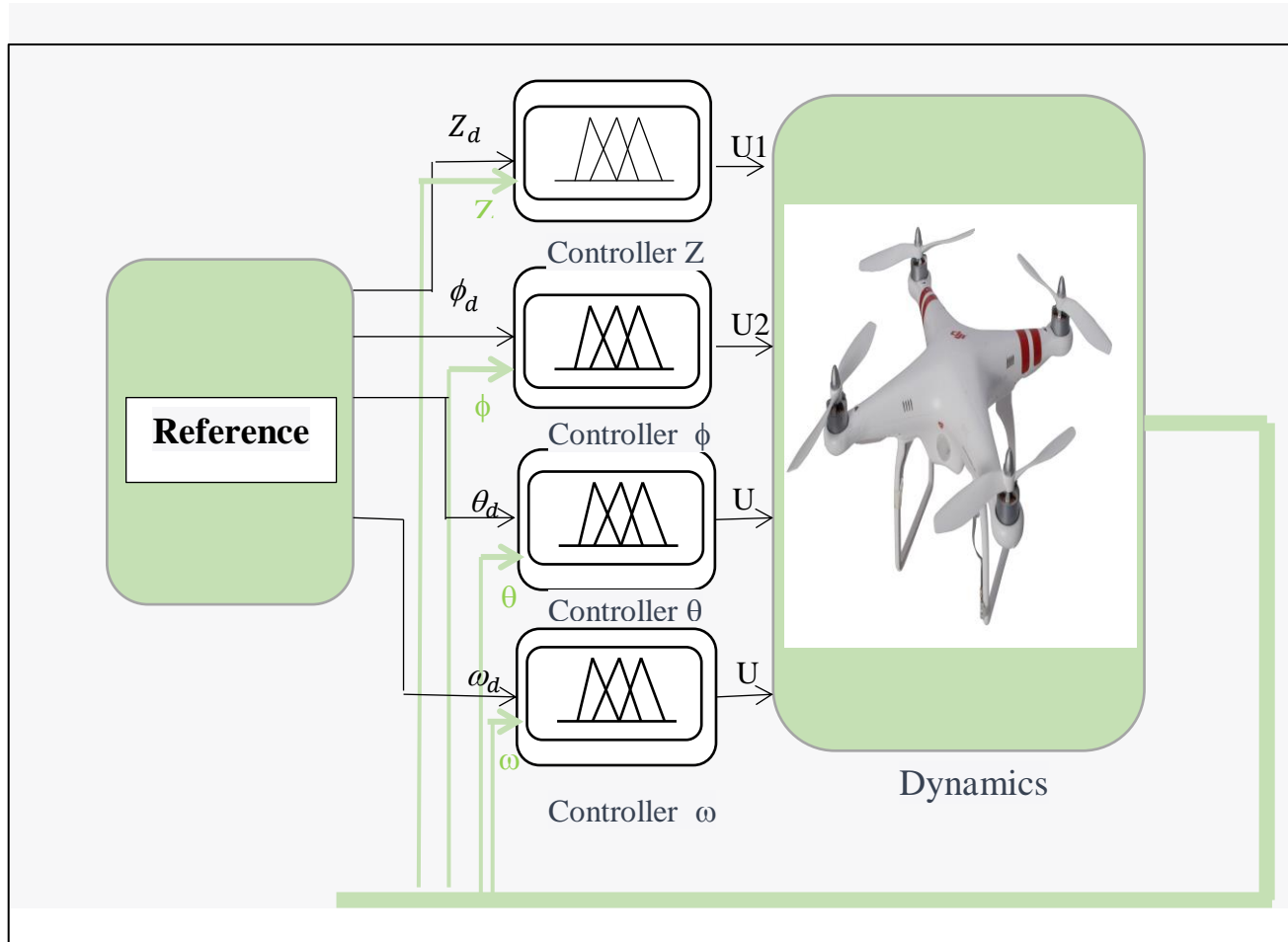


Figure IV.7. Controller archetecture

IV.7.1 The fuzzification procedure

Triangular and trapeze membership functions are used for the fuzzy values of the inputs and outputs of the four controllers. The labels used to express the values of inputs and outputs are given in Table IV.2.

Table IV.2. Linguistic values of the inputs and the outputs

Linguistic Term	Label
Negative	N
Grand Negative	NG
Zero	Z
Positivee	P
Grand Positivee	PG

The membership functions for all the terms of the input and output variables in this controller are shown in Figures IV.8-11.

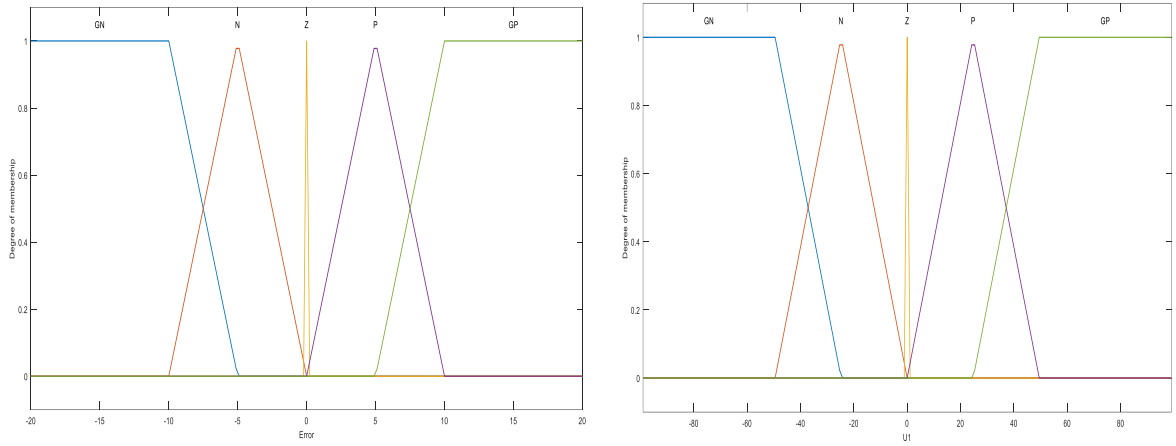


Figure IV.8. The numbership functions of the thrust controller: a) error, b) U1

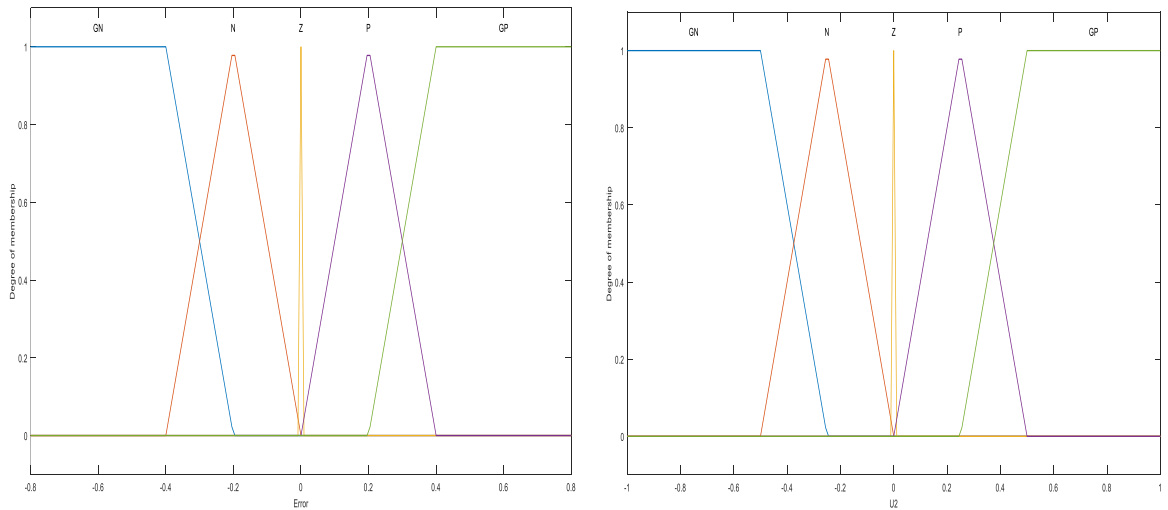


Figure IV.9. The numbership functions of the Roll controller: a) error, b) U2

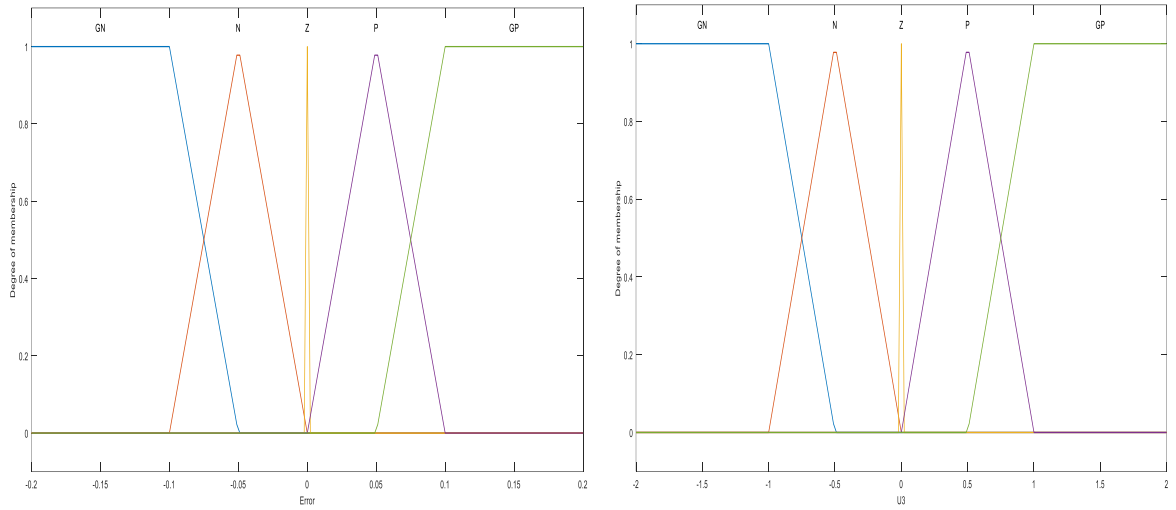


Figure IV.10. The membership functions of the pitch controller: a) error, b) U3

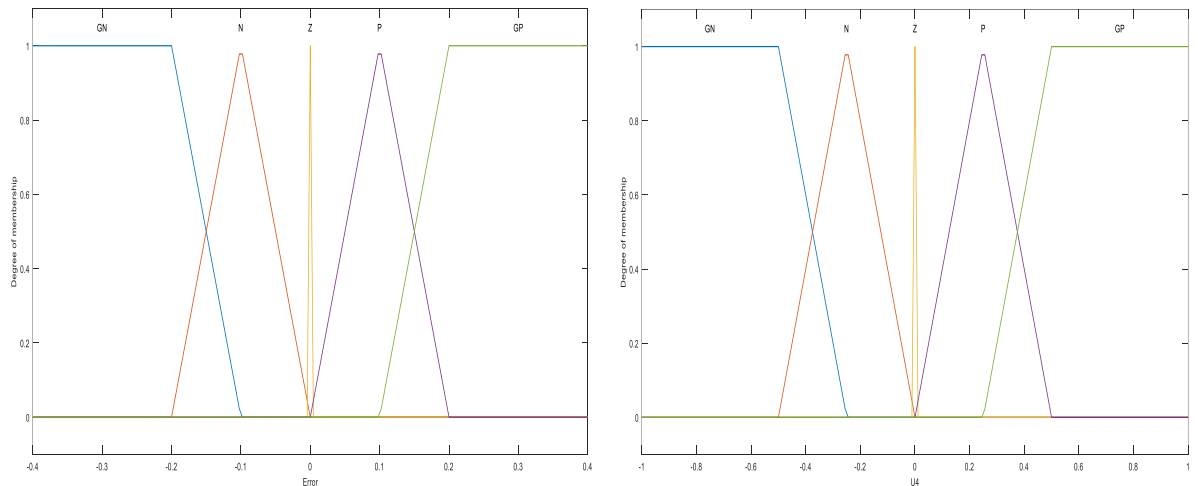


Figure IV.11. The membership functions of the Yaw controller: a) error, b) U4

IV.7.2 The Rule Base Design

Due to the simplicity of design, the rule base of each fuzzy controller contains 5 rules as following:

1. If (input1 is GN) then (output1 is GN)
2. If (input1 is N) then (output1 is N)
3. If (input1 is Z) then (output1 is Z)
4. If (input1 is P) then (output1 is P)
5. If (input1 is GP) then (output1 is GP)

IV.7.3 The Defuzzification Procedure

The “centroid” method is used for the defuzzification procedure. Centroid defuzzification returns the center of the area under the curve.

IV.8. MATLAB Simulink model

The control model is given in Figure IV.12.

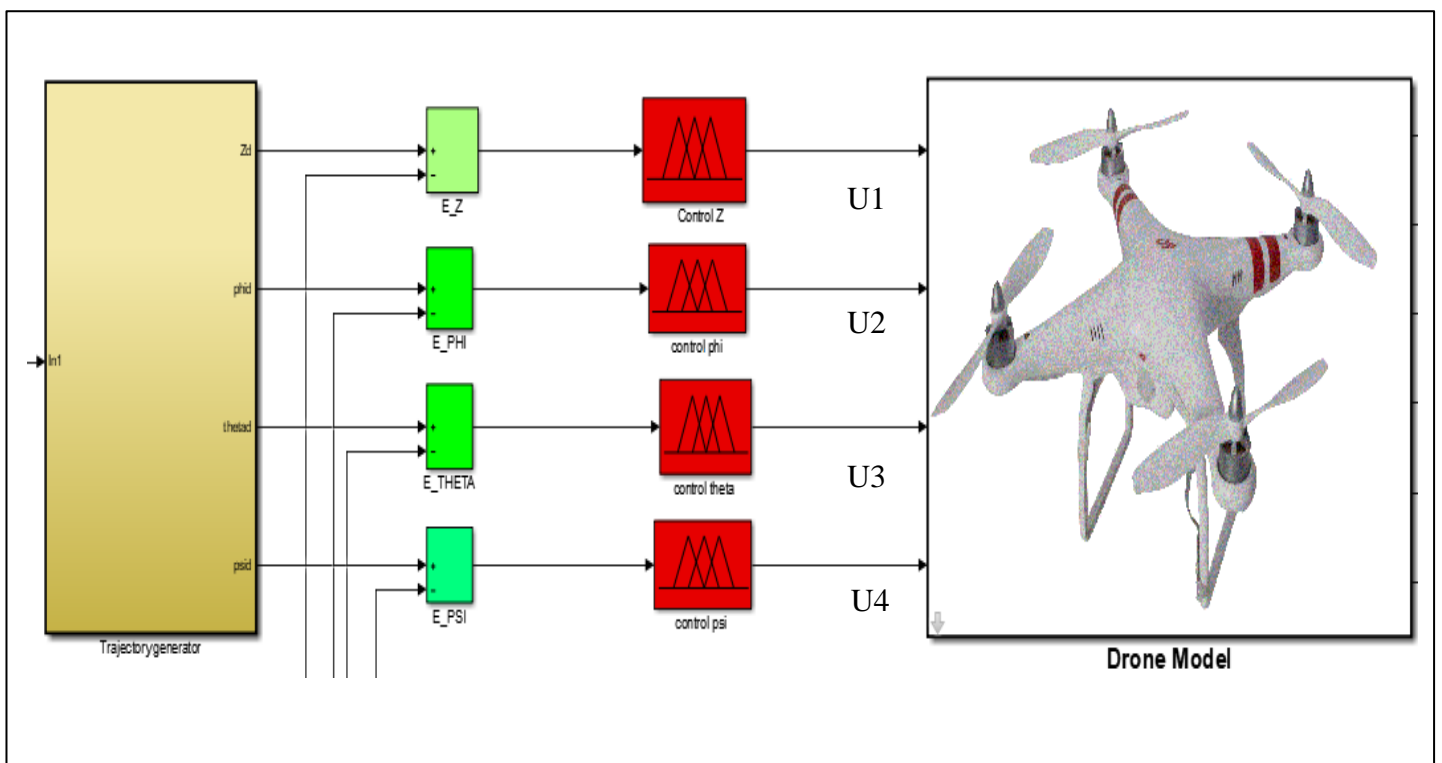


Figure IV.12: Fuzzy Control model

IV.8. Simulation results

The simulation results are given below.

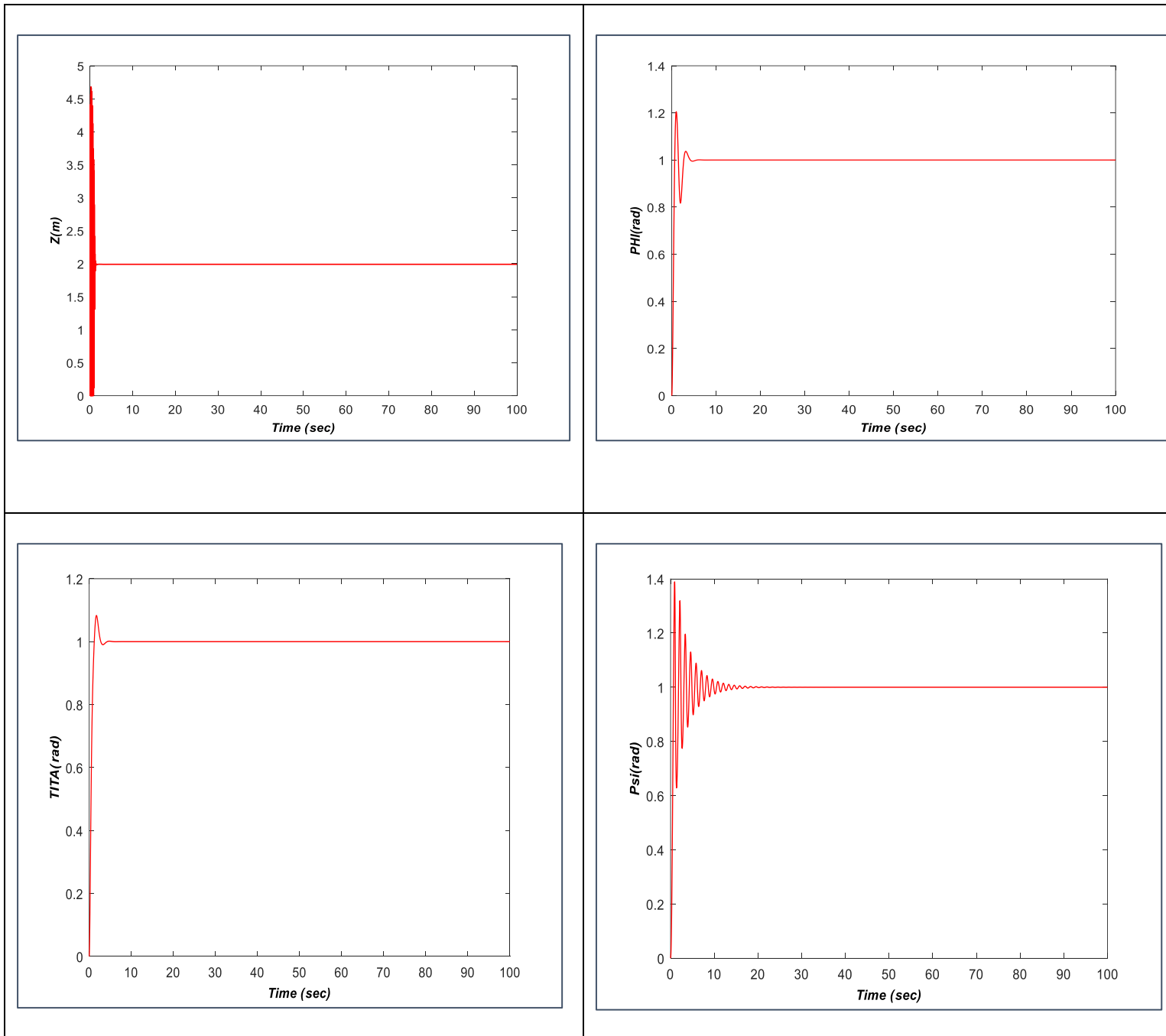


Figure IV.13: Z (height) & Phi (roll) & Theta (pitch) & Psi (yaw) fuzzy control Results

IV.9 Comparison between the PID and Fuzzy controllers

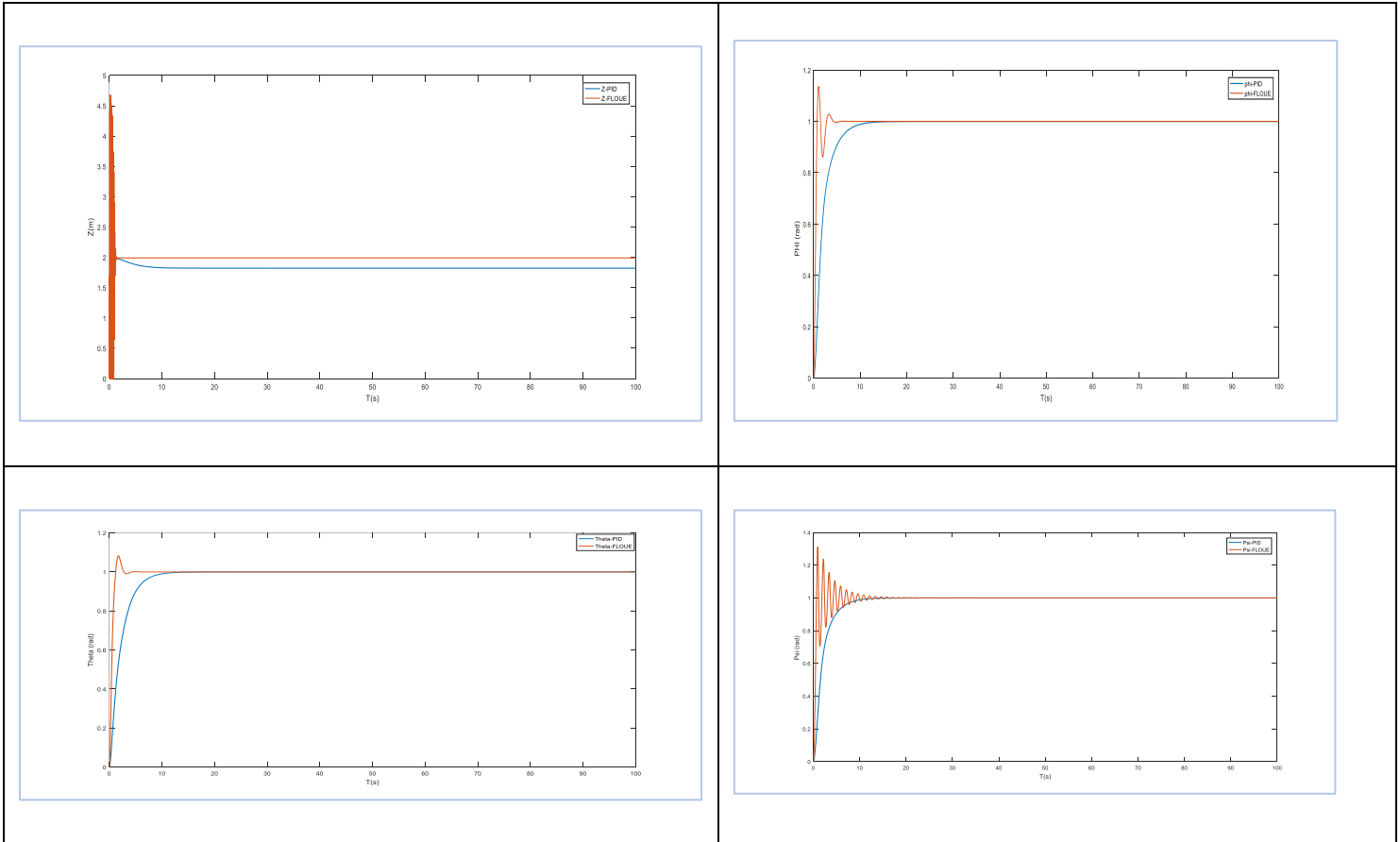


Figure IV.14: Z (height)&Phi(roll)&Theta (pitch) & Psi (yaw) Fuzzy and pid controls

Results

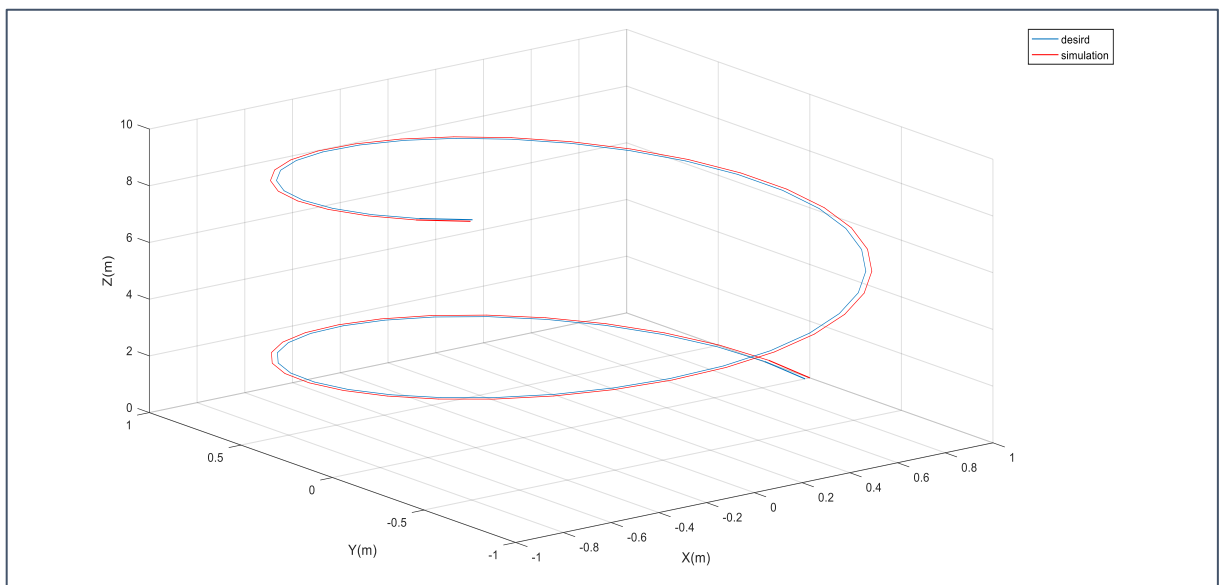


Figure IV.15: The final simulation Fuzzy result of global Trajectories in 3D

IV.10. Conclusion

In the conclusion of this chapter, we employed fuzzy logic to enhance the control capability of the unmanned aerial vehicle (UAV), utilizing fuzzy rules and fuzzy values for different variables.

Upon implementing control using fuzzy logic, we observed a notable improvement in the UAV's performance. It exhibited enhanced stability and more precise tracking of desired paths, even in the presence of unforeseen environmental changes. The impact of vibrations and distortions was also mitigated.

Comparing the results of this chapter with the previous one, where PID control was utilized, we noted that fuzzy logic yields better performance in varying and unexpected conditions. Fuzzy logic control demonstrates a greater capacity to adapt to sudden environmental changes and interact effectively with alterations in the system's state.

Chapter V:

Firefighting Strategy

Chapter V

Firefighting Strategy

V.1 Introduction

The world is currently facing an unprecedented and immeasurable threat in the form of wildfires, which erupt unexpectedly and spread rapidly through forested areas. Dealing with these wildfires poses numerous challenges that need to be addressed.

Unmanned aerial vehicle (UAV) technology has gained increasing popularity in the field of bushfire management systems due to its inherent characteristics such as maneuverability, autonomy, easy deployment, and cost-effectiveness. UAVs equipped with remote-sensing capabilities, along with artificial intelligence, machine learning, and deep learning algorithms, are utilized to detect fire-prone regions, make predictions, make informed decisions, and enhance fire-monitoring tasks.

UAVs serve as valuable tools for monitoring suspicious areas, swiftly reaching fire hotspots, and even directly combating fires. In addition to their speed, accuracy, and versatility in accessing various terrains, UAVs also play a crucial role in ensuring the safety of firefighters by substituting human intervention in hazardous situations.

[<https://france3-regions.francetvinfo.fr/occitanie/gard/nimes/des-drones-pour-lutter-contre-les-incendies-2545852.html>]

V.2 The processing of images

V.2.1 Definition:

The processing of images is the study of digital pictures and their changes in order to enhance their quality or extract information from them. It is a branch of applied mathematics and computer science. The goal of image segmentation, a fundamental phase in the image processing and analysis process, is to divide an image into homogenous regions and group pixels with similar features according to established criteria.

V.2.2 Definition of Image

An image is a representation of a person or an object by painting, sculpture, drawing, photography, film, etc. It is also a structured set of information that, after being displayed on the screen, has a meaning for the human eye. It is also a structured set of information that, after being displayed on the screen, has a meaning for the human eye. It can be described as a continuous analog brightness function defined in a bounded domain, such as the spatial coordinates of a point in the image, and is a function of light intensity and color. Under this aspect, the image is not usable by the machine, which requires its digitization. [H.ANOUAL, 2012]

V.2.2.1 Digital image:

The images manipulated by a computer are digital (represented by a series of bits). The digital image is the image whose surface is divided into elements of fixed size called cells or pixels, each having as a characteristic a level of gray or color taken from the corresponding location in the real image or calculated from an internal description of the scene to be represented.

The digitization of an image is the conversion of this one into a two-dimensional matrix of numerical values $I(n,m)$ or n,m , which are represented by the Cartesian coordinates of a point of the image $I(n,m)$ and the level of gray or color at this point.

V.3 Artificial Neural Networks

V.3.1 Definition:

Artificial neural networks are highly connected networks of elementary processors operating in parallel. Each elementary processor calculates a unique output based on the information it receives. Any hierarchical structure of networks is obviously a "network". The formal neuron is a theoretical model of information processing inspired by observations of the functioning of a biological neuron in order to reproduce intelligent reasoning in an artificial way.

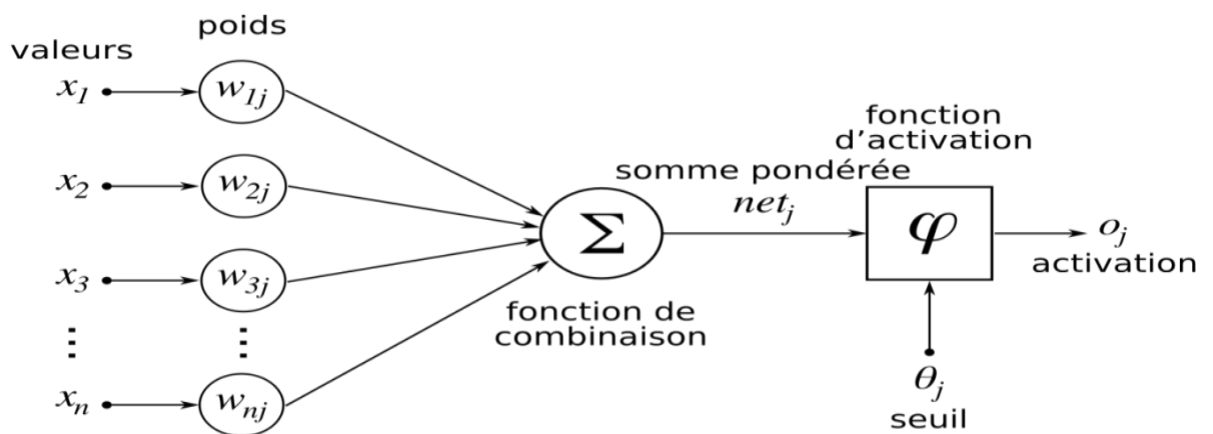


Figure V.1: artificiel Neurone

The formal neuron can be defined, in a more general way, by the following elements:

1. The inputs of the neural network: They can be binary (0, 1) or real.
2. The activation function is a mathematical function that allows one to define the internal state of the neuron according to its total input. The figure below presents some of the most commonly used functions.

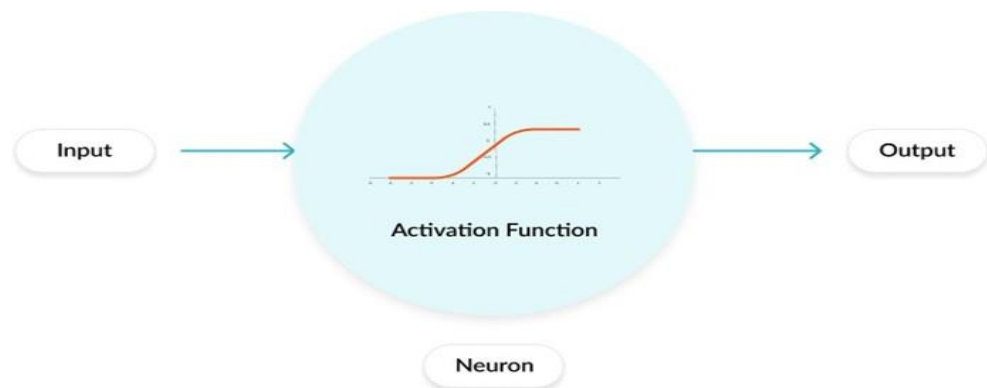


Figure V.2: the activation Fonction

- 1. Output function:** It calculates the output of a neuron according to its activation state. In general, this function is considered the identity function. It can be binary (0, 1), bipolar (-1, 1), or real.
- 2. Connection weights:** A weight w_{ij} is associated with each connection. The weight of an artificial neuron represents the efficiency of a synaptic connection. A negative weight inhibits an input, while a positive weight enhances it.

V.3.2 Different models of neural networks:

A neural network is a structure organized around a set of neurons interconnected, according to a certain topology, by links assigned weights. These links provide each neuron with a channel to transmit and receive signals from other neurons. Artificial neural networks can be classified into two main families:

V.3.2.1. Single-layer neural networks:

Presented by Frank Rosenblatt in 1958, the perceptron is the first model and the simplest form of neural network. The monolayer perceptron is composed of two layers: the input layer and the output layer, which give the response corresponding to the input stimulation

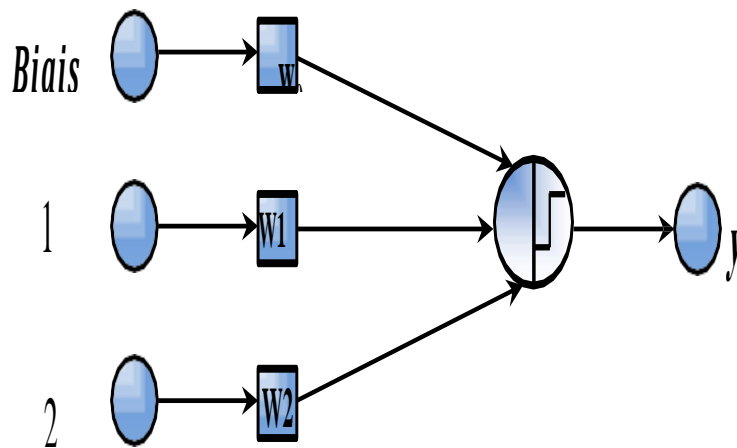


Figure V.3: Model of a simple (single layer) perceptron

A simple perceptron can only handle linearly separable problems where the states can be separated by a straight line, such as AND and OR logic functions. For problems that are not.

V.3.2.2. Multilayer neural networks:

This is an extension of the single-layer perceptron, with one or more hidden layers between the input and output. The (Figure V.4) in general, a multilayer perceptron can have any number of layers and any number of neurons (or inputs) per layer. [R SADOUNI]

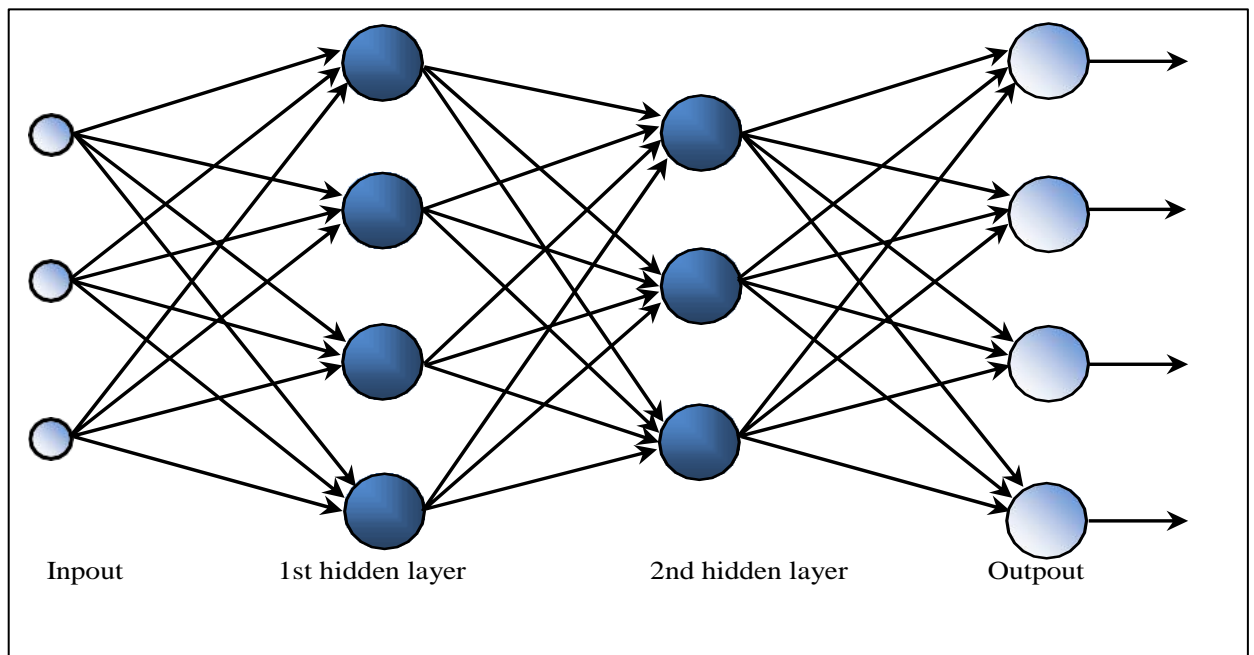


Figure V.4: Model of a Multilayer perceptron

V.3.3 Applications:

Neural networks can be applied in several domains, which we can mention:

- Statistics: data analysis, forecasting, classification, etc
- Robotics: control and guidance of robots or autonomous vehicles
- imaging or pattern recognition
- signal processing
- learning simulation

V.4 Learning a neural network

Learning is probably the most interesting property of neural networks. However, it does not concern all models, but the most commonly used ones.

Learning is a phase in the development of a neural network during which the behavior of the network is modified until the desired behavior is obtained. Neural learning uses examples of behavior. There are two main families of learning:

V.4.1 Machine learning according to the nature of the input data

V.4.1.1 Supervised learning

Learning is said to be supervised when the network is forced to converge to a specific final state, which requires prior (a priori) knowledge of the desired response $d(n)$. The most commonly used method is gradient back-propagation. It consists of presenting examples to

the network, computing its output, and adjusting the weights in order to reduce the gap between this output and the desired response to satisfy a certain performance criterion.

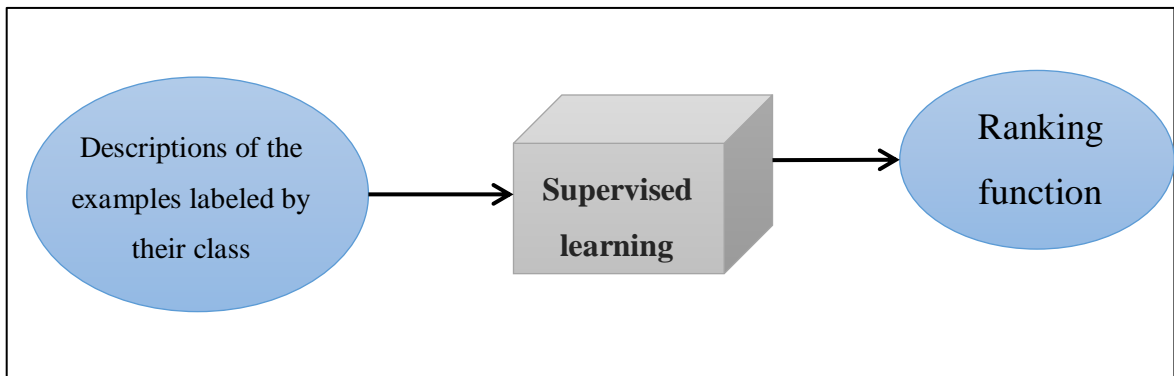


Figure V.5: Supervised learning

V.4.1.2 Unsupervised learning

In unsupervised learning, only the input values are available, and the network is left free to converge to any final state. A priori knowledge of the desired output is not necessary; the learning procedure is based only on the input values. The network is self-organizing in order to optimize a certain cost function. [R SADOUNI]

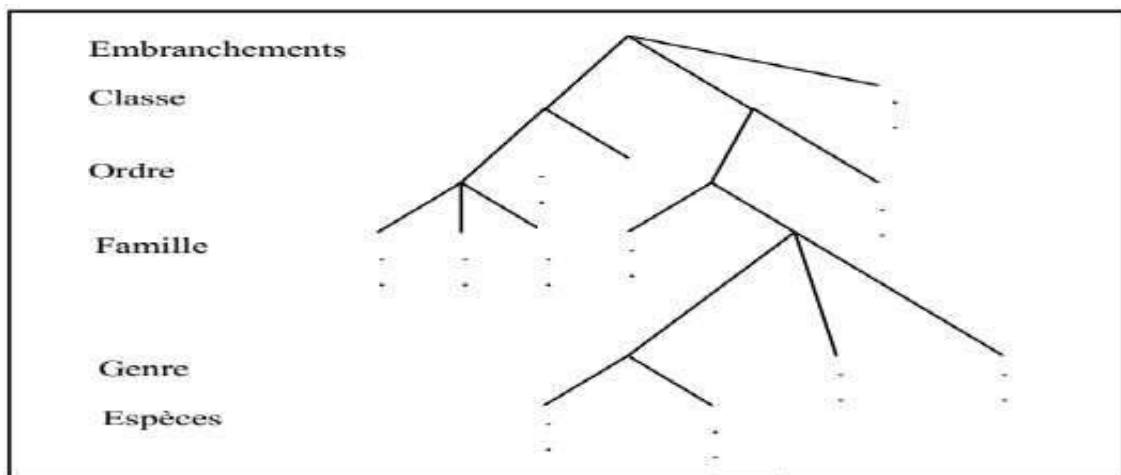


Figure V.6: Unsupervised learning

V.4.1.3 Reinforcement learning

The algorithm learns a behavior given an observation. The algorithm's action on the environment produces a feedback value that guides the algorithm's action.

V.4.2 Machine learning by type of result classification

Classification is a type of supervised learning that identifies the category to which a new

feature belongs based on a training dataset of observations with known categories. Also called data partitioning, it allows you to group objects (observations or individuals) into classes (clusters) of so that objects belonging to the same class are more similar to each other than objects belonging to other classes. There are several types of classification algorithms :

- **Decision tree:** uses a tree structure with "if" and "then" rules, executing the input via a series of decisions until it reaches a termination condition. It can model complex decision processes and is very intuitive, but it can easily overestimate the data.
- **Random Forest:** a set of decision trees with automatic selection of the best-performing tree It offers the strength of the decision tree algorithm without the problems of overlearning.
- **Nave Bayes classifier:** probability-based classifier It calculates the probability that each data point exists in each of the target categories. Simple to implement and accurate for a wide range of problems, but sensitive to the set of selected categories.
- **K-nearest neighbor:** ranks each data point by analyzing its nearest neighbors among the training examples. Simple to implement and understand, it is effective for many problems, especially those of low dimensionality. Provides lower accuracy than supervised algorithms and is computationally intensive.

V.5 Convolutional neural networks

In the field of machine learning, a convolutional neural network (CNN, or ConvNet) is a type of acyclic artificial neural network in which the pattern of connections between neurons is inspired by the visual cortex of animals. The neurons in this region of the brain are arranged in such a way that they correspond to overlapping regions when they cover the visual field. Their operation is inspired by biological processes, and they consist of a multi-layered stack of perceptrons in order to preprocess small amounts of information. Convolutional neural networks have many applications in image and video recognition, recommendation systems, and natural language processing.

V.5.1 CNN architecture principle

Convolutional neural networks (CNNs) are currently the most powerful models for image classification. They have two distinct parts. As input, an image is provided in the form of a matrix of pixels. It has two dimensions for a grayscale image. The color is represented by a third dimension with a depth of 3 to represent the fundamental colors [red, green, and blue]. The first part of a CNN is the convolutional part itself.

It works as an image feature extractor. An image is passed through a succession of filters, or convolution kernels, creating new images called convolution maps (Figure 2.5). Some intermediate filters reduce the resolution of the image by a maximum local operation. In the end, the convolution maps are flattened and concatenated into a feature vector, called the CNN code. This CNN code at the output of the convolutional part is then connected as input to a second part made of fully connected layers (multilayer perceptron). The role of this part is to combine the features of the CNN code to classify the image. The output is a final layer with one neuron per category. The numerical values obtained are usually normalized between 0 and 1, with a sum of 1, to produce a probability distribution for the categories.

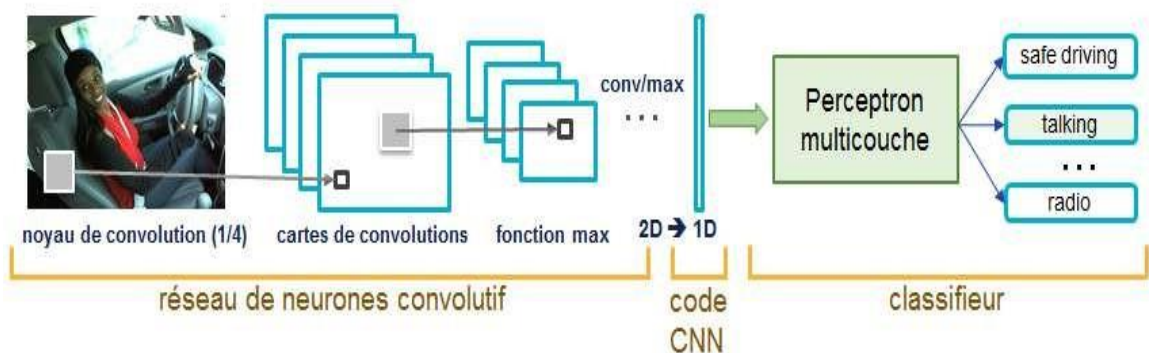


Figure V.7: The convolutional neural networks

V.5.2 The different layers of the CNN

A CNN architecture is formed by the stacking of independent processing layers:

V.5.2.1 The convolution layer (CONV)

Three hyperparameters allow dimensioning the volume of the convolution layer (also called output volume): the 'depth', the 'pitch,' and the 'margin'.

1. **Depth' of the layer:** number of convolution kernels (or number of neurons associated with the same receiver field).
2. **The 'pitch':** it controls the overlap of the receptive fields. The smaller the pitch, the more the receptive fields overlap and the larger the output volume.
3. **The 'zero padding':** it is sometimes useful to add zeros to the limit of the input volume. The size of this zero padding is the third hyperparameter. This padding allows you to control the spatial dimension of the output volume. In particular, it is sometimes desirable to keep the same area as the input volume.

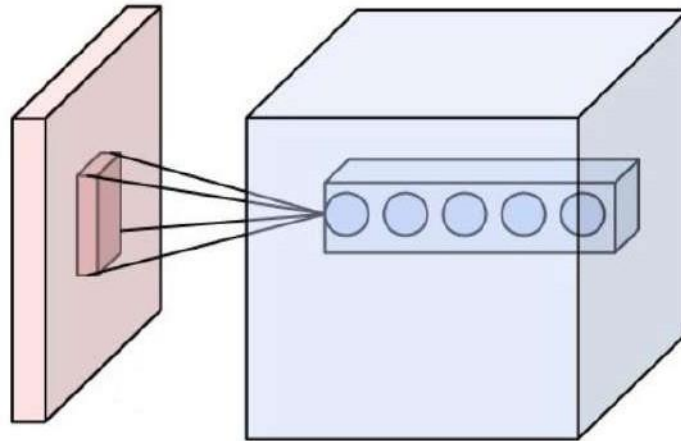


Figure V.8: Set of neurons (circles) creating the depth of a convolution layer (blue). They are linked to the same receiver field (red).

V.5.2.2 Pooling layer (POOL)

Pooling is a specificity of convolutional neural networks. Its function is to progressively reduce the spatial size of the representation in order to reduce the number of parameters and computations in the network without losing the most important information, and thus also to control overfitting. The main advantage of average pooling is that it is effective for detecting weak signals, as in the case of steganalysis. Maximum pooling, on the other hand, is effective for detecting strong signals, such as objects, and also allows the model to be translation invariant. After this subsampling step, we obtain a feature map defined as follows:

- $I^{(l)k} = \text{pool}(s^{(l)k})$,
- With $I^{(l)k}$ a feature map of the layer
- $\text{Pool}()$: the pooling operation
- $S^{(l)k}$ is the output value of neuron k in layer l .

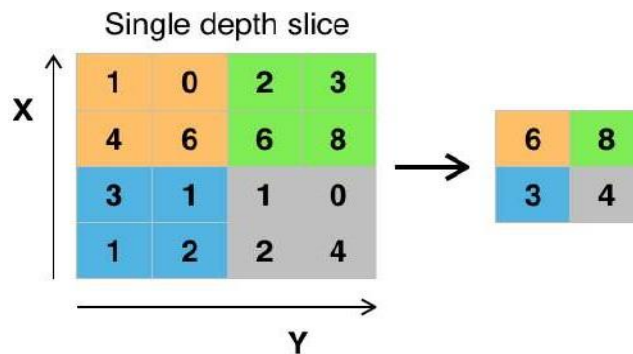


Figure V.9: Pooling with a 2x2 filter and a step of 2.

V.5.2.3 ReLU:

ReLU is a per-element operation (applied per pixel) that replaces all negative pixel values in the feature map with zero. The purpose of ReLU is to introduce nonlinearity into our ConvNet, since most of the real-world data we would like our ConvNet to learn is nonlinear (convolution is a linear operation—multiplication and addition of matrices per element—so we account for nonlinearity by introducing a nonlinear function such as ReLU).

The formula to apply is: $f(x) = \max(0, x)$.

[<https://www.supinfo.com/articles/single/7923-deep-learning-fonctions-activation>]

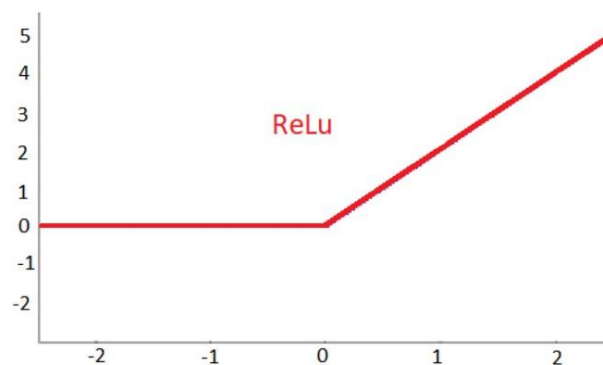


Figure V.10: The ReLu function

V.5.2.4 Fully connected layer:

After several layers of convolution and max-pooling, the high-level reasoning in the neural network is done through fully connected layers. The neurons of a fully connected layer are connected to all outputs of the previous layer (as is usually the case in ordinary neural networks). Their activation functions can therefore be calculated using matrix multiplication followed by bias shifting.

V.5.2.5 Loss Layer (LOSS):

The loss layer specifies how network learning penalizes the difference between the predicted signal and the actual signal. It is usually the last layer of the network. Various loss functions suitable for different tasks can be used in this layer. Solemax loss is used to predict a single class from a set of mutually exclusive classes. The sigmoid cross-entropy loss is used to predict K independent probability values in [0, 1]. Euclidean loss is used to regress to real values.

The following figure shows the architecture of a CNN:

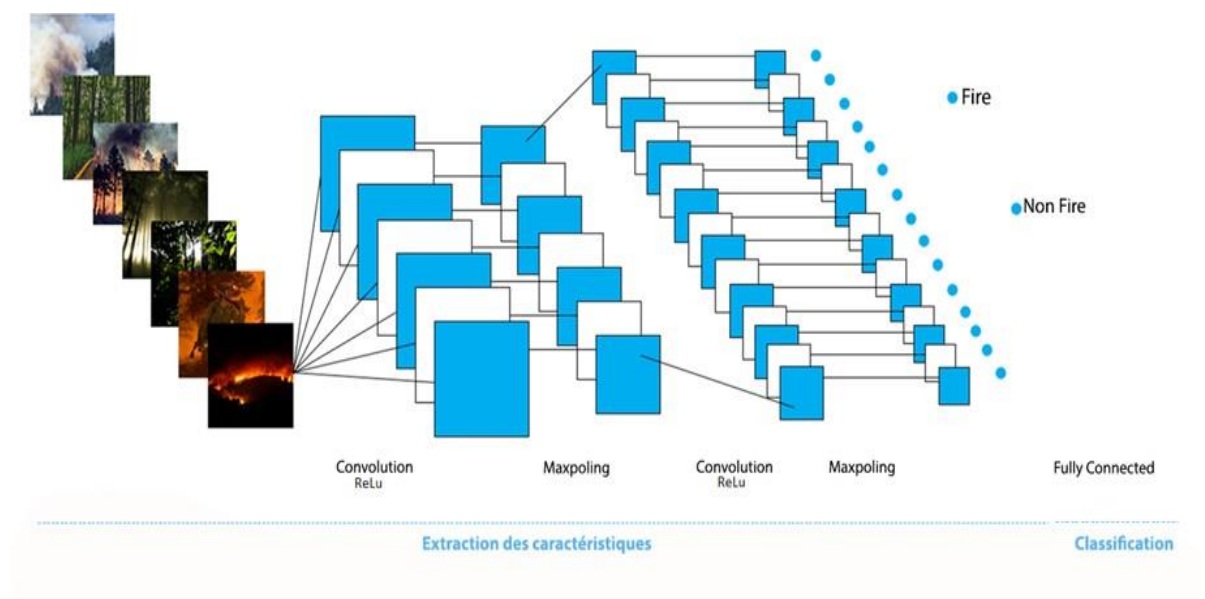


Figure V.11: Operation of a convolutional neural network.

V.5.3. Advantages of CNN:

- A major advantage of convolutional networks is the use of a single weight.
- This improves performance and allows for translation invariance.
- Compared to other image classification algorithms, convolutional neural networks use relatively little pre-processing.
- The absence of initial parameterization and human intervention is a major advantage of CNNs.

V.6 Model development and implementation of CNN:

Recent advances in image processing have enabled vision-based systems to detect fires using convolutional neural networks. In our project, we implemented two CNN architectures for wildfire detection prediction and fire detection, and created a model with **Teachable Machine**

V.6.1 Introduction to Teachable Machine

Teachable Machine is a web-based tool available to anyone, which allows you to create machine learning models quickly and easily

V.6.2 Target Audience of Teachable Machine

Teachers, artists, students, innovators, creators of all kinds. Anyone with an idea to explore. No prior knowledge of machine learning is required.

V.6.3 Working Principle of Teachable Machine

You train a computer to recognize images, sounds, and postures without writing code for machine learning. You then use your model for your projects, websites, apps and more.

V.6.4 Initial Steps for Using Teachable Machine

1. Where to start?

Just go to <https://teachablemachine.withgoogle.com/> ,

Then click on "Get Started". No need to create an account or log in

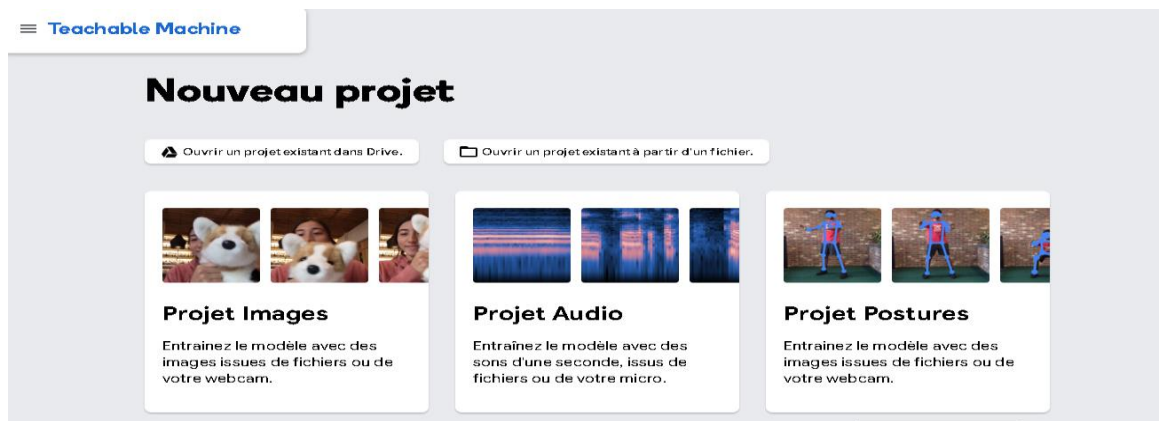


Figure V.12: The main interface of Teachable Machine

2. What can I train it with?

You can currently train Teachable Machine with images (from your webcam or image files), sounds (in one-second clips from the microphone), and postures (where the computer deduces the position of your arms, legs, etc. from an image). Other types of workouts may be available soon.

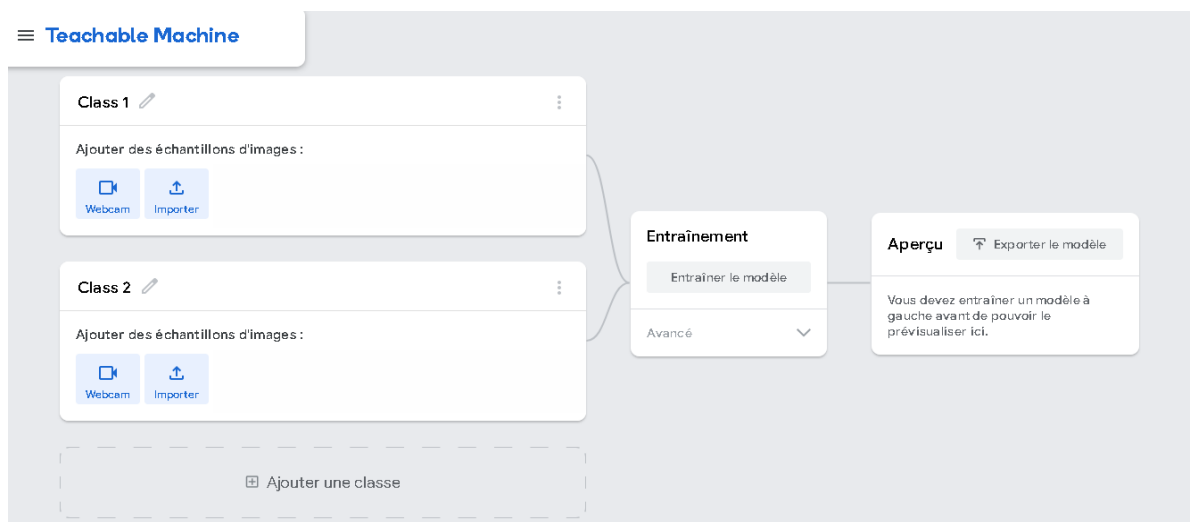


Figure V.13: Start of work

V.6.5 Saving Projects in Teachable Machine

You have several options:

- 1. Save your entire project in Google Drive:** A.zip file including all the samples for each of your classes is then saved in Drive. You can reopen this.zip file later from Teachable Machine to pick up where you left off.
- 2. Download your samples:** you can download all the samples for each class, then import them later if you want to continue using the same data.
- 3. Upload your template:** if you upload your template and close the tab, you can use this uploaded template later, and nothing will be saved on any server.
- 4. Do not save anything:** if you close your tab and do not perform any of the above actions, nothing is saved in the browser or on any server.

V.7. Wildfire detection and prediction using machine learning:

Experts around the world are striving to discover fast and powerful solutions that can help cope with climate change and treat some of its disasters and damages, especially in the context of the recent wave of devastating forest fires resulting from rising temperatures. To this end, a range of new technologies have been developed that can help predict these destructive fires and treat them.

These technologies include computer models that plot potential fire trajectories, drones that detect fire outbreaks and deposit extinguishing balls, as well as other approaches. Here are the available technologies used in our study:

A-Fire prediction:

- A-1. Prediction based on historical fire records.
 - A2. Prediction base on Thermal Data Analysis.
 - A.3. Prediction by aerial imaging using drones.
- B- Fire detection using machine learning.
- C- Firefighting using UAV.

V.7.A.Fire prediction:

V.A.1 Prediction based on historical fire records:

Aiming to use previous fire data to uncover patterns and trends that might aid in predicting future fire occurrences, the technique you suggested entails predicting fires based on historical fire records. By offering early warning systems and preventive steps to lessen the damage of fires, this strategy's main goal is to enhance fire management and response.

Unmanned aerial vehicles (UAVs), sometimes known as drones, can be used to carry out this plan. Drones can collect useful information about the environment and identify possible fire threats since they are outfitted with a variety of sensors and imaging technology. The overall procedure is as follows:

1 Data collection: Drones are used to gather information from the desired location. They can be fitted with various sensors, including multispectral, infrared, and laser range finders, to gather pertinent data on the temperature, vegetation, and other important variables.

2 Advanced algorithms and machine learning approaches are used to interpret and evaluate the obtained data using images. To find trends and correlations, historical fire records and other pertinent data are combined. The study may take into account variables including climate, plant cover, geography, and prior fire events.

3 Fire Risk Assessment: The drone-mounted system creates a fire risk assessment based on the analysis, which offers an estimate of the likelihood and possible severity of flames in various places. It assists in identifying high-risk areas that require further monitoring.

4 Early Warning Systems: The information obtained is utilized to create early warning systems that can notify stakeholders and the authorities about possible fire dangers. This enables effective fire control techniques, resource mobilization, and prompt evacuation preparations.

This technique seeks to enhance efforts at fire prevention and response through the use of historical fire records and drone technology. To reduce the damage caused by wildfires, it helps authorities deploy resources efficiently, execute focused preventative measures, and improve overall fire control skills.

V.A.1.1 Data Mining Algorithms:

We need to employ data mining techniques to forecast the occurrence of forest fires. Using data mining techniques, a number of algorithms may be utilized to forecast the occurrence of forest fires. Based on satellite data, certain classification algorithms have previously been used to create predictive models of the likelihood that a fire would occur, including neural networks, naive bayes, SVMs, and random forests.

In this work, we processed the generated dataset using this method. Neural networks are used in these algorithms. To load the data, build the model, and present the findings, each method makes use of certain routines.

A group of supervised learning algorithms known as artificial neural networks (ANNs) learn repeatedly by being trained on a collection of data [Younes Oulad Sayad and all]

ANNs are frequently employed to address a range of classification and prediction issues. Three layers make up an ANN: the input layer, the intermediate layer, and the output layer.

Performance:

- ✓ Network-wide data archiving
- ✓ the capacity to operate with insufficient information
- ✓ Simultaneously do many tasks

Limitations:

- ✓ Parallel processing-capable processors are needed. It is difficult to demonstrate the
- ✓ Problem to the network.

V.A.1.2 Simulated actions:

there are three steps in the simulation of the dataset:

- 1. Modeling instruction:** The neural network function fit (X, y) , which fits the model to the data matrix X and the targets y , is used by each procedure to train the model.
- 2. Prediction:** The function predicts (X) forecasts the values that the test data (X) , supplied as parameters, will ultimately achieve.
- 3. Evaluation:** Using the score function "score (X, y) ", which provides the average accuracy of the supplied test data (X) and labels (y) , the prediction is assessed.

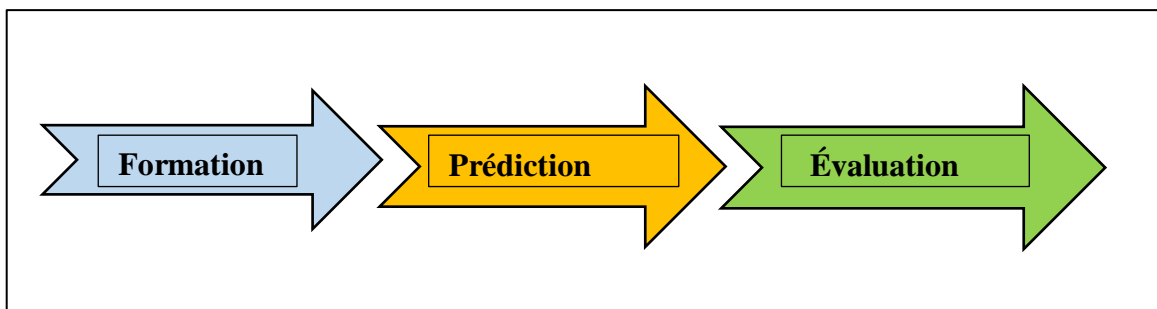


Figure V.14: Steps in simulating the dataset

V.A.2 Prediction base on Thermal Data Analysis

Thermal imaging technology is used in prediction based on thermal data analysis to identify and anticipate fires. In order to identify possible fire dangers, thermal data analysis relies on measuring and interpreting the thermal energy released by landscapes or items. The objective is to use this data to predict and stop fire accidents. An overview of how this tactic functions is given below:

1 Thermal Sensors and Imaging: Thermal data is recorded using specialized sensors, such as thermal cameras or infrared sensors. These sensors are able to pick up infrared emissions from objects and translate them into temperature data. To collect thermal data over designated areas, thermal imaging technology-equipped drones, satellites, or ground-based equipment can be used.

2 Data collection and processing: Thermal pictures or temperature maps are produced by collecting and processing the thermal data that has been obtained. The thermal patterns are analyzed using sophisticated algorithms and image processing methods to pinpoint regions with unusual heat signatures or temperature anomalies.

3 Fire Risk Assessment: A fire risk assessment is carried out by examining the thermal data, trends, and previous fire records. Finding hot spots or heat signatures that might point to possible fire threats is a part of this examination. Other elements that may be taken into account during the study include the state of the weather, the amount of vegetation, and past fire behavior.

4 Early Warning Systems: Early warning systems may be created to inform authorities and stakeholders about probable fire occurrences based on the fire risk assessment. When the thermal data shows a high likelihood of fire, thresholds may be set to start alerts or notifications. This makes it possible to respond quickly and to mobilize resources for evacuation preparations.

5 Proactive Fire control: The examination of thermal data can help with proactive fire control techniques. Thermal imaging hotspots, for instance, might be prioritized for additional surveillance, patrols, or specialized suppression measures. The data can also aid in maximizing the distribution of firefighting resources to efficiently put out prospective flames.

This method improves the capacity to identify and forecast fires based on temperature anomalies by applying thermal data analysis. Authorities are given useful information that enables them to take preventative action, put in place efficient fire prevention policies, and enhance overall fire management skills.

The suggested system can be installed in forested regions that frequently experience yearly forest fires. Additionally, it establishes and validates the existence of fire. A vast number of nodes are established to check for environmental parameters in order to monitor an entire

forest area. When a fire is confirmed, it transmits the notification to the closest node so that the relevant authorities may respond. Fig.

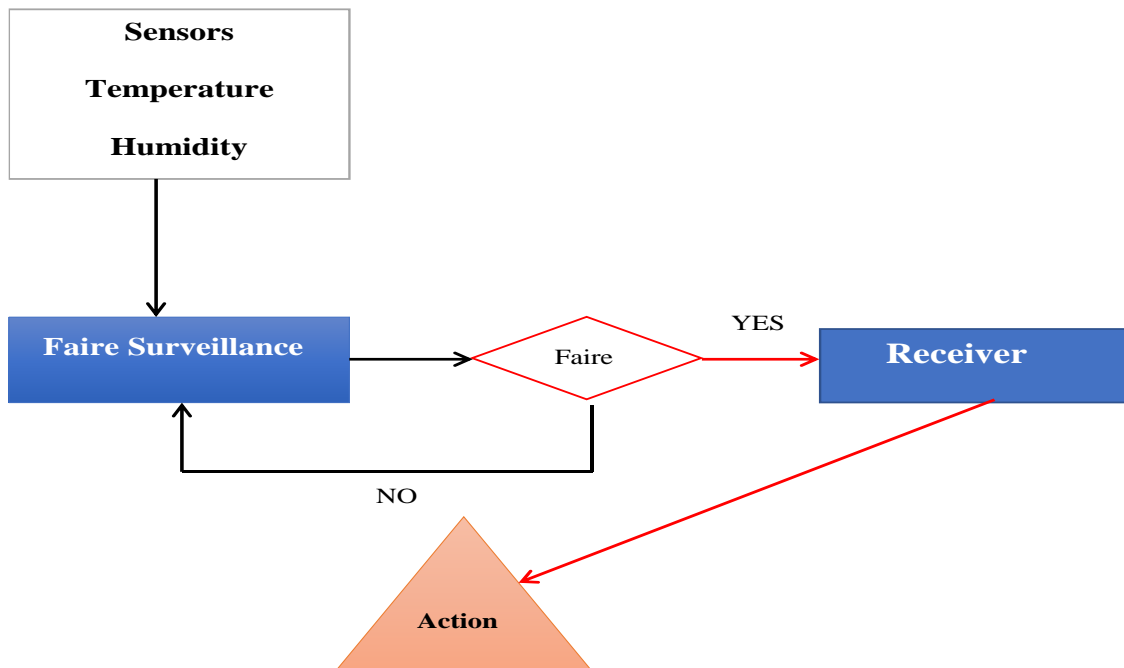


Figure V.15: System overview for monitoring forests

The fire monitoring system keeps track of temperature and humidity data to confirm the existence of a fire.

V.7.A.2.1. Monitoring of temperature and humidity:

As was previously noted, the two most crucial elements that determine the features of the forest ecosystem prior to an early wildfire are temperature and humidity. Initially, sensors are used to collect temperature and humidity data in order to perform temperature and humidity monitoring. The DT-11 temperature and humidity sensor is attached to the analog pins of the Arduino Uno. It has a calibrated digital output. The temperature value is expressed in degrees Celsius, whereas the relative humidity value is expressed in degrees Fahrenheit Moisture (t).

The ratio of the amount of water vapor to its saturation point is known as relative humidity. Because of the fire's tendency to create overheating, dry air, and smoke, temperature and humidity are negatively correlated in the set.

- A potential wildfire hazard is indicated if the temperature is above a specific level and the humidity is below a given threshold. Each geographic area may have a different threshold value.
- The likelihood of an early forest fire is calculated using the link between temperature and humidity.

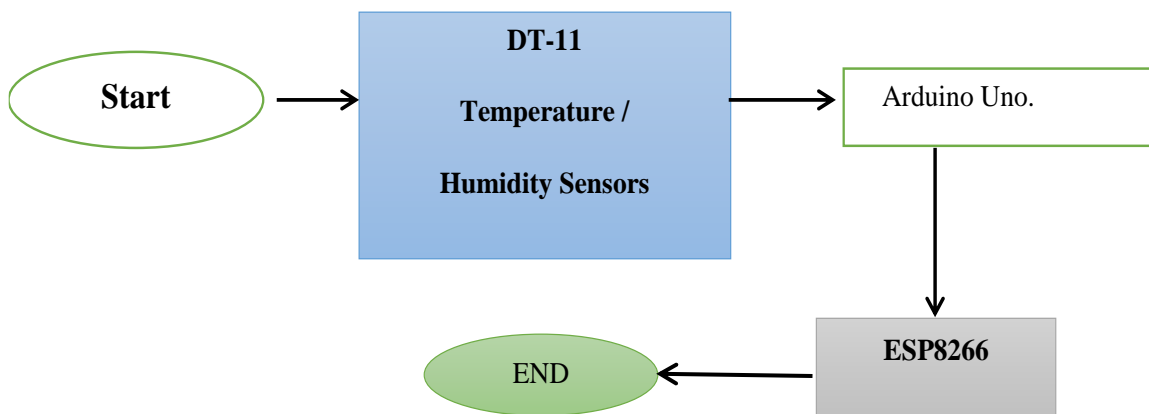


Figure V.15: Temperature and humidity Fire Model

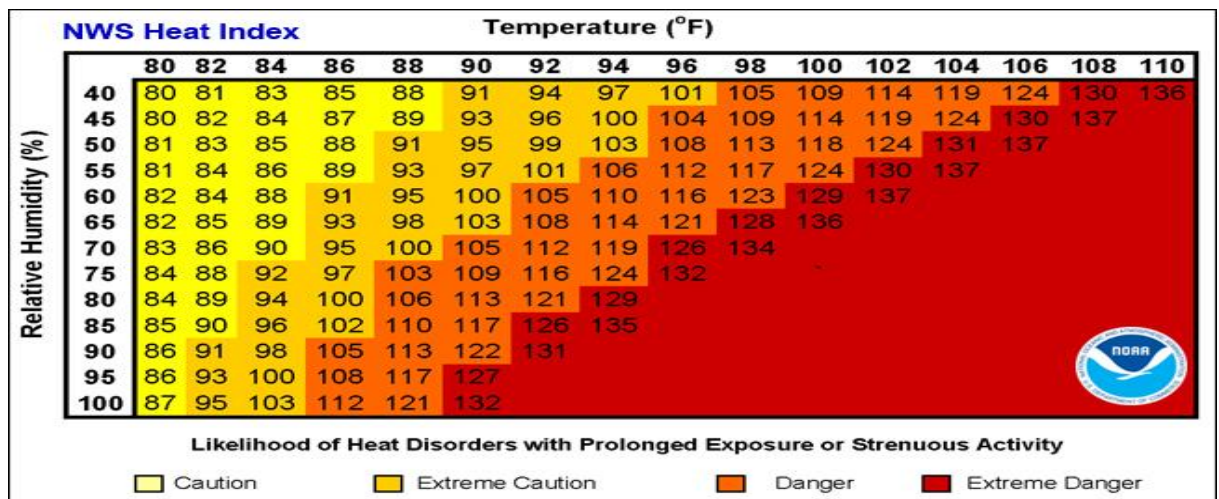


Figure V.16: Heat index chart from [https://www.weather.gov/ama/heatindex]

It not only forecasts flames but also carries out graphic monitoring. Strong proof of an early wildfire arrival is required since temperature and humidity alone cannot confirm the presence of flames.

V.7.A.2.2. Check for fire.

The dataset was produced as part of the NASA space applications challenge in 2018, and its purpose was to be used to build a model that could identify photos with fire. There are two layers and over 999 photos in total in it. The key benefit of utilizing this dataset is the asymmetry, or the fact that there are various numbers of photos on each layer.

It includes 755 pictures of outdoor fires, some of which have dense smoke, and 244 pictures of natural objects (such as trees, grass, rivers, people, foggy forests, lakes, animals, and roads) that don't include fire.



Figure V.17: Forest affected with fire & forest without fire.

Several data augmentation techniques, including flipping, rotation by 300 degrees, brightness enhancement at various scales, magnification, and shearing on the pictures, were used to make the dataset resistant to overfitting.

Occlusion, noise, clutter, flame smoke fluctuation, illumination variance, and view-point difficulties are just a few of the computer vision obstacles that many deep learning models successfully handle. The CNN model was initially fed the training data.

The capacity of artificial intelligence to close the gap between human and computer capabilities has substantially increased. To produce amazing outcomes, both professionals and amateurs focus on several aspects of the field. One of many such subjects is the field of machine vision.

A convolutional neural network (CNN) is a deep learning system that can take a picture as input, assign various characteristics and objects in the image importance (learnable weights and biases), and distinguish between them.

A ConvNet requires significantly less pre-processing compared to other classification techniques. While hand-engineered filters are used in rudimentary techniques, ConvNets can may learn these filters and characteristics with sufficient training.

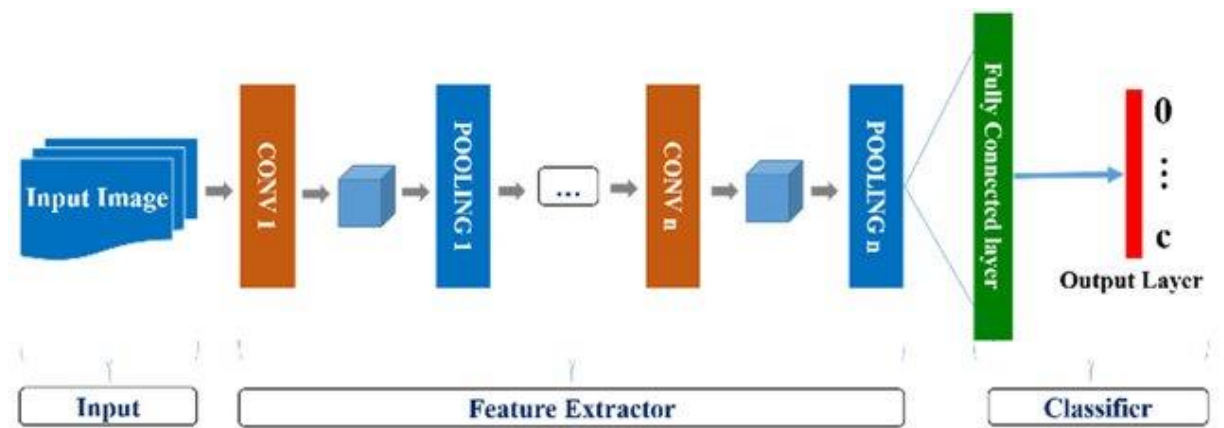


Figure V.18: an overview of convolutional neural network architecture for image classification taken from [P.Nguyen, 2018]

V.7.A.3 Prediction by aerial imaging using drones

Prediction via aerial imaging utilizing drones includes employing unmanned aerial vehicles (UAVs) equipped with image sensors to acquire and analyze data from above to forecast possible fire events. Here's how this method normally works:

1 Drone Deployment: Drones outfitted with imaging sensors, such as visible light cameras, multispectral cameras, or thermal cameras, are deployed into the intended region. These drones can be set to follow pre-defined flight patterns or manually operated by operators.

2 Aerial data collection: As the drones fly over the region of interest, they collect photographs or videos from various angles and elevations. The image sensors on board the drones record visual, multispectral, or thermal data, depending on the specific goal of the research.

3 Image Processing and Analysis: The recorded aerial data is processed and analyzed utilizing powerful computer vision algorithms and image processing techniques. The purpose is to extract important information and detect potential fire dangers. This study might involve vegetation health evaluation, hotspot detection, or finding other indications of fire danger.

4 Fire Risk Assessment: Based on the analysis of the recorded airborne data, a fire risk assessment is undertaken. It entails examining elements such as vegetation density, dryness, temperature anomalies, and proximity to human populations. By merging this information with previous fire records and other pertinent data, the risk of prospective fire events may be assessed.

5 Early Warning Systems: Drone-based aerial photography analysis may be utilized to construct early warning systems. Thresholds can be established to activate warnings or notifications when the data shows a high chance of fire danger. This enables fast reaction, evacuation planning, and resource allocation.

6 Preventive Measures and Fire Control: The acquired aerial data and risk assessment can guide preventive measures and fire control methods. For example, it can help identify regions prone to fires, allowing authorities to adopt focused preventative initiatives such as fuel reduction or enhanced firebreaks. Additionally, the data can help in resource allocation and decision-making during firefighting operations.

By deploying drones for aerial imagery, this technique provides a cost-effective and efficient means to monitor broad regions, detect possible fire dangers, and forecast fire events. It provides early detection, fast reaction, and informed decision-making, eventually increasing fire management and prevention efforts.

V.7.B.Fire detection using machine learning

Fire detection with machine learning entails employing algorithms and models to assess visual or sensor data in order to identify and detect the existence of flames. Here's an outline of how machine learning may be applied to fire detection:

1 Data Collection: To train a machine learning model for fire detection, a huge dataset of fire-related photos or sensor inputs is collected. This data can include photographs or videos collected from security cameras, satellite photography, or sensor data from smoke detectors, heat sensors, or fire alarms.

2 Data Preprocessing: The acquired data is preprocessed to reduce noise, standardize the data, and extract essential characteristics. For visual data, preprocessing may entail scaling, cropping, and transforming pictures into a suitable format. For sensor data, preprocessing may include

3 Model Training: Machine learning models, such as convolutional neural networks (CNNs), recurrent neural networks (RNNs), or support vector machines (SVMs), are trained using the preprocessed data. The models learn to distinguish patterns and characteristics suggestive of fire by modifying their internal parameters during the training phase. The training is generally supervised, and labeled samples of fire and non-fire data are used to assist the learning process.

4 Feature Extraction: In the case of visual data, the trained model can automatically extract key properties from photos, such as color, texture, or form, that identify fire from non-fire

objects. For sensor data, the model may learn to recognize patterns in the sensor values that are indicative of fires, such as abrupt temperature rises or smoke particle detection.

5 Classification: Once the model is trained and features are retrieved, it may be utilized for fire detection. New, unknown data is fed into the trained model, and the model identifies whether the input represents a fire or a non-fire event. The model generates a probability or a binary prediction indicating the presence or absence of fire.

6 Integration and Alert Systems: The fire detection system may be incorporated with existing infrastructure, such as surveillance systems, smoke detectors, or IoT devices. When a fire is discovered, suitable warnings or notifications can be provided to relevant stakeholders, including emergency services, building management, or inhabitants, enabling fast action and evacuation.

Machine learning-based fire detection systems may be continually enhanced by gathering fresh data and retraining the models. This iterative method helps increase the accuracy and performance of the detection system over time, resulting in more reliable fire detection capabilities.

In this forest fire detection strategy, we will follow the system shown in Figure 1. Initially, the proposed model will be developed by training and testing it on the selected forest dataset, which contains fire and non-fire scenes.

After During training, the model's reliability and effectiveness will be verified by observing the quantitative results of the test data. Once the model has performed well, it will be installed in the UAV for real-time fire detection. The UAV is then deployed and maintained by the Forestry Department via the wireless communication network. The UAV can take a real-time photo of the forest and produce a fire or non-fire result using the proposed model. This result is sent to the data center by drones via the communication system. If the data center receives a fire signal, you finally inform the disaster management system to take the necessary measures to control the fire.

The focus is on building a fire detection model **figure V.19** that will be installed on a surveillance drone. The proposed system is an autonomous forest fire detection system that examines forest scenes and extracts features using a customized CNN architecture. To train the supervised learning model, a set of forest fire images, including fire and non-fire scenes, is required. These images were taken from a recently released dataset.

First, the images were augmented, then divided into training (80%) and test (20%) samples. The training samples were normalized (scaled from 0 to 1) to speed up the training

process. The proposed CNN model was then trained using normal training samples. Finally, regular test samples were used to evaluate the performance of the CNN model.[A.K.Z Rasel Rahman and all, 2022].

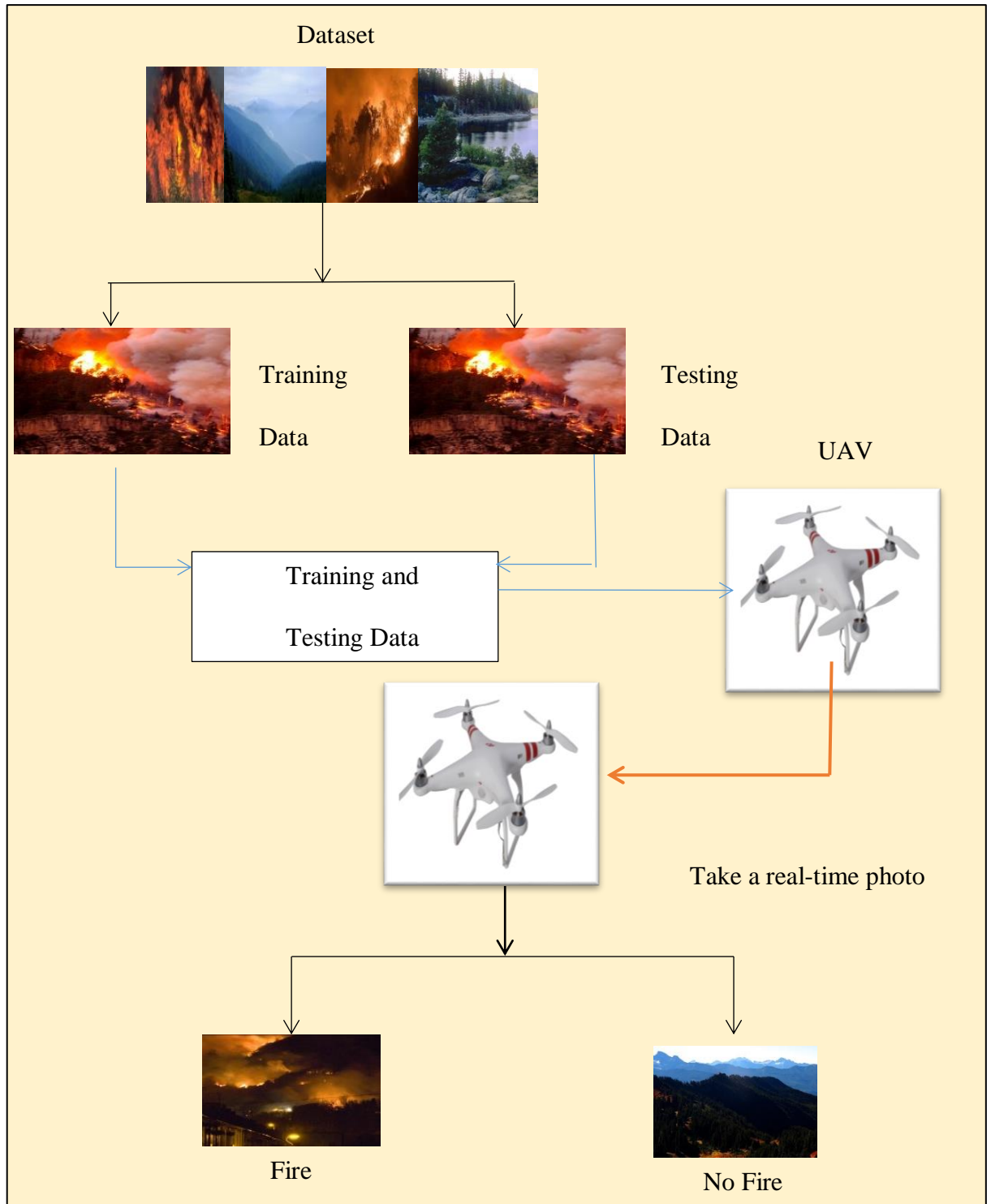


Figure V.19: Ditection fire modle

V.7.B.1 Preparing the dataset (data segmentation)

For the implementation of our model, we used a dataset containing a total of 1550 images. We divided this dataset into two subsets:

- The first subset contains the images used to train our model.
- The second subset contains the images used to validate the same model.

Note that the images in the two subsets are completely different. In other words, any image belonging to one subset must not belong to the other in order to guarantee the relevance of our segmentation.

- **The first subset called "Training"** contains a total of 1250 images. These images are divided into two classes. The first class contains images of fires or forest fires (a folder containing 750 images called "Fire"). The second class contains images without fire (a folder containing 500 images called "NoFire").
- **The second subset called "Tasting"** contains a total of 300 images. These images are divided into two classes. The first class contains images of fires or forest fires (a folder of 180 images called "Fire"). The second class contains images without fire (a folder of 120 images called "NoFire").

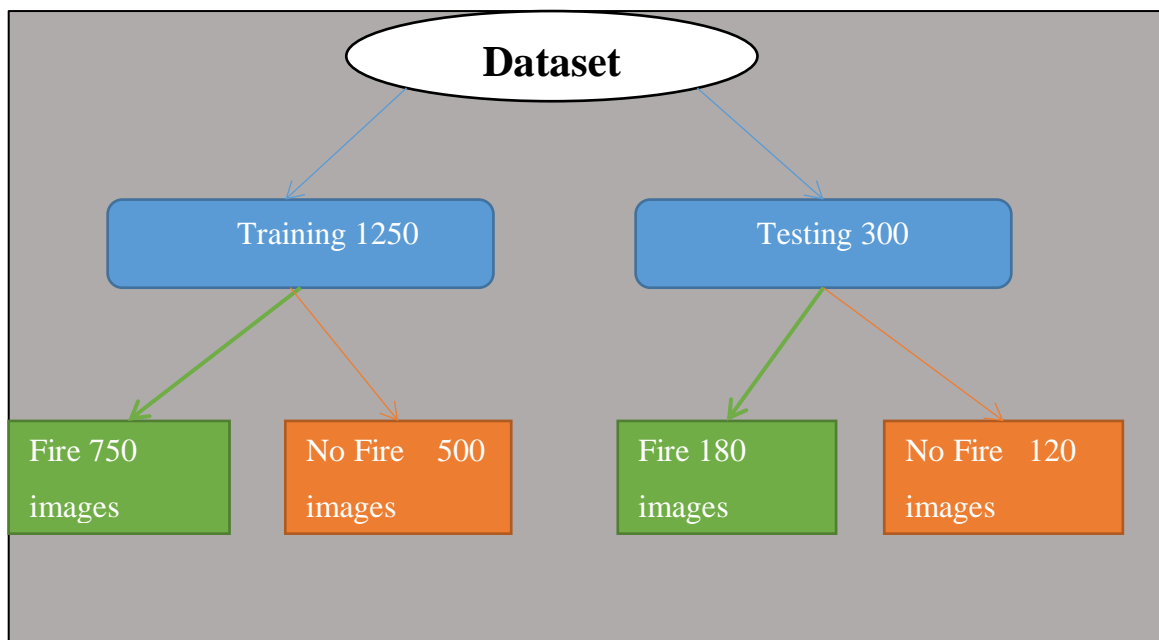


Figure V.20: Segmentation of the model data

V.7.B.2 Experimentation



Figure V.21: Fire images (Training)



Figure V.22: No Fire images (Training)



Figure V.23: Examples of Fire and No Fire images (Testing)

V.7.B.3 Results and discussion

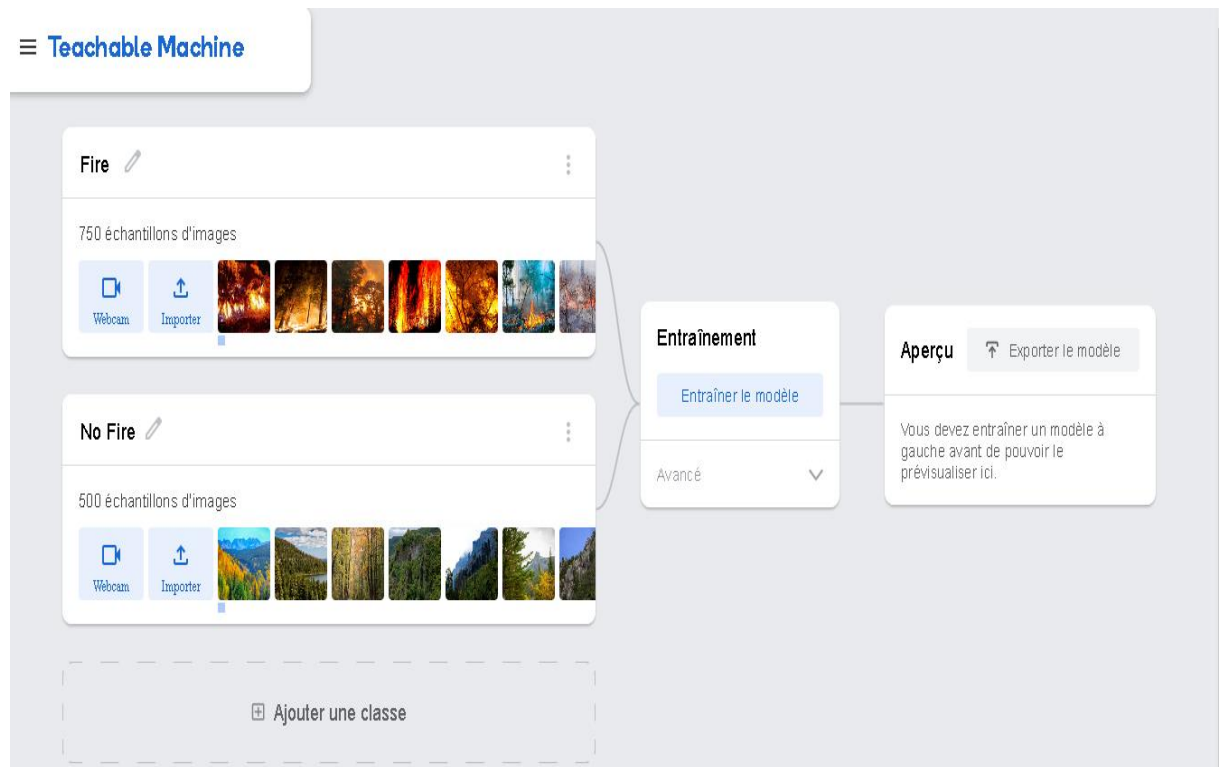


Figure V.24: Preparation the dataset

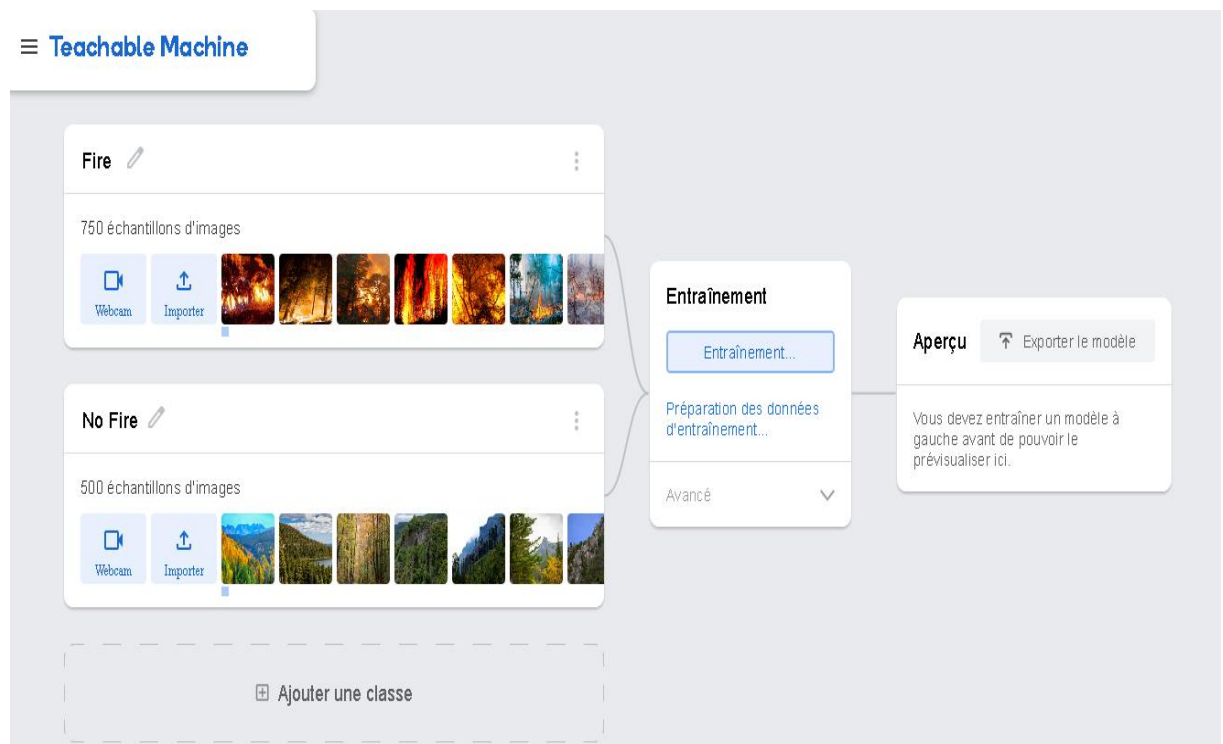


Figure V.25: preparation of training data

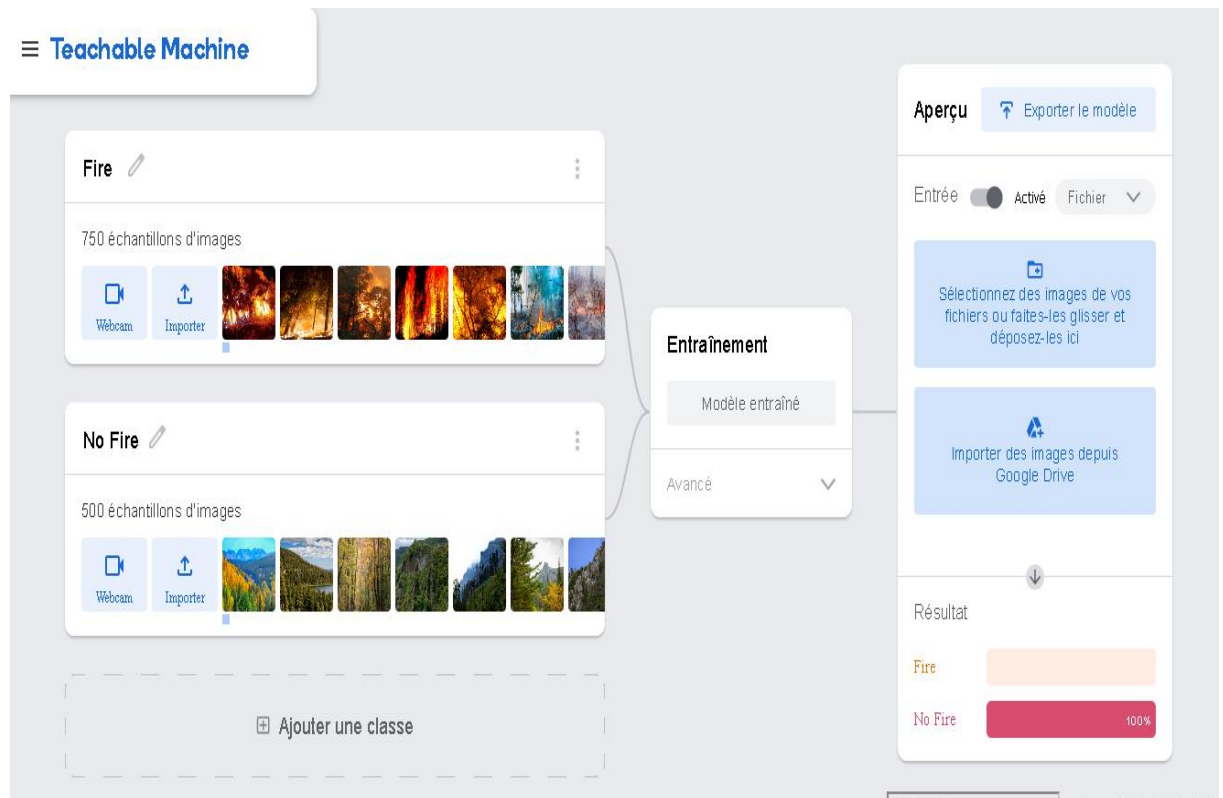


Figure V.26: Training dataset

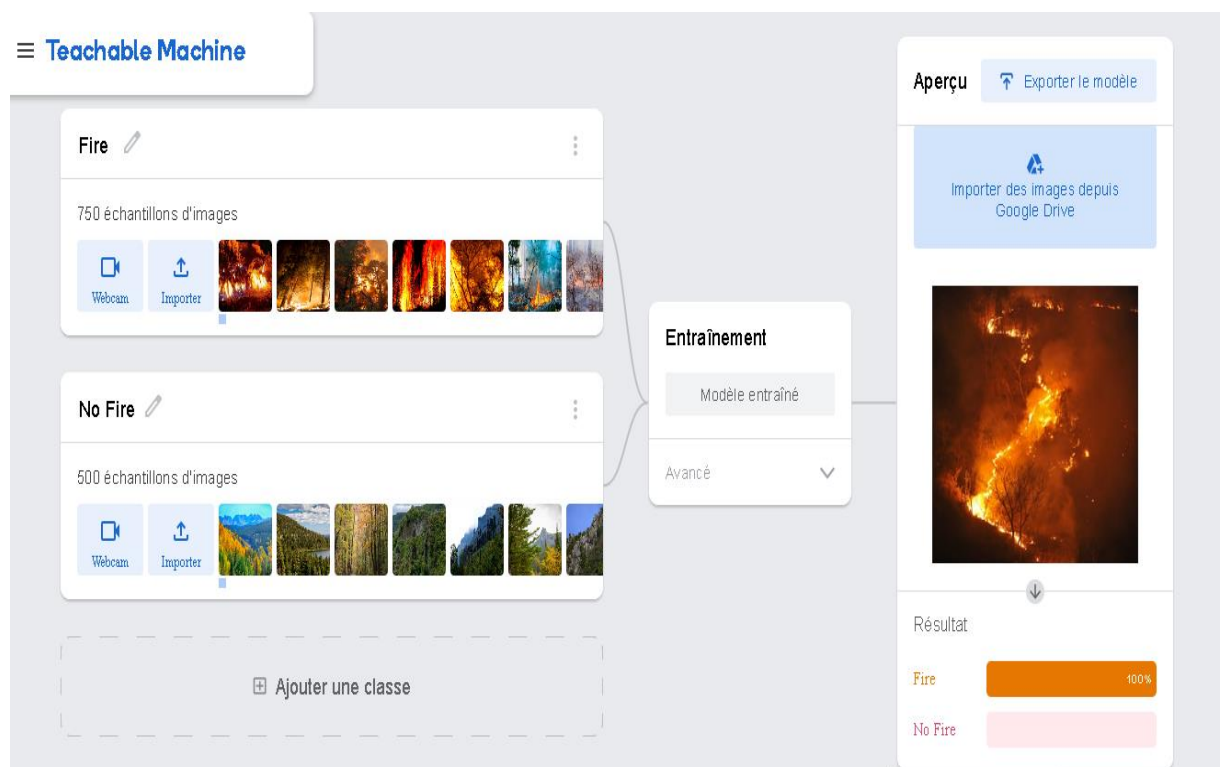


Figure V.27: Tasting the dataset

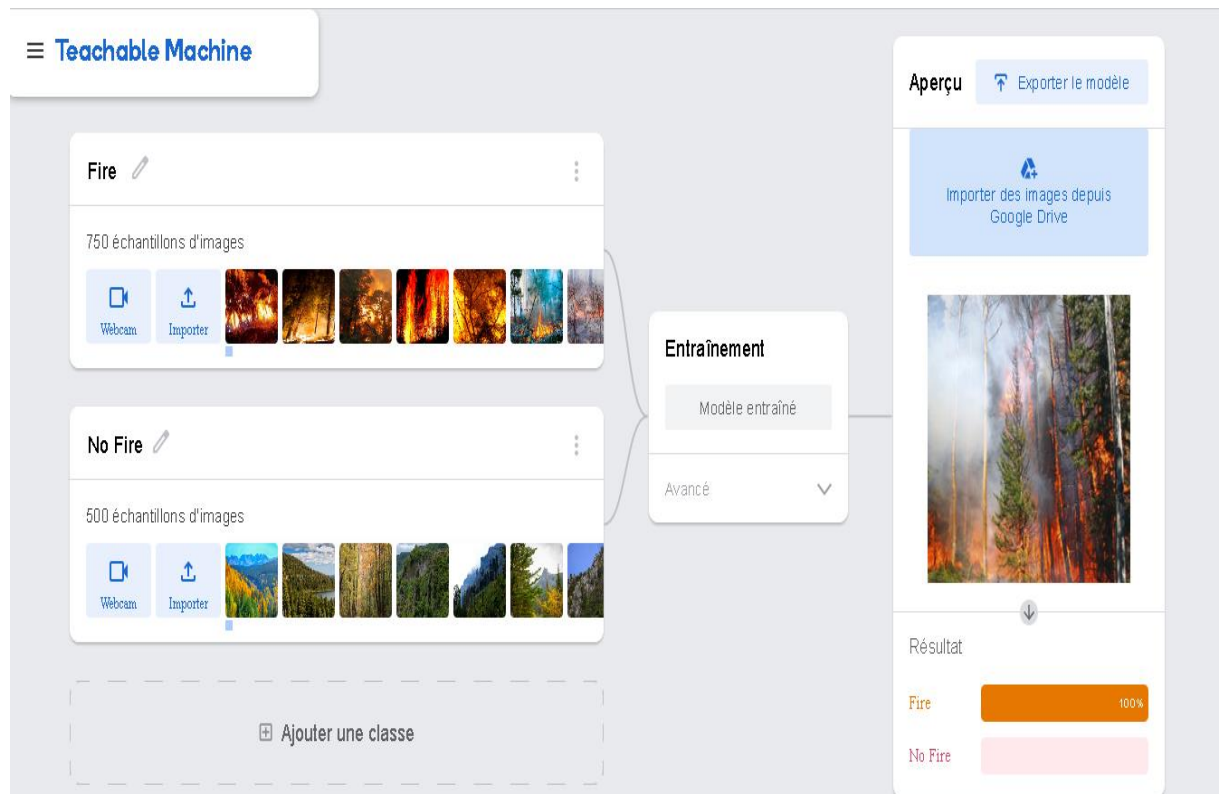


Figure V.28: Result Tasting 'fire'

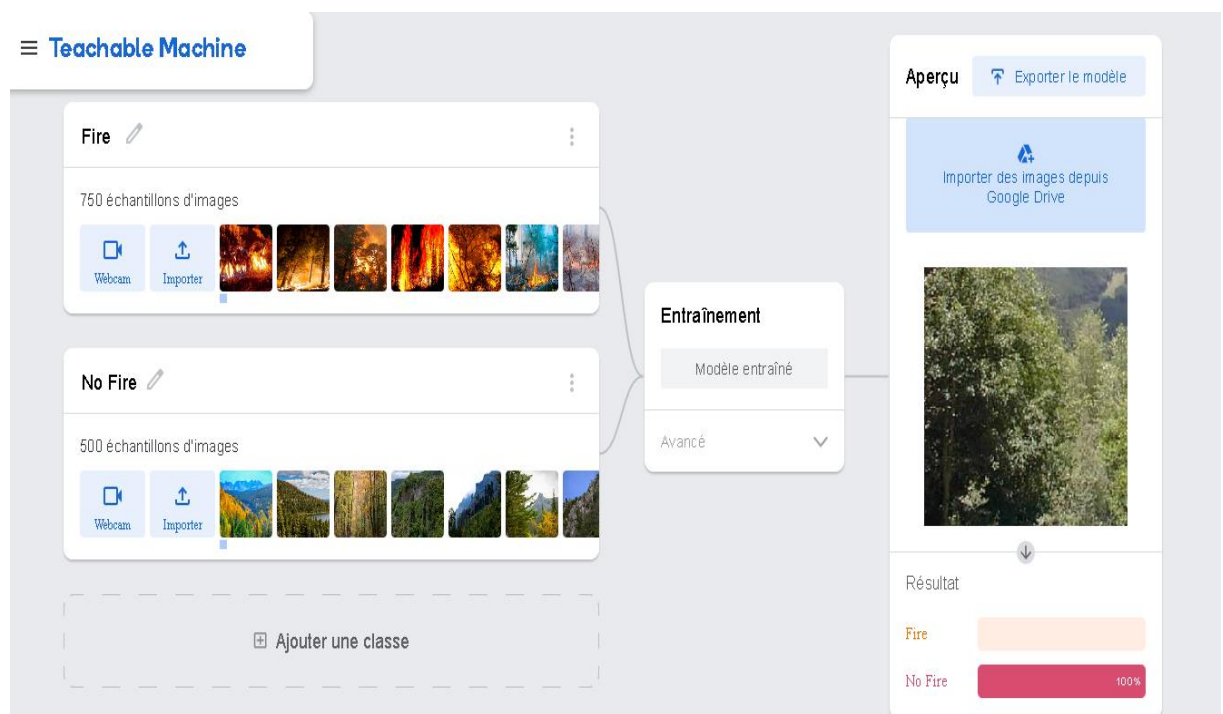


Figure V.29: Result of Tasting 'No fire'

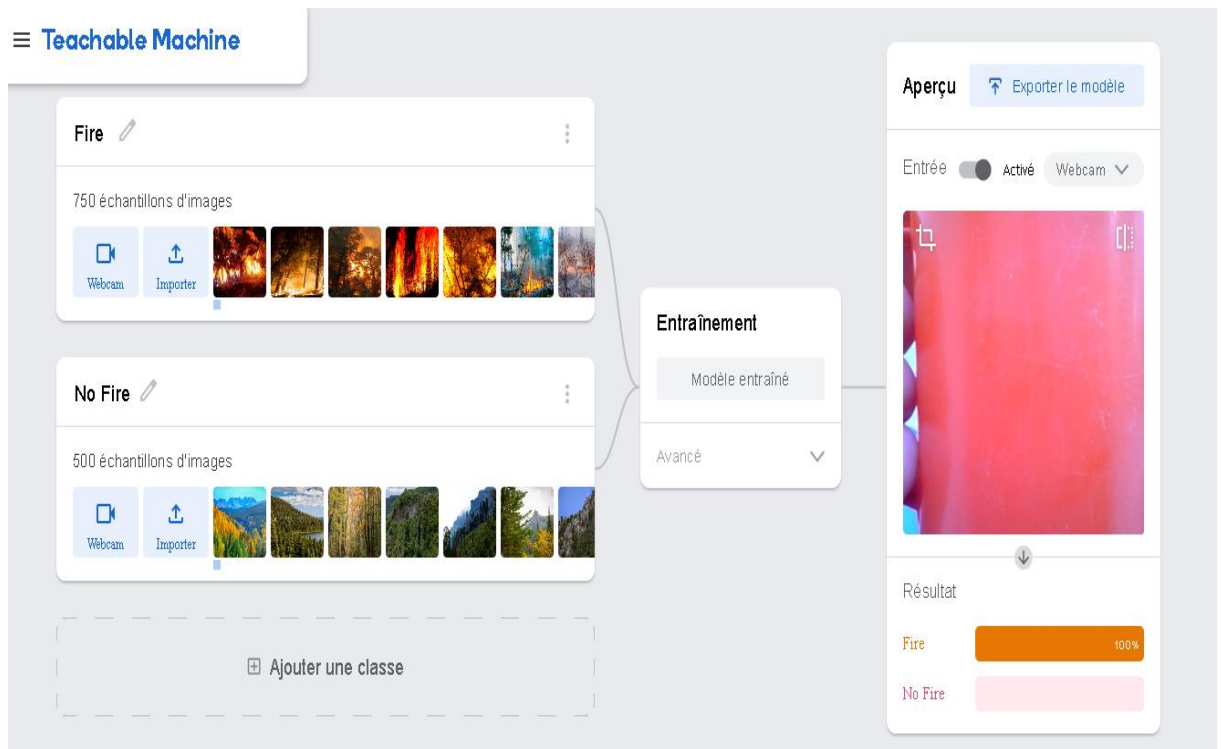


Figure V.30: Result Testing 'Fire'



Figure V.31: Export the model

After conducting the machine learning process and training the fire detection model, highly promising outcomes were attained. The model exhibited exceptional capability in distinguishing between images that contain fires and those that do not. A fresh set of images was used for testing, and the results were scrutinized to assess the model's effectiveness.

The experimental findings demonstrated that the developed model achieved a remarkable accuracy in detecting fires, correctly classifying images into "fire" and "non-fire" categories with a high level of success. Various performance metrics, including precision, recall, and error rate, were utilized to evaluate the model, all of which indicated its superior ability to differentiate fires from other images.

The model underwent testing on a diverse range of experimental data, including forest fire images and rural settings. It demonstrated exceptional proficiency in identifying key fire indicators, such as flames, smoke, and abrupt temperature changes. Moreover, the model displayed its capacity to differentiate fires from other factors that may be present in the images, such as sunlight and clouds.

These research outcomes open up avenues for extensive application of this model in fire detection systems, including forest early warning systems and remote monitoring of urban areas. With its high accuracy and dependable performance, this model holds significant potential in the realm of fire detection applications.

V.7.C.Firefighting using UAV

Firefighting using Unmanned Aerial Vehicles (UAVs) involves utilizing drones equipped with specialized firefighting tools and technologies to assist in firefighting operations. Here's a detailed overview of this strategy:

1. Aerial Surveillance and Situational Awareness:

UAVs allow real-time aerial surveillance of the fire site, delivering a detailed picture of the fire's size, position, and activity. This airborne view helps firefighters achieve situational awareness and make educated decisions on resource allocation, deployment, and strategy planning.

2. Early Fire Detection:

Drones outfitted with thermal cameras or other sensors may identify hotspots and areas of strong heat, even in smoke-filled conditions. This early detection capacity helps firefighters

respond rapidly to possible fire breakouts or discover minor flames before they grow, enabling speedier containment and suppression operations.

3. Airborne Fire Suppression:

Some drones are expressly built to carry and distribute firefighting materials, such as water, foam, or fire retardants. These drones, generally equipped with strong pumps and nozzles, can properly target particular parts of the fire and deliver the firefighting materials straight to the source. This skill is particularly important for reaching inaccessible or dangerous regions.

4. Support for Ground Operations:

Drones can give support to ground firefighting operations by relaying real-time video or pictures of the fire situation. This information serves to monitor fire behavior, detect possible risks, and ease communication between ground teams and incident commanders. Drones may also transfer equipment or supplies to remote or difficult-to-reach regions, lessening the physical load on firefighters.

5. Monitoring and Hotspot Tracking:

UAVs fitted with thermal or multispectral sensors can monitor the fire perimeter and follow hotspot activity. By regularly monitoring the fire's path, drones can detect locations where the fire is growing fast or where new hotspots are appearing. This information assists in deploying firefighting resources effectively and altering methods in real-time.

6. Safety Assessments:

Drones can be used to inspect the structural integrity of structures impacted by the fire. By recording high-resolution photos or videos, drones aid in analyzing possible collapse hazards, locating weakened structures, and directing firemen in selecting safe entry sites.

7. Post-Fire Evaluation and Analysis:

Once the fire is under control, drones can be deployed for post-fire evaluation. They may collect airborne pictures of the impacted region, aiding in damage assessment, evaluating the degree of fire suppression, and locating any residual hotspots or possible re-ignition hazards.

Firefighting with UAVs boosts operational capabilities, improves firefighter safety, and enables more effective resource allocation. The real-time data and aerial viewpoint given by drones lead to more effective decision-making, shorter reaction times, and improved overall firefighting outcomes.

V.8 Conclusion

In conclusion, this chapter covered various important topics in the field of fire detection using machine learning. We discussed image processing concepts and the definition of digital images. We introduced artificial neural networks and explored different models, including single-layer and multilayer neural networks. The applications of neural networks were also highlighted.

The process of learning a neural network was explained, including supervised, unsupervised, and reinforcement learning. We then focused on convolutional neural networks (CNNs) and their architecture, including the different layers such as convolution, pooling, ReLU, fully connected, and loss layers. The advantages of CNNs were emphasized.

We discussed the development and implementation of CNN models using Teachable Machine. The chapter also delved into wildfire detection and prediction using CNNs, covering prediction based on historical fire records, thermal data analysis, and aerial imaging using drones.

Finally, we touched upon the preparation of the dataset, experimentation, and the results and discussion. The use of machine learning and CNNs showed promising results in fire detection and prediction. These techniques have the potential to significantly improve our ability to combat forest fires and mitigate their impact.

Moving forward, further research and development are necessary to enhance these models and techniques, ultimately leading to more accurate and efficient fire detection systems. Continued collaboration between the scientific, engineering, and relevant stakeholders is crucial to maximize the utilization of machine learning in the field of fire detection.



**General
Conclusion**

General conclusion

In conclusion, this thesis has extensively covered various aspects related to the design and development of quadcopter unmanned aerial vehicles (UAVs). The thesis delved into the principles of quadrotor flight, including kinematics and dynamics. It analyzed control modeling techniques, such as PID controllers, and their role in height, roll, and pitch control. Fuzzy logic control and its advantages were also explored, highlighting its applicability in UAVs.

The thesis further investigated image processing techniques, with an emphasis on artificial neural networks and convolutional neural networks. It highlighted their significance in tasks like fire detection and prediction. The implementation of CNNs were explored, demonstrating their effectiveness in wildfire detection.

The thesis proposed a promising solution to address the issue of massive wildfires, relying on an integrated set of four strategies that utilize drones and artificial intelligence. The first strategy is fire prediction using artificial intelligence. The second strategy is early warning and fire detection using drones and artificial intelligence. The third strategy is firefighting, where drones are directed to intervene and extinguish the fire in its initial stage before it expands and spreads. The fourth strategy, named DronesRain, is used in cases where the fire is large and a single drone is unable to extinguish it.

We were unable to cover all the strategies in the thesis, so we focused on one strategy, which is fire detection, as fire images and data are easily accessible.

Regarding the prediction strategy, the lack of data and images posed a major obstacle to its implementation. As for the firefighting strategy, it primarily relies on reaching the prototype stage.

Regarding the DronesRain strategy, it requires more time and addressing it alone goes beyond the scope of a master's thesis. It relies on what is known as collective intelligence or swarm robotics.

Overall, the four strategies require more than just a master's thesis to be fully addressed, and this should be taken into account in future work.

Furthermore, part of our future work plan is to develop a hybrid (vertical take-off and landing) VTOL drone that can operate in challenging environments. This involves the development of long wings to enable gliding, which extends flight time and conserves energy. Additionally, the wings will be equipped with solar cells to harness solar power.



References

References

- [A.Rahuldeo and all.2022] A. Rahuldeo, P.S. Nerkar, B. Borse, Kirubakaran V. Unmanned Aerial Vehicles an Overview and Applications. University. Nashik, Maharashtra, INDIA ‘article 6’.2022.
- [CC, Chang, and all. 2016] Chang CC, Wang JL, Chang CY, Liang MC, Lin MR. Development of a multicopter-carried whole air sampling apparatus and its applications in environmental studies. Chemosphere. 2016
- [J.Bright, and all.2019] J.Bright, R.Suryaprakash, S Akash, A Giridharan .Optimization of quadcopter frame using generative design and comparison with DJI F450 drone frame, Vellore Institute of Technology Chennai, Tamilnadu, India.2019
- [A. Sanchez · and all.2010] A. Sanchez ·L. R. García Carrillo. E. Rondon · R. Lozano · O. Garcia. Hovering Flight Improvement of a Quad-rotor Mini UAV Using Brushless DC Motors. J Intell Robot Syst (2011) 61:85–101. 2010
- [H, L. Chan, and K. T. Woo .2015] H. L. Chan and K. T. Woo .design and control of small quadcopter system with motor closed loop speed control. University of science and technology, Hong Kong china 2015
- [A. Kendall. K.A STOL .2014] A. Kendall. K.A STOL .on-board object tracking control of a quadcopter with monocular vision. <https://www.researchgate.net/publication/270511150> .2014
- [T.A. Brungarta, and all.2019] T.A. Brungarta, S.T Olsonb, B.L. Klinec and Z.W. Yoasd .the reduction of quadcopter propeller noise. Noise Control Engineering Journal .2019
- [K, SA Khuwaja, and all. 2018] K. SA Khuwaja , B S .Chowdhry , K F. Khuwaja , V O,Mihalca and R C ,Țarcă. Virtual Reality Based Visualization and Training of a Quadcopter by using RC Remote Control Transmitter. IOP Conf. Series: Materials Science and Engineering 444 (2018) 052008 .2018

References

- [D.Baek, and all. 2014] D.Baek, Y.Chen , N.Chang , E.Macii , M.Poncino. Energy-Efficient Coordinated Electric Truck-Drone Hybrid Delivery Service Planning. . AEIT International Conference of Electrical and Electronic Technologies for Automotive (AEIT AUTOMOTIVE) 2014
- [DR, Borah, and all, 2016] DR_Borah, L_Debnath, M_Gogoi. A review on Quadcopter Surveillance and Control. ADBU-Journal of Engineering Technology. ADBU-Journal of Engineering Technology .2016
- [S. Ahirwar and all,2019] S.Ahirwar , R_Swarnkar, S_Bhukya and G_Namwade. Application of Drone in Agriculture. ournal homepage: <http://www.ijcmas.com> .2019
- [M.O.Baloola, Ibrahim, and Mas S. Mohktar, 2022] M.O.Baloola ,Ibrahim and Mas S. Mohktar . Optimization of Medication Delivery Drone with IoT-Guidance Landing System Based on Direction and Intensity of Light. Sensors 2022, 22, 4272. <https://doi.org/10.3390/s22114272>.
- [B. Rabta, C. Wankmüller, and G. Reiner, 2018] B.Rabta, C. Wankmüller, G.Reiner, A drone fleet model for last-mile distribution in disaster relief operations.
- [S. Maharana. 2017] S.MAHARANA. COMMERCIAL DRONE .Sroceedings of IRF International Conference, 2017, Mumbai, India, ISBN: 978-93-85832-29-1.
- [E.Brumfield,2014] E_Brumfield, Armed Drones for Law Enforcement: Why It Might Be Time to Re-Examine the Current Use of Force Standard <https://scholarlycommons.pacific.edu/mlr/vol46/iss3/5>
- [Y. Mohd Yamani and all.2021] Y.Mohd Yamani, PS.Wong, Y. Azlina Md, O.Roshartini. The Challenges of Drone Application in the Construction Industry. Journal of Technology Management and Business.2021
- [C.Agho,2017] Courage Agho. Dynamic Model and Control of Quadrotor in the Presence of Uncertainties. University of South Carolin.2017

References

- [M.Mokhtari.2015] M.Mokhtari. Commande Adaptative des Systèmes Non linéaires par l'Approche Backstepping Neuronale.Université Hadj Lakhdar Batna.2015
- [D. Dubois] Etude des correcteurs, D. DUBOIS.
- [Z.Satla, M.Elajrami , K.Bendine,2018] Z.Satla, M.Elajrami and K.Bendine . Easy Tracking of UAV Using PID Controller.. Periodica Polytechnica Transportation Engineering 2018.
- [T.Bresciani,2008] T.Bresciani. Modeling Identification and Control of a Quadrotor Helicopter. Department of Automatic Control Lund University.2008
- [Ch.CHUEN, 1990] CH.CHUEN. Fuzzy Logic in Control Systems: Fuzzy Logic Controller. 1990.
- [R. R. Yager,1992] R. R. Yager , An Introduction to Fuzzy Logic Applications in Intelligent Systems © Kluwer Academic Publishers 1992
- [R. SADOUNI] R SADOUNI, Course notes: Commande Intelligente, University of Ghardaia.
- [P.Nguyen Kieu, 2018] P.Nguyen Kieu Applying Multi-CNNs model for detecting abnormal problem on chest x-ray images 11/2018
- [A. K. Z Rasel Rahman and all, 2022] A. K. Z Rasel Rahman and all, Unmanned Aerial Vehicle Assisted Forest Fire Detection Using Deep Convolutional Neural Network, 2022
- [Y.Oulad Sayad and all,] Younes Oulad Sayad and all, "Predictive Modeling of Wildfires: A New Dataset and Machine Learning Approach"
- [H.ANOUAL ,2012] Hinde ANOUAL. Modélisation, Observation et Commande d'un Drone Miniature Birotor Coaxial. Thèse de Doctorat, 2012.

References

Internet references

<https://www.weather.gov/ama/heatindex>

<https://france3-regions.francetvinfo.fr/occitanie/gard/nimes/des-drones-pour-lutter-contre-les-incendies-2545852.html>

<https://www.supinfo.com/articles/single/7923-deep-learning-fonctions-activation>

<https://teachablemachine.withgoogle.com>